

**The joint impact of storm surge,
fluvial flood and operation of
man-made structures on the high
water level frequency in the
Lower Rhine Delta**

**The joint impact of storm surge, fluvial flood and
operation of man-made structures on the high water
level frequency in the Lower Rhine Delta**

Proefschrift

ter verkrijging van de graad van doctor
aan de Technische Universiteit Delft,
op gezag van de Rector Magnificus prof. ir. K.C.A.M. Luyben,
voorzitter van het College voor Promoties,
in het openbaar te verdedigen op
woensdag 19 Maart 2014 om 10:00 uur

door

Hua ZHONG

Bachelor of Science in Hydrology and Water Resources,
Hohai University, China
geboren te Gongyi, China

Dit proefschrift is goedgekeurd door de promotoren:

Prof. drs.ir. J.K. Vrijling
Prof. dr.ir. P.H.A.J.M. van Gelder

Copromotor Dr.ir. P.J.A.T.M. van Overloop

Samenstelling promotiecommissie:

Rector Magnificus,	voorzitter
Prof. drs.ir. J.K. Vrijling,	Technische Universiteit Delft, promotor
Prof. dr.ir. P.H.A.J.M. van Gelder,	Technische Universiteit Delft, promotor
Dr.ir. P.J.A.T.M. van Overloop,	Technische Universiteit Delft, copromotor
Prof. W.Wang,	Hohai University, China
Prof. dr.ir. M. Kok,	Technische Universiteit Delft
Dr.ir. J. Beckers,	Deltares
Dr.ir. T. Wahl,	University of South Florida, United States
Prof. dr.ir. S.N. Jonkman,	Technische Universiteit Delft, reservelid

This research has been financially supported by “the China Scholar Council (CSC)”.

Copyright © 2014 by Hua ZHONG

Published by: VSSD, Delft, the Netherlands

ISBN: 97890-6562-3522

All rights reserved. No part of the material protected by this copyright notice may be reproduced or utilized in any form or by any means, electronic or mechanical, including photocopying, recording or by any information storage and retrieval system, without the prior permission of the author.

In memory of my grandmother

Summary

Most deltas of the world and their highly urbanized environments, are vulnerable to flooding, and thus, the consequences in terms of human fatalities and economic losses are serious. Floods and the consequent damages have triggered significant developments of flood protection measures.

Flood risk is expected to be much more serious in the future. On the one hand, climate change is exacerbating mean sea level rise and intensifying extreme river floods, consequently increasing high water level frequency. On the other hand, deltas are rapidly experiencing urbanization, which results in increasing vulnerability of deltas.

High water levels in deltas are the result of interaction between natural flood sources (high astronomical tides, storm surges, river flooding, high intensive precipitation, or combination of more than one variable) and human interventions (flood control measures to reduce flood sources).

In this thesis the joint impact of storm surges, fluvial floods as well as the operational water management system on the high water level frequency is estimated in the Lower Rhine Delta. A fully probabilistic approach is developed for resampling extreme hydrodynamic boundary conditions of the Lower Rhine Delta as well as the time revolution.

The first application of a joint probability approach in the Lower Rhine Delta dated back to 1969 (Van der Made, 1969). It only considered the peak values of the sea level and the Rhine flow, assuming the other associated variables (such as the storm surge duration) to be pre-determined as constant values. Nevertheless, at present these associated variables play an important role in determining the water level in the delta. For example, the Maeslant barrier and the Haringvliet Dam with sluices should be closed when a storm surge occurs. A storm surge duration can affect the closure duration of the Lower Rhine Delta and therefore can influence the water level in the inland delta. In the fully probabilistic approach these associated variables will be taken into account.

In the fully probabilistic approach, joint probability distributions of extreme hydraulic load variables derived from the observed flood events are applied to re-sample a large number of scenarios of storm surges, Rhine floods as well as Meuse floods. These scenarios drive a deterministic model to result in water levels at the locations of interest. These water levels can be converted into high water level frequency at locations.

This approach enables assessment of the high water level frequency in a changing environment with associated effects from climate change and human interventions. In the Lower Rhine Delta, the impact of climate change on the high water level frequency is also quantified for the year 2050 in order to assist

in decisions regarding the adaptation of the operational water management system and the flood defense system.

To protect the Lower Rhine Delta from flooding, one of critical measures is to reduce the high water level frequency by taking advantage of the present operational water management system. This system refers to the man-made structures, such as large sluices, storm surge barriers and pumps, either at the mouth of the delta or along the rivers and canals, as well as their operational controls. This system is applied to control the water levels and flows within the delta for the aims (1) avoiding high water levels (due to high river discharges or storm surges or the combination of both), (2) avoiding low water levels (in case that problems with regard to freshwater supply and navigation) (van Overloop, 2009; 2011). The Dutch policy primarily aimed at the prevention of flooding by means of strengthening and heightening dikes, and therefore little attention has been given to the potential reduction of the high water level frequency as a result of developments of the operational water management system. In this thesis, the effect of the present and future operational water management system on the high water level frequency will be discussed.

Construction of new structures such as storm surge barriers, flood gates has been proposed to improve the operational water management system for a better performance of high water level frequency reduction. In this thesis the effect of new structures on the high water level frequency is presented.

The traditional approach applied only a very limited number of sampling scenarios (Mantz and Wakeling, 1979; Samuels and Burt, 2002) to the high water level frequency estimation with a detailed model. Computational burden for the usage of detailed models strongly limits the number of stochastic scenarios. However, a large number of stochastic scenarios are necessary not only for the statistical uncertainty reduction, but also for the present operational water management system controlling different extreme hydrodynamic boundary conditions. It requires unaffordable computational resource with a detailed model. Therefore, a simplified model derived from a detailed model is necessary.

The particular contribution of this thesis is that it introduces a fully probabilistic approach for stochastic simulation of extreme hydrodynamic boundary conditions of the Rhine Delta. The approach takes the probability related to time evolution into account, and drives a deterministic model to estimate the high water level frequency based on the importance sampling Monte Carlo method. The impact of climate change and developments in the operational water management system is assessed. The approach can also be extended to the assessment of the flood probability and the flood risk in order to assist the flood risk management in the Lower Rhine Delta. This approach can also be applied to other deltas all over the world.

Samenvatting

De meeste delta's in de wereld en hun zeer geurbaniseerde omgeving, zijn kwetsbaar voor overstromingen, en de gevolgen, in termen van verlies voor mens en economie, zijn aanzienlijk. Overstromingen en de daaruit voortvloeiende schade vormen de aanleiding tot de ontwikkeling van beschermingsmaatregelen.

Het risico van overstromingen zal in de nabije toekomst steeds ernstiger toenemen. Enerzijds leidt klimaatverandering tot een gemiddelde zeespiegelstijging en tot een intensievere en een meer extreme overstroming van rivieren, met een steeds hoger wordende gemiddelde waterhoogte tot gevolg. Anderzijds zijn de delta regio's aan urbanisatie onderhevig, hetgeen de kwetsbaarheid van de delta's vergroot.

Hoge water niveau's in delta's zijn het gevolg van een combinatie van een aantal interactieve natuurlijke factoren (hoge astronomische getijden, stormvloed, rivier overstromingen, hoge intensieve neerslag, of combinatie van meer dan één variabele) en van menselijke interventies (overstroming controlemaatregelen ter vermindering van overstroming bronnen).

In dit proefschrift wordt het totale effect van deze natuurlijke factoren, zoals stormvloed, overstromingen van rivieren, etc., evenals de werking van kunstmatige, door de mens gecreëerde structuren, op de frequentie van het hoog- waterniveau in de lage Rijndelta geschat. Een volledig probabilistische aanpak is ontwikkeld om de frequentie van het hoog-waterniveau in de lage Rijndelta in te schatten.

De eerste toepassing van een gezamenlijke probabilistische benadering in de lage Rijndelta dateert uit 1969 (Van der Made, 1969). Deze gezamenlijke probabilistische aanpak overwoog slechts de piekwaarden van de zeespiegel en de Rijn stroom, ervan uitgaande dat andere, bijbehorende variabelen (zoals duur van de storm golf) vooraf bepaald werden als constante waarden. Echter, in deze tijd spelen deze bijbehorende variabelen een belangrijke rol bij de bepaling van het waterniveau in de delta. Zo moeten bijvoorbeeld de Maeslant stormvloedkering en de Haringvlietdam sluizen worden gesloten wanneer zich een stormvloed voordoet. De duur van een stormvloed kan van invloed zijn op de duur van de sluiting van de lage Rijndelta en hierdoor het waterniveau in de delta beïnvloeden. In dit proefschrift zullen meerdere variabelen worden besproken in de probabilistische analyse van de hydrodynamische randvoorwaarden.

In de geheel probabilistische benadering, worden de gezamenlijke probabilistische distributies van extreme hydrodynamische randvoorwaarden afgeleid van de waargenomen overstromingen en gebruikt om opnieuw een groot aantal scenario's van stormvloed in de Rijn alsmede Maas

overstromingen te testen. Deze scenario's met stochastische en hydrodynamische randvoorwaarden creëren een deterministisch model wat op de locaties van belang tot hoge waterstanden en hoge frequenties leidt .

Deze aanpak maakt het mogelijk de frequentie van een hoog water niveau in een veranderende omgeving met gecombineerde effecten van klimaatverandering en menselijk ingrijpen te beoordelen. In de lage Rijndelta, is het effect van klimaatverandering op de frequentie van een hoog water niveau ook voor het jaar 2050 gekwantificeerd, om de besluitvorming met betrekking tot de aanpassing van het operationele water managementsysteem en overstroming afweer systeem nader te bepalen..

Om de Rijn delta tegen overstroming te beschermen, is het gebruik van het huidige operationele water managementsysteem een optimale maatregel voor vermindering van hoog water niveau. Dit systeem verwijst naar de al bestaande structuren en operationele controles, zoals sluizen, stormvloedkeringen en pompen, hetzij aan de monding van de delta of langs de oevers van rivieren en kanalen. Dit systeem wordt toegepast om de waterstanden en stroming in de delta onder controle te houden, met als doel (1) voorkomen van te hoge waterstanden (als gevolg van hoge rivierafvoer, stormvloed, of de combinatie van beide), (2) het voorkomen van lage waterstanden (mbt problemen in verband met drinkwater voorziening en navigatie) (van Overloop, 2009). Het Nederlandse beleid was in eerste instantie gericht op de preventie van overstromingen door middel van versterking en verhoging van de dijken, en hierdoor werd weinig aandacht geschonken aan de potentiële vermindering van de frequentie van hoog water niveau ten gevolge van ontwikkelingen van het operationele water managementsysteem. In dit proefschrift, zal het effect van het huidige en toekomstige operationele water managementsysteem op de frequentie van een hoog-water niveau worden besproken.

De bouw van nieuwe structuren zoals stormvloedkeringen en sluizen ter verbetering van de operationele water managementsysteem en hun effect voor betere resultaten in relatie tot vermindering van hoog water niveau frequentie wordt in dit proefschrift gepresenteerd.

De traditionele benadering, is slechts in een zeer beperkt aantal scenario 's (Mantz en Wakeling, 1979; Samuels en Burt, 2002) toegepast op de hoog-water frequentie schatting met een gedetailleerd model. De computationele last voor het gebruik van gedetailleerde modellen, beperkt sterk het aantal stochastische scenario's. Een groot aantal stochastische scenario's zijn echter niet alleen nodig voor de vermindering van de statistische onzekerheid, maar ook om het huidige operationele water managementsysteem te controleren op verschillende extreme hydrodynamische randvoorwaarden. Het gedetailleerde model vereist kostbare computationele middelen. Om deze reden is een vereenvoudigd model afgeleid van een gedetailleerd model noodzakelijk.

De bijzondere bijdrage van dit proefschrift is de introductie en het overzicht van een geheel probabilistische aanpak voor stochastische simulatie van de hydrodynamische randvoorwaarden van de Rijndelta. In deze benadering wordt met meer variabelen rekening gehouden, en stuurt een deterministische model om de hoog-water niveau frequenties op basis van de Monte Carlo methode te bepalen. Het effect van klimaatverandering en de ontwikkelingen op het vlak van operationeel water management worden beoordeeld.

Een geheel probabilistische aanpak is ontwikkeld voor de hoog-water niveau frequentie schattingen. De benadering kan ook worden uitgebreid voor de beoordeling van de kans op overstromingen en de overstromingsrisico's ter ondersteuning van de overstromingsrisicobeheer in de Rijndelta. Deze benadering kan worden toegepast op andere Delta's over de hele wereld.

Table of Contents

Summary	v
Samenvatting	vii
Chapter 1. Introduction	1
1.1. Background	1
1.2 The Lower Rhine Delta	5
1.2.1 Climate Change	6
1.2.2 The operational water and flood management system	7
1.2.3 The flood safety and the proposal adaptation.....	9
1.3 Problem outline	11
1.3.1 Problem statement	11
1.3.2 Research question.....	12
1.3.3 Approach	12
1.3.4 Contribution	13
1.4 Overview of the thesis.....	14
Chapter 2. Probabilistic analysis of the hydrodynamic boundary conditions	16
2.1 Introduction	16
2.2 The joint probability analysis.....	17
2.2.1 Data analysis.....	17
2.2.2 Division of three categories.....	20
2.2.3 The joint probability distribution of storm surges & normal Rhine flows. 21	
2.2.4 The joint probability distribution of high Rhine flows & normal sea water levels.....	32
2.2.5 The joint probability distribution of storm surges & high Rhine flows	35
2.3 Monte Carlo Simulation of stochastic scenarios	35
2.4 The effect of Climate change	37
2.5 Discussions.....	37
2.5.1 Interaction between astronomical tide and wind induced storm surge	38
2.5.2 Statistical uncertainty in parameters of distributions	38
2.5.3 Incorporating information of rare floods in previous centuries	39
2.5.4 Dependence between North Sea storm surge and high Rhine river discharge	39
2.6 Conclusions	40
Chapter 3. High water level frequency assessment with a conceptual model	41
3.1 Introduction	41
3.2 The conceptual model: Equal Level Curves.....	42

3.2.1 Equal Level Curves with the open delta.....	44
3.2.2 Equal Level Curves with the closable delta	46
3.3 Results	50
3.3.1 High water level frequency in the open Rhine delta	51
3.3.2 High water level frequency in the closable Rhine delta.....	53
3.4 Discussion	55
3.5 Conclusions and recommendations	56
Chapter 4 High water level frequency assessment with a simplified 1-D hydrodynamic model.....	58
4.1 Introduction	58
4.2 The simplified 1-D hydrodynamic model	58
4.2.1 Introduction of the simplified 1-D model.....	59
4.2.2 Assumptions in the simplified 1-D model.....	65
4.2.2.1. Rhine river discharge distribution at the bifurcation points	65
4.2.2.2 Bathymetry and roughness	66
4.3 The present operational water management system.....	66
4.3.1 Man-made structures	67
4.3.2 The present operational control rule.....	69
4.4 Results	72
4.4.1 Exceedance probabilities of the present design water levels	73
4.4.2 High water level frequency curves in Rotterdam and Dordrecht.....	74
4.4.3 Comparison of high water level frequency curves between the conceptual model and the simplified 1-D model.....	75
4.5 Conclusions and recommendations	76
Chapter 5. An alternative stochastic storm surge model.....	78
5.1 Introduction	78
5.2 Methodology	79
5.2.1 Detect storm surge events.....	81
5.2.2 Parameterization.....	83
5.2.3 Monte Carlo Simulation	87
5.2.4 High water level frequency assessment with the alternative stochastic storm surge model	89
5.4 Results	91
5.5 Discussion	94
5.6 Conclusions	94
Chapter 6. The effect of four new floodgates on the high water level frequency reduction.....	95
6.1 Introduction	95

6.2 The adaptation of the operational water management system	96
6.3 Results	98
6.4 Conclusions and recommendations	102
Chapter 7. Effect of statistical uncertainty in the hydraulic boundary conditions on the high water level frequency	104
7.1 Introduction	104
7.2 Methodology	106
7.2.1 Statistical uncertainty in the marginal distributions	106
7.2.2 Uncertainty-incorporation marginal distributions	107
7.2.3 Impact on the high water level frequency	108
7.3 Results	108
7.3.1 Statistical uncertainty in the marginal distributions	108
7.3.2 Uncertainty-incorporation marginal distributions	111
7.3.3 Impact on the high water level frequency	113
7.4 Conclusions and Recommendations.....	115
Chapter 8. Conclusions and recommendations	116
8.1 Summary of conclusions	116
8.1.1 High water level frequency assessment in the Lower Rhine Delta.....	116
8.1.2 Statistical uncertainty of the hydraulic boundary conditions	117
8.1.3 The proposed adaptation of the operational water management system..	118
8.2 Recommendations	118
References:	120
Index of notation and abbreviations	130
Acknowledgements	131
Curriculum Vitae.....	133
Publications	133

Chapter 1. Introduction

1.1. Background

Deltas or estuaries are landforms that are formed at mouths of rivers where rivers flow into oceans or seas. Deltas are coastal features developed from the accumulation of sediment near the mouths of rivers (Syvitski and Saito, 2007). A delta's size ranges from a few square kilometers to thousands of square kilometers. Small rivers are associated with small deltas; large rivers are associated with large deltas.

Over 500 million people live in coastal areas and most of them live in deltas where rivers reach the ocean (Kuenzer and Renaud, 2012). Flat topography, fertile soils for agriculture, available fresh water resources and good transportation in terms of navigation etc, there are numerous advantages for settlement of humanity in deltas. Many mega cities are located in deltas: Tokyo, New York, London, Greater Cairo, Jakarta, Hong Kong and Rotterdam etc. Besides mega cities, many deltas are also fairly populated, including the Mississippi delta in the United States, the Po delta in Italy, the Elbe delta in Germany, the Mekong delta in Vietnam, to name only a few.

Most deltas of the world, where urbanized cities are located, are vulnerable to flooding, and the consequences in terms of human losses and economic damages are serious. Generally many low-lying delta cities are at risk of flooding from (1) intense precipitation, (2) storm surges, (3) upstream fluvial flooding. Moreover, flood risks of deltaic areas increase because of population growth, economic development, land subsidence and climatic changes such as sea-level rise (Kuenzer and Renaud, 2012; Chan et al., 2013).

Floods and consequence damages have triggered developments of flood defense systems to protect deltas all over the world. For example, in the Mekong River Delta of Vietnam the big flooding induced by the typhoon Linda destroyed more than 300,000 houses and huge loss in economy in 1997, and another three consecutive flooding events in 2000, 2001 and 2002 killed nearly 1,000 people, many of whom were children (Nguyen et al., 2007; Weichselgartner, 2005). After suffering high frequency of floods, the flood defense system including dikes and sluices were strengthened in Mekong Delta. In the mega city of New York, recent storm surge Sandy indicated the vulnerability to storm surges (de Moel et al., 2013) and accelerated the improvement of the flood defense system in New York. A series of storm surge barriers were under discussion as possible way to deal with the increasing risks of storm surges (Rosenzweig et al., 2011; Bowman et al., 2013). In the Rhine Delta of the Netherlands, after the North Sea flood of 1953, the Dutch Delta Works Commission installed the so-called "Delta plan". Since then, a total of

about 3000 kilometres of primary flood protection structures including dikes, dunes, storm surge barriers, dams and floodgates have been constructed to protect the Rhine delta in the Netherlands (Pilarczyk, 2007). Without the flood defence system, many delta areas would be flooded during storm surges at sea or high fluvial discharges in the rivers.

Climate change is exacerbating mean sea level rise and enhancing extreme river floods, consequently increase flood frequency significantly (Nicholls and Cazenave, 2010; Hanson et al., 2011; Bulkeley, 2013). Meanwhile it can be more worse that, because of sediment compaction from the removal of oil, gas and water from the delta's underlying sediments, the sediment trapping in reservoirs upstream and floodplain engineering in combination with rising mean sea level, most of the deltas are now sinking faster than before (Syvitski et al., 2009). Moreover, deltas are rapidly experiencing urbanization, which results in increasing vulnerability of deltas.

One critical challenge is to protect deltas from flooding, and to explore possible climate adaptation measures. Adaptation measures should be based on the flood risk assessment.

Flood risk assessment provides a rational basis for monitoring the performance of flood management activities. A widely used approach to assess the flood risk is based on the Source-Pathway-Receptor-Concept (Oumeraci, 2004). The concept is shown in Figure 1-2.

Based on the above concept, first, flood sources are analyzed. Probabilities of flood sources can be transformed into failure probabilities of the flood defence structures given the conditions of the flood defence structures. Breach models (for dykes or hydraulic structures) and flood propagation models are applied to identify inundation conditions. Finally, potential losses in terms of human beings and economy are quantified in the protected areas. The scope of flood risk assessment has extended from the national level (Hall et al., 2003) to regional level (Gouldby et al., 2008; Dawson et al., 2005).

Therefore, a general expression for flood risk R is given by:

$$R = P \cdot D \tag{1.1}$$

here P is occurrence probability of flooding; D is relevant damage.

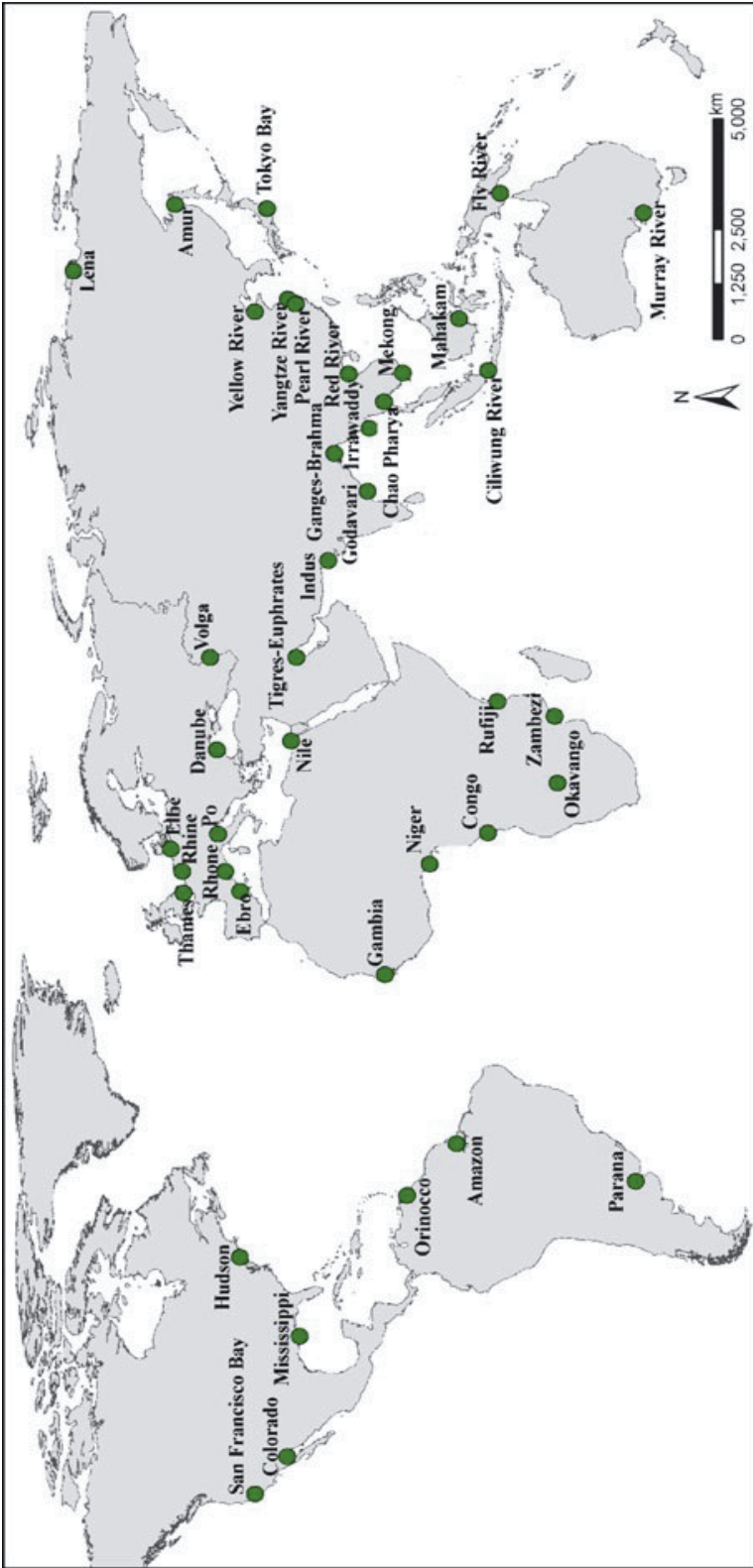


Figure 1-1: The 40 largest river deltas globally
 (This figure does not contain all the river deltas and estuaries that exist in the world; the 40 largest deltas (with respect to delta and river size) were selected).
 (Kuenzer and Renaud, 2012)

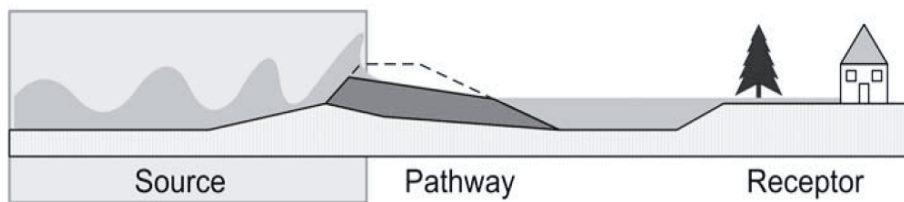


Figure 1-2: Source-Pathway-Receptor Concept for flood risk assessment (Oumeraci, 2004)

This thesis focuses on the investigation of flood sources in delta areas. On the one hand, estimation of flood sources as well as probabilities of flood sources is of importance for the whole flood risk assessment in delta areas. Flood sources can be either from sea or from rivers or from direct rainfall-runoff in delta areas. There are many variables to determine conditions of flood sources, like astronomical tides, wind induced storm surges, river discharges, precipitation. On the other hand, impacts from climate change and human interventions on flood sources can affect the flood risk assessment in delta areas. Importantly, flexible man-made structures, including storm surge barriers, pump stations, floodgates and dams, are gaining popularity to influence natural flood sources in delta areas all over the world. It is expected that these structures can reduce frequency of flood sources in order to reduce the total flood risk.

High water level frequency refers to how often a flood of a high water level will occur in delta areas in a year period. The high water level is the result of interaction between natural flood sources (high astronomical tides, or storm surges, or river flooding, or high intensive precipitation, or combination of more than two variables) and human interventions (flood control measures to reduce flood sources).

As homogeneous observations in delta areas were always interrupted and strongly influenced by man-made structures in the past years, the non-homogeneous extreme records derived cannot be used for estimation of flood frequencies in delta areas. As a given high water level at a delta may result from a number of combinations of sea level and upstream fluvial flow and from how the operational water management system reacts to the situation at hand, the occurrence of all these combinations together determines the frequency of the given water level.

Then a traditional way to estimate flood frequencies is the joint probability approach, using a 1-D hydrodynamic model (Mantz and Wakeling, 1979; Acreman, 1994; Gorji-Bandpy, 2001; Samuels and Burt, 2002; Adib et al., 2010; Lian et al., 2013). The joint probability approach considers flood sources derived from hydrodynamic boundary conditions. The relevant variables in

terms of astronomical tides, wind surges, river flows and precipitation are jointly investigated and result in joint probability distributions.

Developments of the computational technology make a hydrodynamic model available for complex river networks for flood drainage. Several numerical simulation models for delta river networks are available, such as MIKE-11 (MIKE, 2012; Chu et al., 2013), HEC-RAS (Hydrologic Engineering Center, 2002) and SOBEK (Delft Hydraulics, 2005). These models not only represent flood characteristics in complex river systems, but also can reflect the impacts of various flood control infrastructures, such as dikes, storm surge barriers, sluices, pumping stations, etc.

Traditionally, a number of simulated scenarios derived from the joint probability distribution, reflecting the multivariate boundary conditions leading to flood, are forced into the 1-D model to assess the joint probability of high water levels in delta areas.

1.2 The Lower Rhine Delta

The Lower Rhine Delta is located in the Netherlands. The Rhine and Meuse rivers run from the East and the South into the North Sea at Hook of Holland, into the Haringvliet in the West and into the Lake IJsselmeer in the North. The area of the Lower Rhine Delta is a center of high economic activity, maritime transportation and is densely populated. Since a large part of the delta is located below the mean sea level, it is vulnerable to flooding by both river and sea. The water system of the Netherlands is shown in Figure 1-3.

At the upstream boundary, the Rhine flow comes from rainfall-runoff and from snowmelt in the Alps; the Meuse flow is mainly determined by rainfall in France and Belgium. At the downstream boundaries, the extreme still water level (excluding waves) arises from a combination of the astronomical tides and the meteorologically induced storm surge components. In this thesis, the extreme still water level is the so-called ‘storm surge’. Astronomical tides are driven by astronomical forces and are deterministic, while the wind induced storm surges occur stochastically, driven by meteorological forces.

A large part of the Lower Rhine Delta is located below mean sea level. As a result, once high water breaks the flood defense system, the high water will inundate the low land area quickly and result in huge loss in terms of human lives and economy. For example, the 1953’s sea flooding caused more than 1800 casualties, the flooding of over 150,000 hectares of land, demolition of about 9,000 buildings, damage of 38,000 buildings; 67 breaches occurred and hundreds of kilometers of dikes were heavily damaged (Jonkman and Kelman, 2005). The total economic loss was estimated at over 900 million Euros.

During the flooding in 1993 (Rhine) and 1995 (Meuse) 200,000 inhabitants were evacuated in the Upper Rhine Delta (Chbab, 1995b).

Therefore it is of critical importance to estimate the high water level frequency in the Lower Rhine Delta, as it is not only the base of the design and construction of the flood defense system, but also an important component to estimate potential flood risks.



Figure 1-3: Location of important waters (rivers, lakes and estuaries) in the Netherlands

1.2.1 Climate Change

Climate change will affect the high water level frequency in the Lower Rhine Delta. Winter precipitation with earlier snowmelt (Middelkoop and Kwadijk, 2001) is expected to increase in frequency and magnitude and lead to extreme

Rhine flows (Hooijer et al., 2004; Pinter et al., 2006; Linde et al., 2010). Mean sea levels along the Dutch coast with a range of 0.15 to 0.35 m rise until 2050, and with a range of 0.35 to 0.85 m rise until 2100, corresponding to the reference year of 1990, are commonly used extrapolation values (van den Hurk et al., 2006; Second Delta Commission, 2008). In fact, the relative mean sea level rise will be larger when taking mean land subsidence, due to glacial isostasy and subsoil compaction, into consideration. Present research demonstrates that the storm climate has not undergone significant systematic changes during the 20th century at the mouth of the Lower Rhine Delta (WASA-Group, 1998; Alexandersson et al., 1998; 2000) and no discernible long term trend in storm activity has been detected (Barring and von Storch, 2004). The effects of climate change on the characteristics of the wind induced surge along the Dutch coastline were investigated and no evidence was detected for significant changes on storm surge peak height (Sterl et al., 2009). It is assumed that the wind induced surge characteristics (peak height and duration) are not influenced by climate change.

Although there are still inherent uncertainties in the prediction of climate change on the hydraulic boundary conditions within climate change scenario studies, it can be assumed that applying an appropriate climate change scenario can assess future changes in high water level frequency. In this thesis, estimates of mean sea level rise and increases of peak Rhine discharge in the future scenario of 2050 are included to assess future flood frequencies.

The negative consequences of climate change for the low land delta needs quantification. Moreover, the increasing population density and growth of local economies in the Lower Rhine Delta force to pursue sustainable adaptation measures, which can increase flood safety and cope with climate change.

1.2.2 The operational water and flood management system

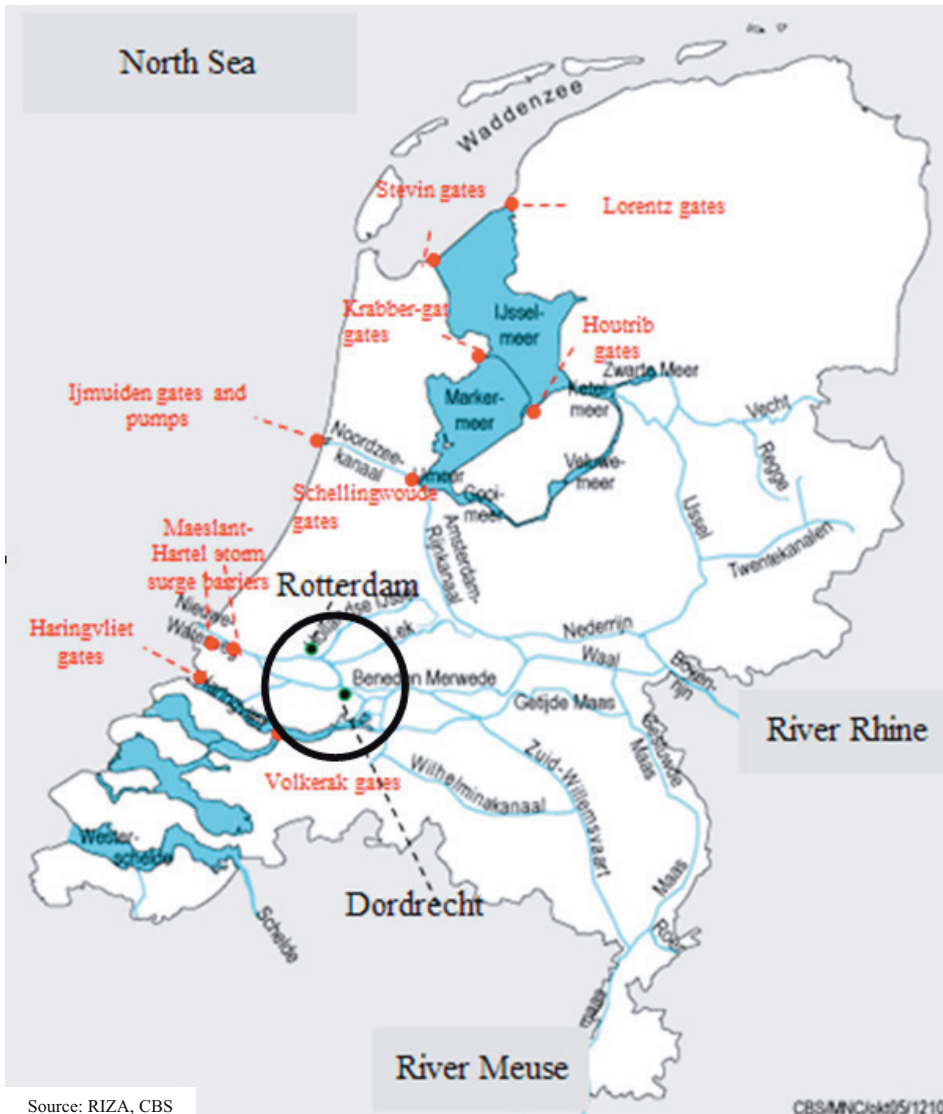
The Dutch are well known for their knowledge and their expertise in the prevention of flooding by building flood defense systems, such as dikes, storm surge barriers and other different types of flood proof structures. To protect the delta from sea flooding, the delta can be closed off from the sea by large dams and controllable gates and pumps. In addition, controllable structures have been constructed along the rivers in order to regulate the upstream flows. These structures work in combination with the dikes, dunes and dams as the primary flood defense system in the delta.

Dutch policy has been primarily aimed at the prevention of flooding by means of strengthening and heightening the dikes. In contrast, less attention has been paid to the potential flood reduction as a result of the operational water management system. The operational water management system in the Lower Rhine Delta refers to the man-made structures, such as large sluices, storm

surge barriers and pumps, either at the mouth of the delta or along the rivers and canals, as well as their operational control.

This system is able to control the water levels and flows within the delta mainly for the objectives of protection against high water levels (due to high river flows or high sea water level or the combination of both), supply of water during dry periods, and navigation (van Overloop, 2009; 2011).

At present, the system is divided into several subsystems that are managed by separate regional divisions of the Dutch national water board. The existing large man-made structures in the water system of the Netherlands are shown in Figure 1-4, where most of our attention is focused on the urbanized area in the Lower Rhine Delta (see the bold black circled area). These structures are under the present operational control of the National Water Board.



Source: RIZA, CBS

CBS/MNC/okt/05/1210

Figure 1-4: Existing structures for the operational water management system

1.2.3 The flood safety and the proposal adaptation

In 2008, the Dutch government asked the Delta Committee for advice to come up with recommendations on how to protect the Dutch coast and the low-lying hinterland against the consequences of climate change (Second Delta Commission, 2008). For the Lower Rhine Delta, two recommendations were offered to enhance the flood safety anticipating climate change.

Recommendation 1

'The present flood protection levels of all dike rings must be raised by a factor of 10. To that end, the new standards must be set as soon as possible (around 2013). In some areas where even more protection is needed, the Delta Dike concept is promising (these dikes are either so high or so wide and massive that the probability that these dikes will suddenly and uncontrollably fail is virtually zero). With regard to specific or local conditions, this will require a tailor-made approach. All measures to increase the flood protection levels must be implemented before 2050.' (Second Delta Commission, 2008: Page 10)

Recommendation 10

'For the Rijnmond an open system that can be closed when needed ('closable-open') offers good prospects for combining flood protection, fresh water supply, urban development, nature development and navigation in this region. The extreme discharges of the Rhine and Meuse will then have to be re-routed via the south-western delta. Further research into the 'closable-open' Rijnmond system should be initiated soon. The Rijnmond will have to be developed in such a way that the area is no longer exposed to the influence of storms and extreme river discharges in an uncontrolled manner.' (Second Delta Commission, 2008: Page 11)

The concept of 'closable-open' for the urbanized area in the Lower Rhine Delta is recommended: the area can be closed off by barriers when faced with extremely high water levels. The high water levels may be derived from the storm surge in the North Sea or the Rhine floods from the upstream or the combination of both. The concept offers safety, while at the same time allowing the development of attractive living environments (city water fronts) and nature reserves.

The application of the concept of 'closable-open' depends on the operational water management system of the Netherlands. It requires the operation of the Maeslant and Hartel Barriers, and the Haringvlietdam with its sluices (all of which will need replacing between 2050 and 2100), possibly supplemented with other closable barriers on the Spui, Oude Maas, Dordtse Kil and Merwede.

Van Overloop (2011) stated that 'the present operational water management system can be characterized as a single objective, local and non-anticipatory. Most of the structures serve a single objective, safety for the area in its neighborhood, and bases its actions on local measurements. Also, predictions for the coming days are not taken into account. This way of managing the system is straightforward and very robust.

1.3 Problem outline

1.3.1 Problem statement

Like many other delta areas, climate change and its negative consequences in terms of mean sea level rise and extreme fluvial flooding, as well as the impact of socio-economic development and population density, continue to contribute to and increase the flood risk in the Lower Rhine Delta.

Although a lot of research has been done on the quantification of the mean sea level rise, the increase of frequency of Rhine and Meuse floods by climate change and the improvement of the operational control of the relevant man-made structures, their continued impact on the high water level frequency has rarely been shown.

The operational water management system has an important role in the high water level frequency reduction and, as a consequence, flood risk reduction. As many flexible controllable structures have been constructed, development of the theory and technology regarding the operational water management system is an important research topic.

More in-depth research on how climate change and the operational water management system affect the high water level frequency in the Lower Rhine Delta is necessary. On the one hand, several factors need to be taken into account: the Rhine flow, the Meuse flow and the sea level are factors affected by climate change and the operational water management system can regulate the water system in the delta in order to influence the high water level frequency. On the other hand, the lack of extreme flood events results in difficulties in the high water level frequency estimation. It is critical to understand these effects on the high water level frequency for a correct management and strategy of flood risk.

To cope with climate change in the future, proposed adaptation measures for the present operational water management system will be presented. New man-made active structures are under discussion. An advanced operational control method, Model Predictive Control, is under development. The new control system is currently tested on several historical flood events and the results indicate the significantly better performance on the flood reduction. However, the proposed adaptation measures have never been evaluated based on the high water level frequency analysis.

The flood risk map of the Netherlands indicates that the urbanized areas Rotterdam and Dordrecht are more hazardous and vulnerable than the others, and so, has higher fatalities (De Bruijn and Klijn, 2009). As a result, Rotterdam

and Dordrecht are taken as the areas of research interest for the high water level frequency estimation in the Lower Rhine Delta.

1.3.2 Research question

Based on the problem statement, the following main research question is derived:

How can an appropriate approach be developed to quantify the high water level frequency and applied to the Lower Rhine Delta under the joint impact of storm surges, fluvial floods, as well as the effect of climate change and the operational water management system?

In order to answer this research question, the following questions must be answered. The chapter numbers in which these questions are answered are shown between brackets.

- How to resample extreme hydrodynamic boundary conditions of the Lower Rhine Delta? And what is the influence of climate change on extreme hydrodynamic boundary conditions? (Ch.2)
- What kind of hydrodynamic models are appropriate to run with the large number of stochastic scenarios of the hydrodynamic boundary conditions? And does the operational water management system affect the high water level frequency significantly? (Ch.3 and Ch.4)
- Does the stochastic storm surge model affect the high water level frequency? And how does the storm surge duration affect the high water level frequency? (Ch.5)
- How does the proposed adaptation measure (four new flood gates to be constructed in the Lower Rhine Delta) affect the high water level frequency in the present and in the future? Will the proposed adaptation measure make the cities of Rotterdam and Dordrecht climate-proof? (Ch.6)
- How does the statistical uncertainty, derived from marginal distributions of the joint probability distribution, affect the high water level frequency? (Ch.7)

1.3.3 Approach

In this thesis a fully probabilistic approach is applied to estimate the high water level frequency in the Lower Rhine Delta. In this approach, the statistical

methods are used to estimate the hydrodynamic boundary conditions with the historical flood events and further to re-sample a large number of pseudo storm surges, Rhine floods as well as Meuse floods. These stochastic scenarios can further drive a deterministic model to result in the high water level frequency at the locations of interest. In the deterministic model, the water movement process can be simulated from the hydrodynamic boundary conditions into the water levels at the transitional locations of interest. The existing hydraulic structures can be operated to influence the water movement process, which has been coupled with the models used.

The approach enables assessment of the high water level frequency in a changing environment with associated effects from climate change and human interventions. Climate change will lead to (1) a mean sea level rise at the mouth of the delta, (2) the increase of the probability of extreme flood events from Rhine and Meuse River; and therefore, (3) increase the high water level frequency in the transitional locations of interest. Sustainable adaptation measures are required to make the lower delta climate flood proof. One important measure is to take advantage of the present operational water management system to reduce the increasing risk of flooding. Further, construction of new adjustable structures and adoption of new advanced operational control methods are to improve the operational water management system and a better performance of flood reduction.

1.3.4 Contribution

The contribution of this thesis is that it introduces and summarizes a holistic approach which will not only estimate the high water level frequency, but will also assess the impact of climate change and human interventions in the Lower Rhine Delta. It also develops statistical methods on re-sampling of the hydrodynamic boundary conditions mainly relating to (1) consideration of the extra variables which have been pre-determined in the previous study, but take important roles on the operational water management system; (2) division of extreme hydrodynamic boundary conditions and indication of the high water level frequency; (3) development of the joint probability distributions of the relevant variables; (4) coupling Monte-Carlo sampling input variables with a deterministic model .

The operational water management system of the Lower Rhine Delta is unique in its scale, its concept as well as its operation control method. To our best knowledge it is the first time that the impact of this operational system on the high water level frequency is evaluated. To cope with climate change in the future, the proposed adaptation measures of this operational system are under discussion (Second Delta Commission, 2008; van Overloop et al., 2010). In this thesis the high water level frequency reductions are assessed.

The results in terms of the high water level frequency in the specific locations and the impact of climate change and adaptation of this operational water management system can be valuable for the decision-making relating to the flood risk management in the Lower Rhine Delta.

1.4 Overview of the thesis

The objectives of this thesis are to (1) quantify the high water level frequency in the Lower Rhine Delta; (2) quantify the impact of climate change and the operational water management system on the high water level frequency; (3) quantify the statistical uncertainty of the distributions in terms of storm surge and Rhine discharge, and their impact on the high water level frequency; (4) investigate into adaptations of the operational water management system and optimization of the control parameters, as well as their effect on the high water level frequency.

The outline of the thesis is presented: Chapter 1 gives the introduction of this thesis, followed by probabilistic analysis of the hydrodynamic boundary conditions in Chapter 2, a conceptual model and the high water level frequency assessment in Chapter 3, and a simplified 1-D model and the high water level frequency assessment in Chapter 4. Chapter 5 presents an alternative stochastic storm surge models and the high water level frequency derived, followed by the adaptation measure of the operational water management system in Chapter 6. The statistical uncertainty, derived from marginal distributions of the joint probability distribution in Chapter 2, is presented in Chapter 7. Chapter 8 summarizes key conclusions and recommendations for this thesis. The framework is shown in Figure 1-5.

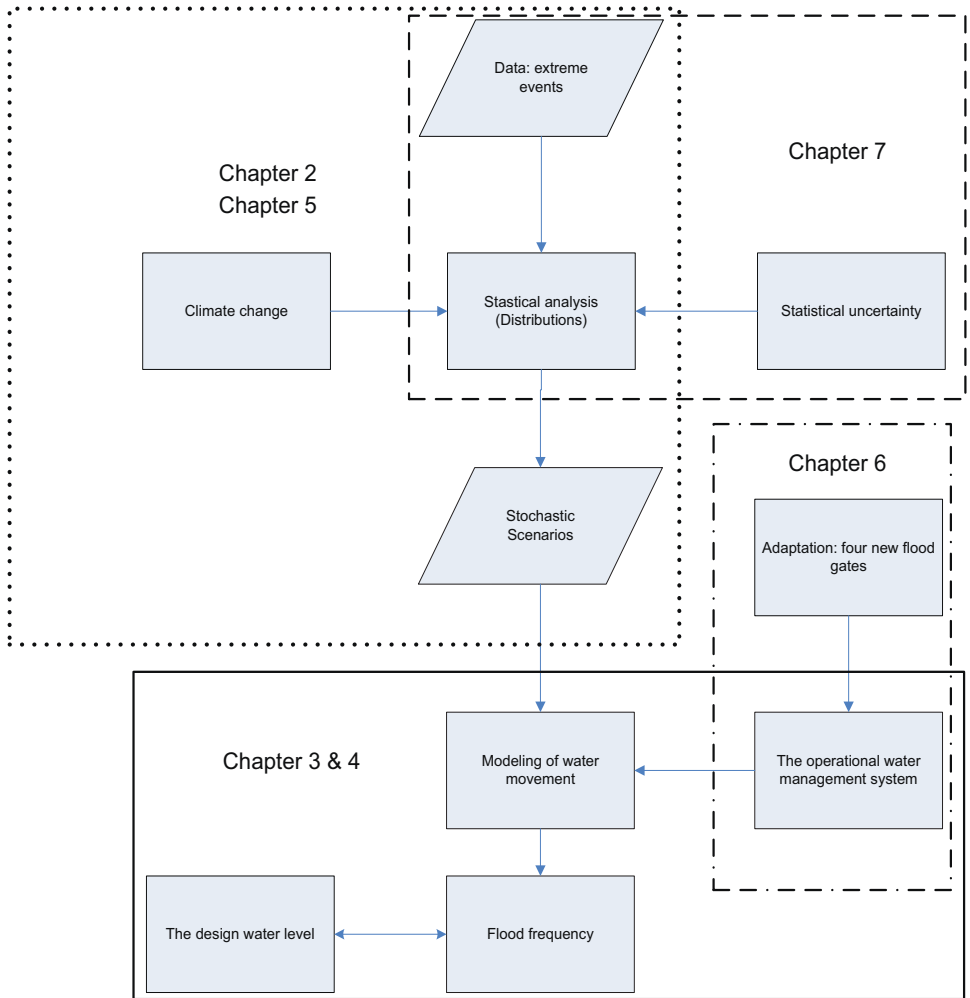


Figure 1-5: Framework of this thesis

Chapter 2. Probabilistic analysis of the hydrodynamic boundary conditions

2.1 Introduction

The Lower Rhine Delta is at risk of flooding induced by infrequent events of storm surges from the North Sea or the fluvial flooding from the Rhine River, or even more infrequent events of the combination of both. As a given high water level at a location in the inland delta may result from a number of combinations of sea level from the North Sea and fluvial flows from Rhine River and Meuse River, the occurrence of all these combinations together determines the frequency of the given water level. The term ‘storm surge’ describes the extreme still water level (excluding waves) that arise from the combination of the astronomical tide component and the meteorologically induced surge component. Therefore, a joint probability analysis of the astronomical tide, the wind induced surge and the flows of the River Rhine and Meuse is necessary for assessing extreme hydrodynamic boundary conditions which result in high water levels at locations of interest in the delta.

The first application of a joint probability approach in the Lower Rhine Delta dates back to 1969. Van der Made (1969) defined three joint probability distributions for three individual categories: high sea levels and normal discharges, normal sea levels and high discharges, high discharges and high sea levels, all of which can result in high water levels at transitional areas. The joint probability distributions were estimated from the observed events of three categories: the peak values of the storm surges as well as the accompanying Rhine flows on the same day, the peak values of the high Rhine flows as well as the accompanying peaks of the sea levels on the same day, the peaks of the storm surges and high Rhine flows on the same day.

The above joint probability approach only considered the peak values of the sea level and the Rhine flow, assuming the other associated variables (such as the storm surge duration) to be pre-determined. However, these associated variables also play an important role in determining the water level in the delta, and become more important with the occurrence of more human interventions. For example, the Maeslant barrier and the Haringvliet Dam with sluices should be closed when a storm surge occurs, and then the water level in the inland delta also relates to the barriers closure duration which is determined mostly by the surge duration (Zhong et al., 2012). Recent research (De Michele et al., 2007; Wahl et al., 2012) have contributed to include more variables in the probabilistic analysis of the hydrodynamic boundary conditions. More associated variables needs to be taken into account.

In this chapter, the hydrodynamic boundary conditions are assessed and a new approach is introduced to estimate the above three joint probability distributions corresponding to three potential flooding causes: storm surges and normal Rhine discharges, normal sea levels and high Rhine discharges, storm surges and high Rhine discharges. For each category, the corresponding joint probability distribution is applied with the Importance Sampling Monte Carlo Simulation to generate a large number of scenarios. These scenarios will be forced into deterministic hydrodynamic models to result in the water levels at locations of interest in the Rhine delta.

Future climate change will affect the hydrodynamic boundary conditions in the Lower Rhine Delta. The hydrodynamic boundary conditions in the year of 2050 are assessed in order to estimate the future high water level frequency.

This chapter is organized as follows: in Section 2.2, the new joint probability approach adopted in this thesis is presented. The following Monte Carlo Simulation of new scenarios of boundary conditions is introduced in Section 2.3. The effect of climate change on the hydraulic boundary conditions is depicted in Section 2.4. Discussions and Conclusions are presented in Section 2.5 and Section 2.6.

2.2 The joint probability analysis

2.2.1 Data analysis

Probabilistic analysis of extreme flood events, such as annual maximum flows (floods) or annual maximum sea levels, has been commonly based on the assumption that the underlying events can be described by independent and identically distributed random variables (Sveinsson et al., 2005). However, the behavior and course of a river or sea condition may change considerably over long time periods due to artificial or natural causes, which therefore result in changes in a series of annual maximum flows and maximum sea levels. Change in a series can occur in numerous ways: e.g. gradually (a trend), abruptly (a step-change), or in a more complex form (Kundzewicz and Robson, 2004).

Three statistical tests are introduced to check whether a change exists in the data to be used. The Mann-Kendall test is commonly applied to assess the significance of trends in hydro-meteorological time series such as stream flow, temperature and precipitation (Mann, 1945). The Spearman's rho (SR) test is another rank-based non-parametric statistical test that can also be used to detect monotonic trends in a time series (Lehmann, 1975; Sneyers, 1991). The Wilcoxon's Rank Sum test is used to test if abrupt points exist in a time series (Wall, 1986).

The available data is shown in Table 2-1. The selected annual maximum series of sea level and Rhine discharge are used to detect whether or not there is a trend or shift in the extreme events. The annual maximum data is shown in Figure 2-1.

Table 2-1: The observation data in the boundary conditions of the Lower Rhine Delta

Station	Data	time	data description
Hook of Holland	observed sea level (m MSL)	1939-2009	1939-1970 water level per 1 hour; 1971-2009 water level per 10 min
Hook of Holland	predicted astronomical tidal level (m MSL)	1939-2009	time unit is the same as the above sea level
Lobith	Rhine discharge (m ³ /s)	1901-2009	daily-average discharge
Borgharen	Meuse discharge (m ³ /s)	1911-2009	daily-average discharge

Note: the source of these data is the Rijkswaterstaat website: <http://www.rijkswaterstaat.nl/waterbase>.

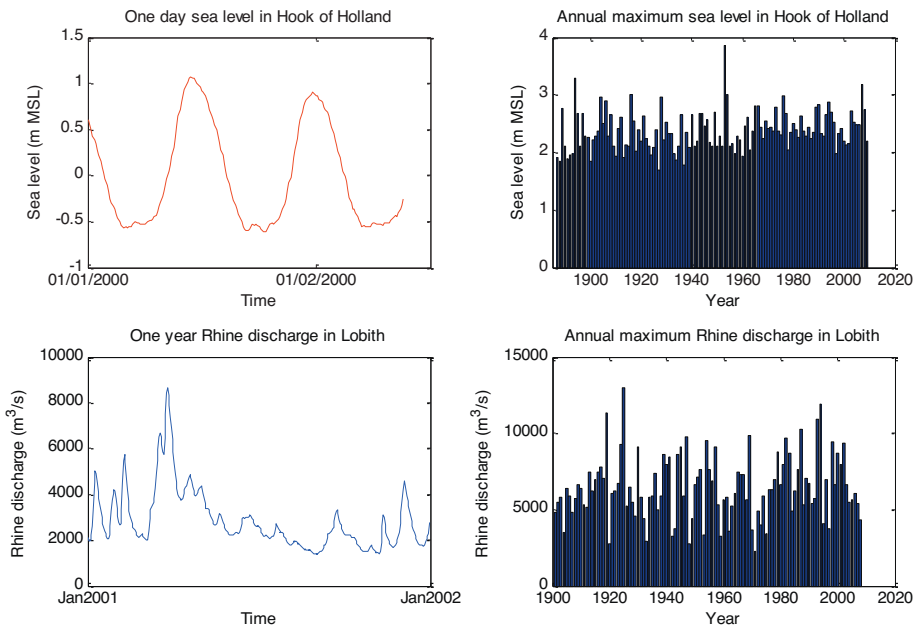


Figure 2-1: The annual maximum data of sea water level at Hook of Holland and Rhine discharge at Lobith

Table 2-2: Tests on the annual maximum sea level in Hook of Holland

Annual maximum sea level in Hook of Holland	Trend test		Jump test
Test (at the significance level 0.05)	Mann Kendall test	Spearman's rank correlation coefficient method	Wilcoxon Rank sum test
Null hypothesis (H_0)	No trend	No trend	No abrupt points
P-value	0.006	0.006	0.132
Reject H_0	Yes	Yes	No

Table 2-3: Tests on Rhine discharge at Lobith

Rhine discharge in Lobith	Trend test		Jump test
Test	Mann Kendall test	Spearman's rank correlation coefficient method	Jump test
Null hypothesis (H_0)	No trend	No trend	No abrupt points
P-value	0.98	0.96	0.16
Reject H_0	No	No	No

In Table 2-2, the results of trend tests show that there is a trend in the annual maximum sea level series at Hook of Holland. In the First Delta Plan a 0.2 m sea level rise during the 20th century was accepted, included and was widely used (Dantzig et al., 1960). After the annual maximum sea level data is corrected by 0.002 m mean sea level rise per year, the results then satisfy the null hypotheses in Table 2-4. On the contrary, annual maximum Rhine discharge data accept the null hypotheses in Table 2-3. Although the Rhine upstream area has undergone a great deal of changes over the past 100 years, these changes are of minimal importance in extreme Rhine discharge. Therefore, these data are assumed to be homogenous.

Table 2-4: Tests on the annual maximum sea level in Hook of Holland corrected for 0.002 m/y sea level rise

Annual maximum sea level in Hook of Holland	Trend test		Jump test
Test	Mann Kendall test	Spearman's rank correlation coefficient method	Jump test
Null hypothesis (H_0)	No trend	No trend	No abrupt points
P-value	0.71	0.69	0.21
Reject H_0	No	No	No

In conclusion, no significant trends or shifts have been detected with these three tests in the annual maximum series of sea level and Rhine discharge except that a least squares linear regression suggests a gradual increase of 0.20 m mean sea level rise per century. The result is in line with the previous research (Dantzig et al., 1960; van Gelder, 1996). The sea level data used in the following analysis has been corrected for this trend.

2.2.2 Division of three categories

The division into three categories is based on thresholds of the peak surge residual and the peak of Rhine flow occurring at the same day: 1.00 m in Hook of Holland and 6000 m³/s at Lobith. This threshold value for the peak surge residual is chosen for two reasons: first of all, this value is related to the operation of the Maeslant Barrier. The peak surge residual of 1.0 m coincides with the high astronomical tide level and high Rhine flow may make the Rotterdam water level exceed the critical value of 3.0 m MSL (the decision level of the closure of the barrier). Secondly, the threshold of 1.0 m has been applied before for the estimation of the frequency of the wind induced surge peak level (Bijl, 1997).

The threshold of 6000 m³/s for Rhine discharge is determined by three reasons: first of all, this value is related to the operation of the Maeslant Barrier (Bol, 2005). Secondly, this value is related to the floodplains inundated along the lower Rhine branch. A discharge exceeding 6000 m³/s with a small amount is assumed the critical value which resulted in the highest floodplains inundated (Kwadijk and Middelkoop, 1994). Thirdly, the threshold value of 6000 m³/s has been applied by Chbab (1995) with the generalized Pareto distribution to estimate the frequencies of high Rhine flows. In this study, the application of this threshold as well as the fitted generalized Pareto distribution function leads to a Rhine design discharge (with a probability of 1/1,250 per year) of 15250 m³/s, which is comparable to commonly used values.

The selected events from 1939 to 2009 in Figure 2-2 are applied to estimate the joint probability distributions of three categories. The largest storm surge flooding of the last century occurred in 1953 misses in the website of Rijkswaterstaat (<http://www.rijkswaterstaat.nl/waterbase>). According to Gerritsen, (2005), the peak level and duration of the 1953 surge residual was 3.00 m and 50 hours, respectively.

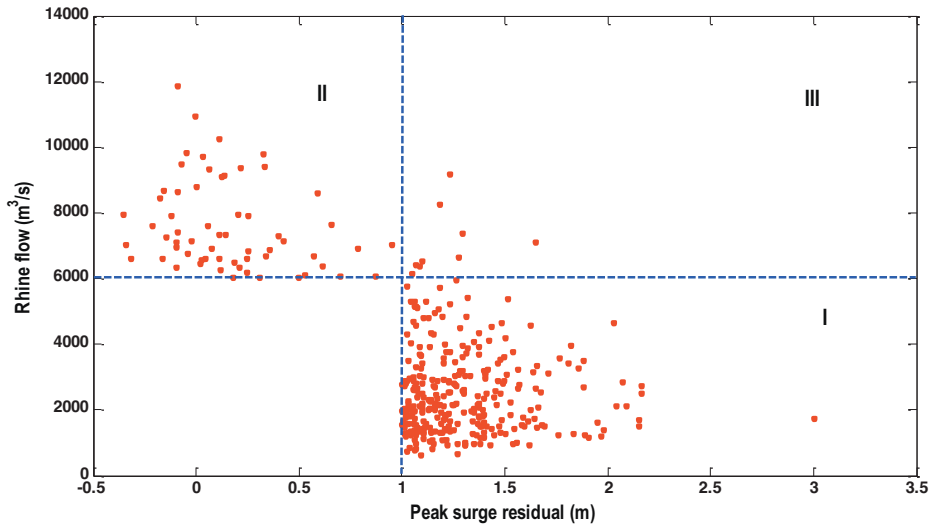


Figure 2-2: Selected events: Category I, storm surge and normal Rhine flow; Category II. high Rhine flow and normal sea water level; Category III. storm surge and high Rhine flow

2.2.3 The joint probability distribution of storm surges & normal Rhine flows

The selected events of storm surges coinciding with normal Rhine flows are shown in Category I of Figure 2-2. The probability distribution of the storm surges in the Eastern Scheldt was estimated by separating the astronomical tide component and the wind induced surge component (Vrijling and Bruinsma, 1980; Praagman and Roos, 1987). This method is introduced and further validated in the gauge station of Hook of Holland at the mouth of the Lower Rhine Delta.

From a statistical point of view, the occurrence of the astronomical tide component is independent to the occurrence of the wind induced surge component at the mouth of the Lower Rhine Delta. However, these two components can interact each other when they propagate into the delta (de Ronde, 1985). Their nonlinear interaction generally increases the surge height at rising astronomical tide and decreases the surge height at high astronomical tide (Bijlsma, 1989). Quantifying the nonlinear effect is beyond the scope of

this study. For the sake of the convenience, it can be assumed that the wind induced surge is independent to the astronomical tide as seen in Figure 2-3.

These surge residual curves are taken into the probability analysis with two parameters: the peak surge residual h_{smax} and the surge duration T_s . The probability distributions of these two parameters are applied to simulate many pseudo surge residual curves with an appropriate shape function. The astronomical tide curves can also be simulated by the same logic. As a result, the simulated surge residual curves and the simulated tide curves can be linearly combined into the simulated sea level curves.

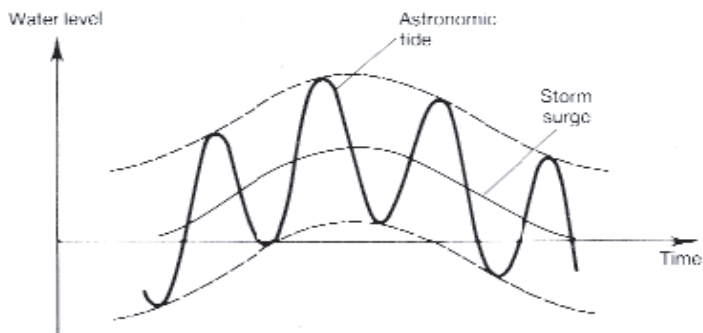


Figure 2-3: Variation with time of the extreme sea water level

In order to estimate the surge curve in Hook of Holland, 300 extreme surge residuals in Category I in Figure 2-2 are analyzed. The observed peak surge residuals and associated durations are plotted in Figure 2-4. Their linear correlation coefficient is 0.0474, and therefore they are assumed linearly independent. For a surge event at Hook of Holland, the peak surge residual and duration are generated and constrained by complex physical factors like the offshore surge, the shallow water depth, the interaction between tide and surge, etc. However, in statistical perspective, the assumption of independence between the peak surge residual and the duration is acceptable.

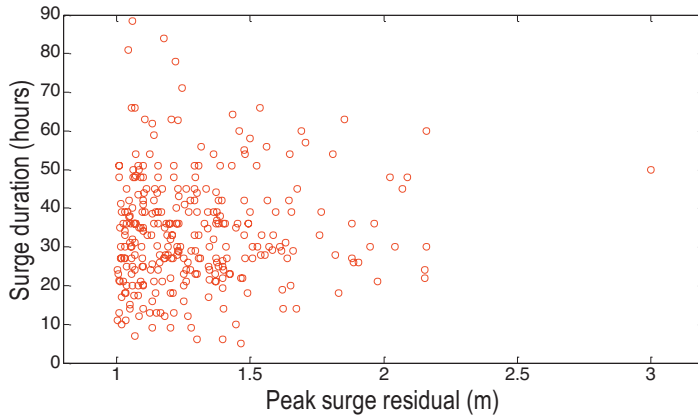


Figure 2-4: The peak surge residuals and associated durations

The design surge residual curve function can be approximated by a squared cosine function. In Figure 2-5 the comparison between the observed surge residual curves and the design curves for six extreme storm surge events agrees this reasonable assumption. In Figure 2-6 a symmetric curve is also shown for the surge residual curve of the 1953 big sea flooding (Gerritsen, 2005).

The design surge residual curve function can be derived from the observed surge residual curves:

$$h_s(t) = h_{s,max} \cdot \cos^2\left(\frac{\pi \cdot t}{T_s}\right) \quad (2.1)$$

where $h_{s,max}$ is the peak value of the surge residual level, and its unit is m; T_s is the duration of the surge, and its unit is hours. Here, the surge peak is assumed to occur when $t = 0$.

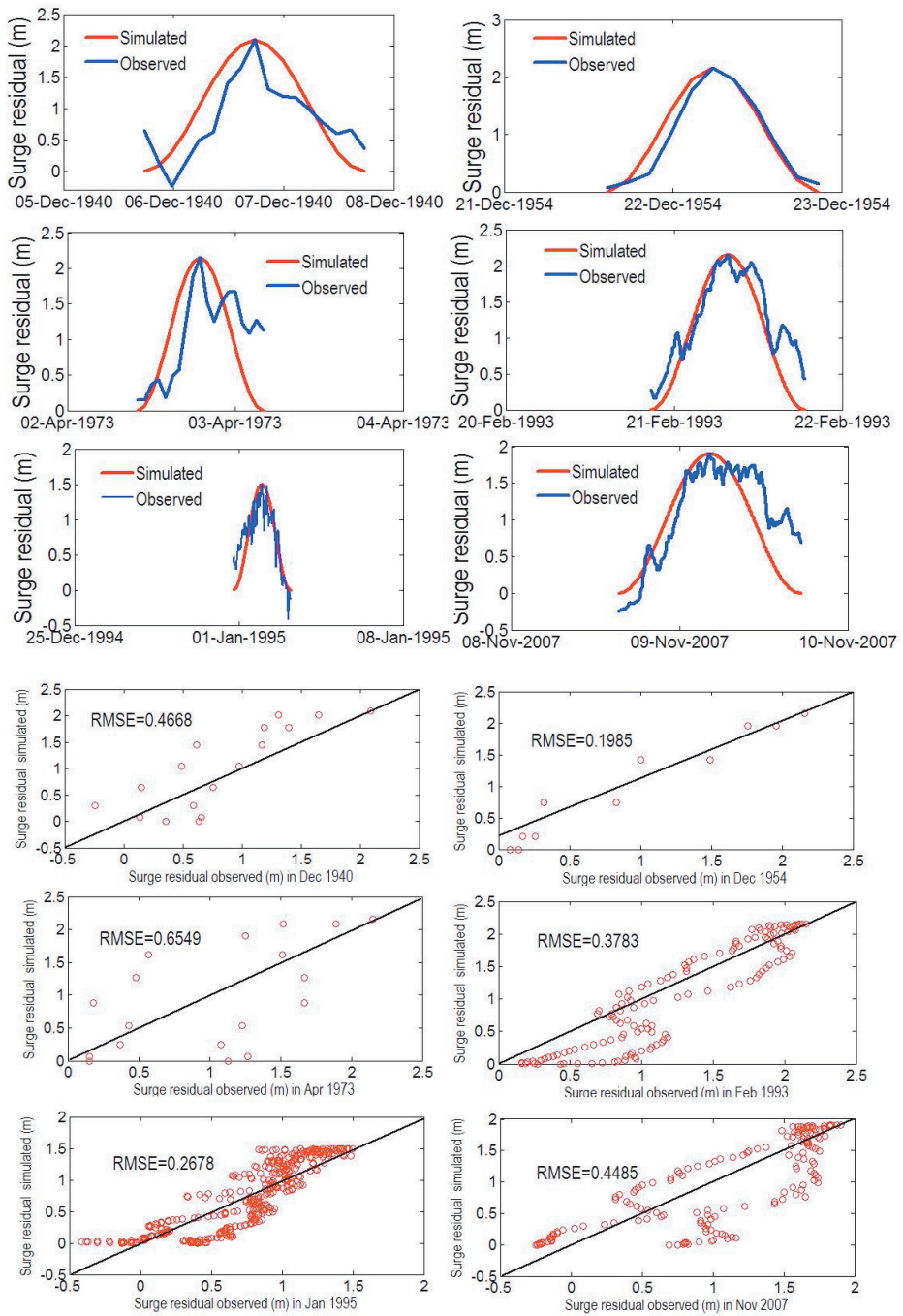


Figure 2-5: The observed surge residual curves and the design surge residual curve function (Upper 6 graphs); the correlation coefficient squared R^2 (Lower 6 graphs)

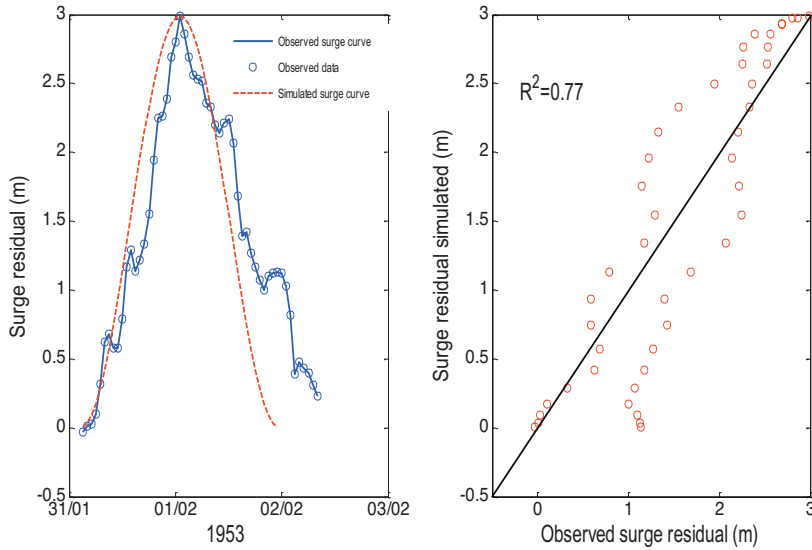


Figure 2-6: (Left) The surge residual curve of the largest flood in 1953 and the design surge residual curve function; (Right) the correlation coefficient squared R^2

The generalized Pareto distribution and the Weibull distribution fit the distributions of peaks (h_{smax}) and durations (T_s) of these selected surge residuals, respectively, as can be seen in Figure 2-7 and 2-8, and the distribution functions show in Eqn. (2.2) and (2.5). In this dissertation, all parameters of distributions are estimated by the maximum likelihood method.

$$f(h_{smax}) = \frac{1}{\sigma} \left(1 + \xi \frac{h_{smax} - u}{\sigma} \right)^{-\frac{1}{\xi} + 1} \quad (2.2)$$

In this equation the shape parameter ξ is -0.0677 ; the scale parameter σ is 0.3140 m; the location parameter u is 1.0 m.

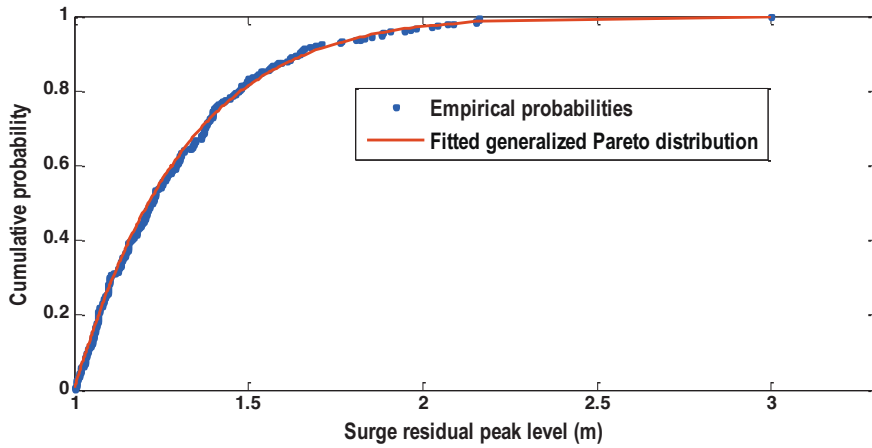


Figure 2-7: Fitting the generalized Pareto distribution to the surge residual peak level

In addition, the Peak over Threshold (POT) method (1.0 m for the peak surge residual in Figure 2-2) is applied to detect the storm surge events and in average 4.38 storm surges per year are chosen. The number of storm surges occurring in one year fits a Poisson distribution and the parameter λ is 4.38. The Poisson distribution is:

$$f(k; \lambda) = p(x = k) = \frac{\lambda^k e^{-\lambda}}{k!} \quad (2.3)$$

where k means the number of storm surges occurring in one year. From the Poisson distribution, the probability that at least one storm surge exceeding 1.0 m (the threshold level) in one year is 0.9875.

The Poisson-GPD process can be transformed to a GEV distribution for annual maxima. The detail information is available from (Smith, 2004). Then the Poisson-GPD model of the peak surge residual h_{smax} is transformed to the GEV model. As a result, for the h_{smax} generated from the transformed GEV model, its probability $p(h_{smax})$ refers to the occurrence probability in one year, see Eqn. (2.4):

$$f(h_{smax}) = \frac{1}{\sigma} \left(1 + \xi \left(\frac{h_{smax} - \mu}{\sigma}\right)\right)^{-\frac{1}{\xi} + 1} e^{-\left[1 + \xi \left(\frac{h_{smax} - \mu}{\sigma}\right)\right]^{\frac{1}{\xi}}} \quad (2.4)$$

In this equation the shape parameter ξ is -0.0677 ; and the scale parameter σ is 0.2841; the location parameter μ is 1.4417 m. h_{smax} should be larger than 1.0 m.

The Weibull distribution fit the durations (T_s) of these selected surge residuals, see Eqn. (2.5)

$$f(T_s) = \frac{k}{\lambda} \left(\frac{T_s}{\lambda}\right)^{k-1} e^{-\left(\frac{T_s}{\lambda}\right)^k} \quad (2.5)$$

In the equation, $T_s > 0$, k is the shape parameter, 2.5237; λ is the scale parameter, 38.0887 hours.

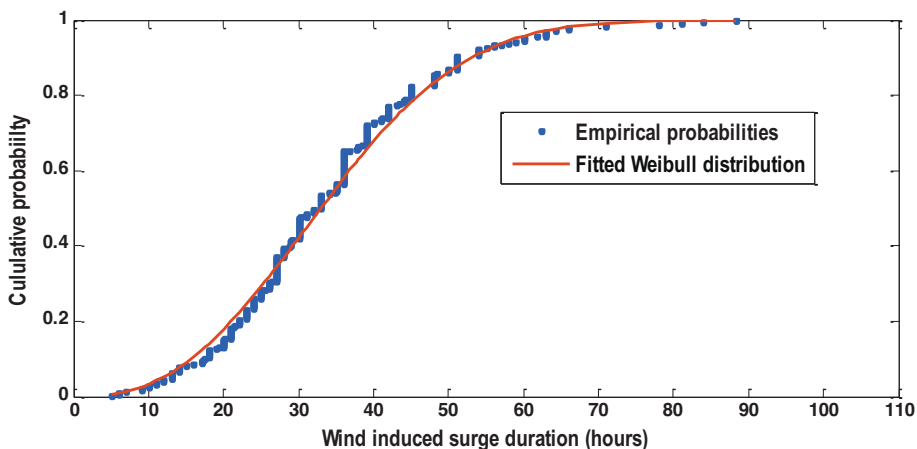


Figure 2-8: Fitting the Weibull distribution to the wind induced surge duration

The semi-diurnal astronomical tide in Hook of Holland, is almost symmetric, and can therefore be approximated by a sinusoidal-curve and modeled as a periodical fluctuation of the water level h_a with a period of 12.4 hours and with amplitude of $h_{HW} - h_{LW}$. Where h_{HW} is the high tide level; h_{LW} is the low tide level; their unit is m MSL; u is the time shift between peaks of tide and surge. Figure 2-9 shows that the simulated tide level from the sinusoidal function represents the tide well.

$$h_a(t) = \frac{h_{HW} - h_{LW}}{2} \cdot \sin\left(\frac{2\pi}{12.4}(t+u)\right) + \frac{h_{HW} + h_{LW}}{2} \quad (2.6)$$

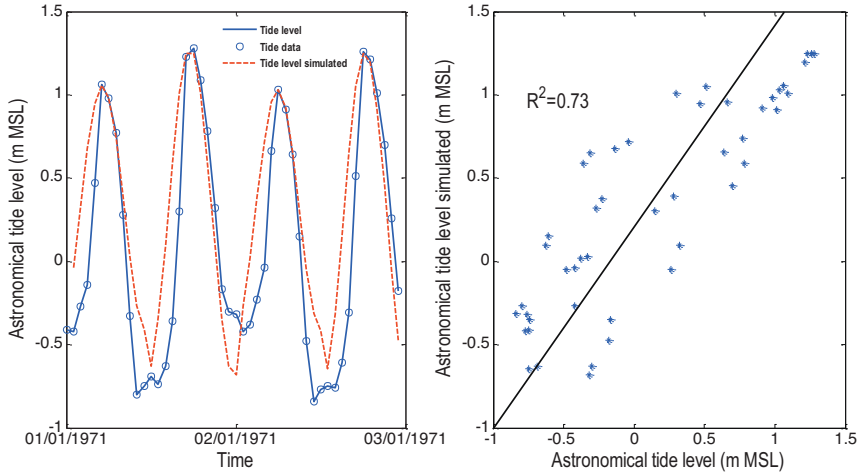


Figure 2-9: The stochastic astronomical tide curve function

As a consequence of the assumed independency of the tide and the surge, the time shift between peaks u fits a uniform probability density function. Time shifts u larger than 12.4 hours are irrelevant, thus considering a symmetrical shape, the probability density function of u becomes:

$$f(u) = 0 \quad |u| > \frac{1}{2} \cdot 12.4 \text{ hours} \quad (2.7)$$

$$f(u) = \frac{1}{12.4} \quad |u| < \frac{1}{2} \cdot 12.4 \text{ hours}$$

In conclusion, the storm surge water level is:

$$h(t) = h_s(t) + h_a(t) + h_0 \quad (2.8)$$

here h_0 is mean sea level.

The characteristics of the high tide level (h_{HW}) at Hook of Holland can be captured in a normal distribution (estimated by one year data of high astronomical tide levels that are derived from the harmonic analysis of water level observations, see Figure 2-11). The influence of the nodal cycle is not considered. Note that the maximum value for h_{HW} is 1.6 m MSL in Hook of Holland, so any values higher than 1.6 m need to be discarded in the following sampling procedure. In Figure 2-11, the low tide level (h_{LW}) is approximately a linear function of h_{HW} .

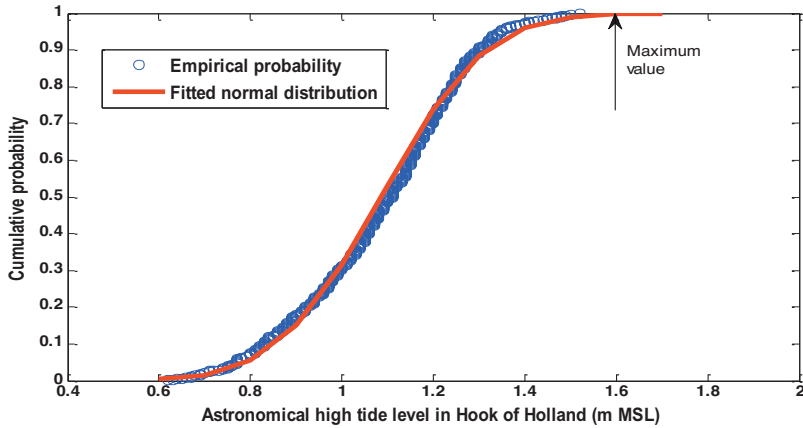


Figure 2-10: Fitting the normal distribution to high tide level

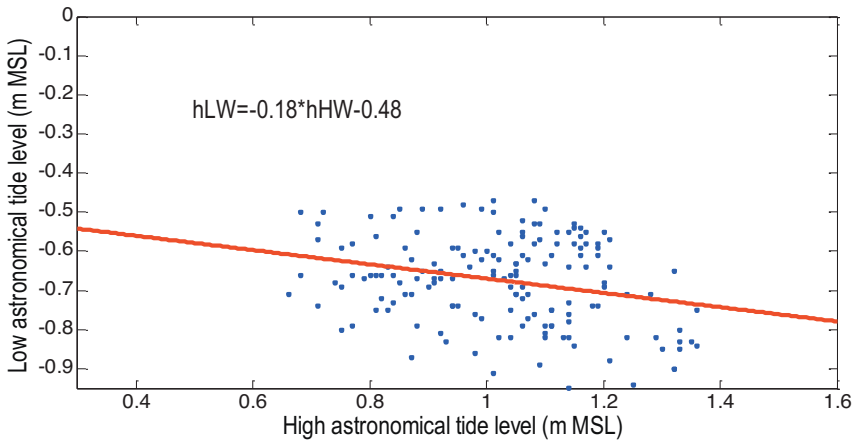


Figure 2-11: Linear relationship between h_{HW} and h_{LW}

The probability distribution of the associated normal upstream discharge can be estimated by the accompanying daily-average Rhine and Meuse flows. The dependence structure between Rhine discharge Q_r and Meuse discharge Q_m can be described by a copula function. The copula function offers the flexible of modeling multivariate distribution through the choice of margins from different families of univariate distributions and the selection of a suitable dependence structure (Sklar, 1959). Some criteria (e.g., the Akaike information criterion (AIC), Bayesian information criterion (BIC), and root mean square error (RMSE)) are widely used to select appropriate copula. A graphical based goodness of fit test suggests a Gaussian Copula function, where the marginal distributions fit the Lognormal distribution for Q_r and the Gamma distribution for Q_m , seen in Eqn. (2.9) and (2.10). Some other goodness of fit tests can be applied, including the Rosenblatt transform (Rosenblatt, 1952; Genest et al., 2009). Although there are two outliers in the left upper part, generally the

simulation Gaussian Copula presents the dependence well between daily-average Rhine and Meuse discharges.

$$f(Q_r) = \frac{1}{\sigma \cdot Q_r \cdot \sqrt{2\pi}} e^{-\frac{(\ln Q_r - \mu)^2}{2\sigma^2}} \quad (2.9)$$

In the equation, Q_r is the daily Rhine flow, μ is the mean value, 7.6808; σ is the stand deviation value, 0.4782.

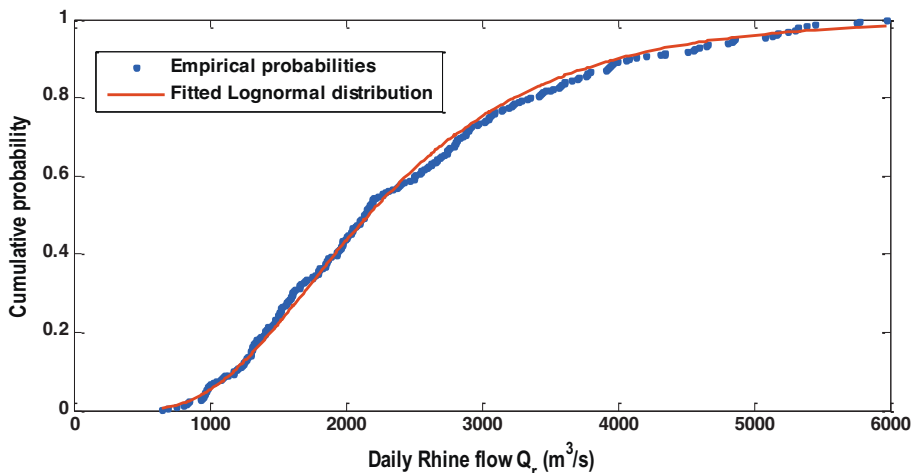


Figure 2-12: Fitting the Lognormal distribution to daily Rhine discharge

$$f(Q_m) = \frac{1}{\Gamma(\kappa)\theta^\kappa} \cdot Q_m^{\kappa-1} \cdot e^{-\frac{Q_m}{\theta}} \quad (2.10)$$

$$\Gamma(\kappa) = (\kappa - 1)!$$

In the equation, Q_m is daily Meuse flow; κ is the shape parameter; θ is the scale parameter; and their values are 1.2924, 329.14 m³/s respectively.

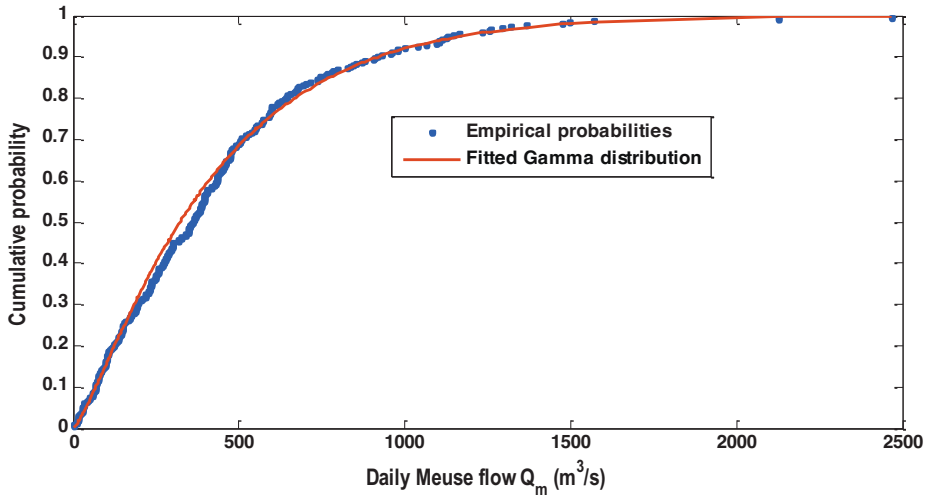


Figure 2-13: Fitting the Gamma distribution to daily Meuse discharge

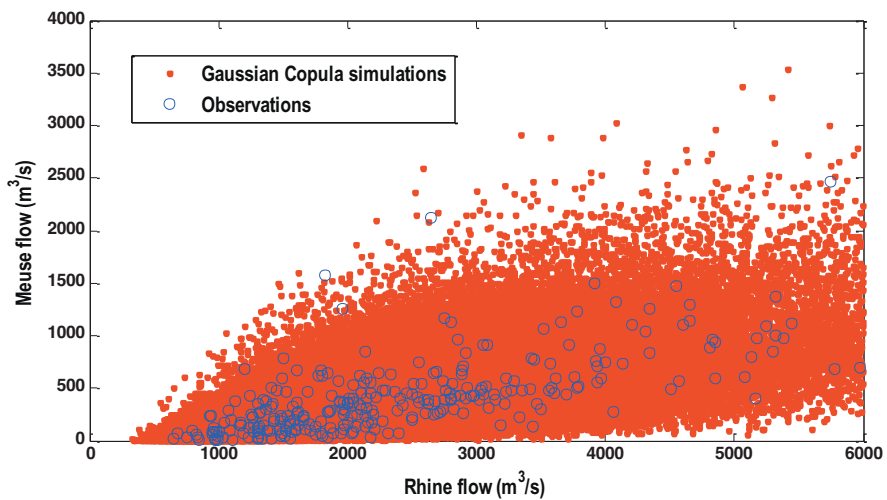


Figure 2-14: Results from a graphical based goodness fit of the Gaussian Copula simulation

The Gaussian Copula dependence structure as well as the marginal distributions is considered to simulate the upstream discharges for Category I where a small percentage of occurrences of Rhine flows exceeding 6000 m³/s are maximized at 6000 m³/s.

The accompanying low Rhine and Meuse flows can be assumed to be constant during the storm surge period, which is not supposed to influence the water levels in the transition areas in model calculation.

Eqn. (2.11) computes the exceedance probability of the transition water level h_R^* in one year for Category I. The method of Peak over Threshold (POT) is applied to detect the wind induced surge events (1.0 m for the peak surge residual in Figure 2-2) and in average 4.38 surges per year are selected. The number of surges occurring in one year fits a Poisson distribution and the parameter λ is 4.38. The Poisson-GPD process can be transformed to the GEV distribution for annual maxima. The probability $P(h_R^*)$ refers to the exceedance probability of a specific h_R^* in one year:

$$\begin{aligned}
 P(h_R \geq h_R^*) &= \iiint \iiint I(h_R^*) f(h_{s,max}) f(T_s) f(h_{HW}) f(u) f(Q_r, Q_m) dh_{s,max} dT_s dh_{HW} du dQ_r dQ_m \\
 I &= 1: h_R(h_{s,max}, T_s, h_{HW}, u, Q_r, Q_m) \geq h_R^* \\
 I &= 0: h_R(h_{s,max}, T_s, h_{HW}, u, Q_r, Q_m) < h_R^*
 \end{aligned} \tag{2.11}$$

where I is an indicator function and h_R is calculated from the specific input parameters using the hydrodynamic model. In a event in Category I, the upstream Rhine flow is independent of the storm surge (Dantzig et al., 1960; Jorigny et al., 2002).

2.2.4 The joint probability distribution of high Rhine flows & normal sea water levels

The events of high Rhine flows coinciding with normal sea water levels are shown in Category II of Figure 2-2. This category focuses on this kind of combinations which result in extreme water level in Rotterdam. It is assumed that the wind induced surge component can be discarded when the peak level of the surge residual is lower than 1.0 m. Therefore, in this kind of combinations, the astronomical tide is the only component to be considered in the sea water level.

The high Rhine flows come from large scale storm depressions which probably also bring about the associated high Meuse flows. The Gumbel copula is applied to describe this dependency, as it exhibits a stronger dependency in the positive tail. The associated Meuse flows are selected at the same day when the Rhine peaks occur. A generalized Pareto distribution and a Lognormal distribution fit the selected Rhine and Meuse flows, respectively seen in Figure 2-15 and 2-16 and the distribution functions are shown in equations below.

$$f(Q_r) = \frac{1}{\sigma} \left(1 + \xi \frac{Q_r - \mu}{\sigma}\right)^{\left(-\frac{1}{\xi}\right)-1} \tag{2.12}$$

In the equation, Q_r is Rhine flow; ξ is the shape parameter; σ is the scale parameter; μ is the location parameter; and the parameters' values are -0.0667, 1629.7 m³/s and 6000 m³/s respectively.

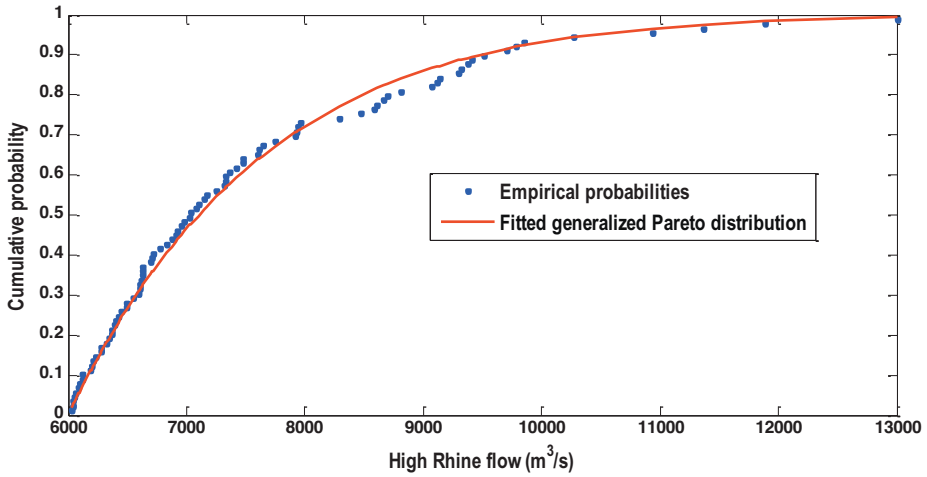


Figure 2-15: Fitting the Generalized Pareto distribution to high Rhine flow

$$f(Q_m) = \frac{1}{\sigma \cdot Q_m \cdot \sqrt{2\pi}} e^{-\frac{(\ln Q_m - \mu)^2}{2\sigma^2}} \quad (2.13)$$

In the equation, Q_m is Meuse flow, μ is the mean value 6.8667; σ is the stand deviation value, 0.3752.

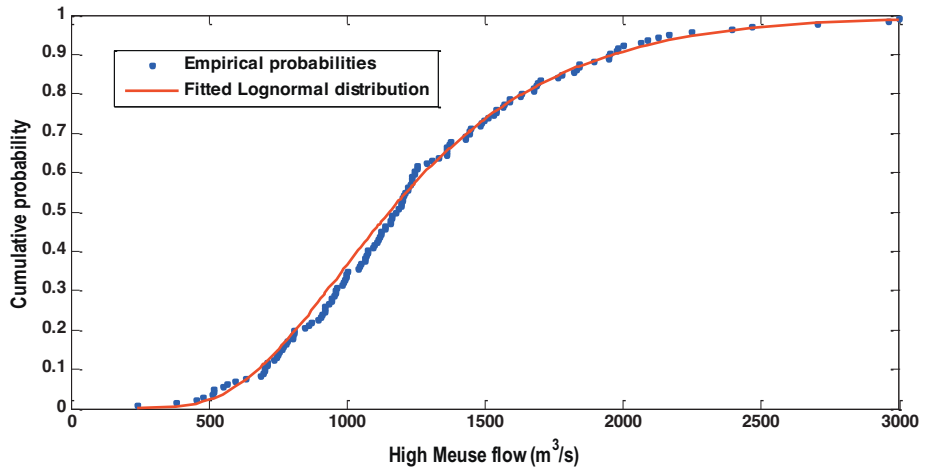


Figure 2-16: Fitting the Lognormal distribution to high Meuse flow

The Gumbel copula function presents here:

$$F_{Q_r, Q_m}(Q_r, Q_m) = C_\alpha(u, v) = \exp\{-[(-\ln u)^\alpha] + (-\ln v)^\alpha\}^{\frac{1}{\alpha}}$$

where $u = F_r(Q_r)$

$$u = F_m(Q_m)$$

$$\alpha = \frac{1}{1-\tau}$$
(2.14)

The relationship between the Gumbel copula parameter α and the Kendall's tau τ is also shown. α is estimated as 1.7158; F_r is the marginal distribution of high Rhine flow; F_m is the marginal distribution of the associated Meuse flow; $F_{Q_r, Q_m}(Q_r, Q_m)$ is the joint cumulative probability.

The Chi-square (χ^2) test is used to determine the goodness of fit between observed data with expected values derived from the Gumbel copula. The calculated value of χ^2 being 27.8 is far below the critical value of 61 for 47 degrees of freedom at the significance level of 0.5%. In addition, the graphical based goodness fit is shown in Figure 2-17.

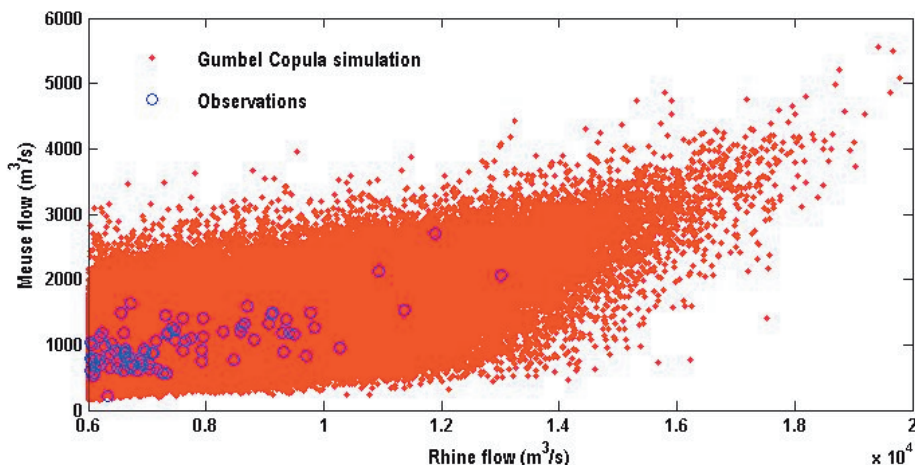


Figure 2-17: Results from a graphical based goodness fit of the Gumbel Copula simulation

Eqn. (2.15) computes the exceedance probability of a certain transition water level h_R^* in one year for Category II.

$$\begin{aligned}
 P(h_R \geq h_R^*) &= \iiint I(h_R^*) f(h_{HW}) f(Q_r, Q_m) dh_{HW} dQ_r dQ_m \\
 I &= 1: h_R(h_{HW}, Q_r, Q_m) \geq h_R^* \\
 I &= 0: h_R(h_{HW}, Q_r, Q_m) < h_R^*
 \end{aligned} \tag{2.15}$$

High Rhine and Meuse flow curves can be generated by the design hydrographs (Parmet et al., 2002a; Parmet et al., 2002b) multiplied by the ratio between the generated values and the design peak values.

2.2.5 The joint probability distribution of storm surges & high Rhine flows

The very limited number of observations of the joint high surge residual and high Rhine flow events in Category III is not appropriate for estimating the joint probability distribution. A rather simple method is introduced. As seen in Figure 2-2, only 9 events have occurred in Category III since 1939 and therefore it can be assumed that the occurrence probability of this combination event is 9/70 per year. The marginal distributions of the peak surge residual, the surge duration, the astronomical tide and the high Rhine flow can be assumed to be the same as Category I and II respectively. The high peak surge residual is assumed to be independent to high Rhine flow (Dantzic et al., 1960; Jorigny et al., 2002).

Eqn. (2.16) computes the exceedance probability of a certain transition water level h_R^* in one year for Category III.

$$\begin{aligned}
 P(h_R \geq h_R^*) &= \frac{9}{70} \cdot \iiint \iiint I(h_R^*) f(h_{s,max}) f(h_{HW}) f(T_s) f(u) f(Q_r, Q_m) dh_{s,max} dh_{HW} dT_s du dQ_r dQ_m \\
 I &= 1: h_R(h_{s,max}, h_{HW}, T_s, u, Q_r, Q_m) \geq h_R^* \\
 I &= 0: h_R(h_{s,max}, h_{HW}, T_s, u, Q_r, Q_m) < h_R^*
 \end{aligned} \tag{2.16}$$

2.3 Monte Carlo Simulation of stochastic scenarios

A large number of boundary stochastic scenarios need to be generated based on the joint probability distribution for each category. Then the 1-D model can run with these scenarios and the outputs are the same number of peak water levels at locations of interest in the Lower Rhine Delta. The resulting series of peak

water levels as well as the accompanying occurrence probabilities can be transformed into the high water level frequency curves in the delta.

Importance Sampling is applied to reduce the number of samples in the Monte Carlo simulation but still get sufficiently accurate estimations (Glynn and Iglehart, 1989; Roscoe and Diermanse, 2011). In the Monte Carlo simulations, the exceedance probability P_f of a specific h_R^* is simply taken to be n_f/n , where n_f is the number of samples which lead to $h_R \geq h_R^*$, and n is the total number of generated samples. In the Importance Sampling method, the number of samples which lead to $h_R \geq h_R^*$ increases largely because boundary inputs are not generated from their original probability distributions, but from alternative distributions which focus on exceedance of the critical water level at Rotterdam h_R^* . The normal distributions are used for the most important input variables $h_{s,max}$, T_s , Q_r (high Rhine flow) and Q_m (high Meuse flow), centered around the values that lead to h_R^* . Note that for different h_R^* , the corresponding Normal distributions are different in order to locate around the area leading to $h_R \geq h_R^*$. The changes in distributions need to be compensated for.

$$P_f(h_R^*) = \frac{1}{n} \sum_{i=1}^n I(*) \frac{f}{g} \quad (2.17)$$

$$I = 1: h_R^* \leq h_R$$

$$I = 0: h_R^* > h_R$$

where $P_f(h_R^*)$ is the exceedance probability of a specific Rotterdam water level h_R^* ; n is the total number of samples; I is an indication function inside which the input parameters are generated from the distributions g , f stands for the original probability density distributions of related variables and g is the corresponding normal density distribution.

In the Importance Sampling method only input parameters $h_{s,max}$, T_s , Q_r (high Rhine flow) and Q_m (high Meuse flow) applied with the new Normal distributions instead of the original distributions. The other input parameters were sampled from their original probability distributions. Generally, there are no upper bounds for these Normal distributions.

To get the reliable simulation results, a large number of events were generated with the Importance Sampling method and the model outputs were the same number of peak water levels at locations of interest in the delta.

2.4 The effect of Climate change

Future climate change will affect the flood frequencies in the Lower Rhine Delta. For the Rhine flow, climate change is expected to increase winter precipitation with earlier snowmelt (Middelkoop and Kwadijk, 2001), which will lead to an increase in the frequency and magnitude of extreme Rhine flows (Hooijer et al., 2004; Pinter et al., 2006; Linde et al., 2010).

For mean sea levels along the Dutch coast, a range of 0.15 to 0.35 m rise until 2050 and a range of 0.35 to 0.85 m rise until 2100 corresponding to the reference year of 1990 are commonly used extrapolation values (van den Hurk et al., 2006; Second Delta Commission, 2008). In fact, the relative mean sea level rise will be larger when taking mean land subsidence due to glacial isostasy and subsoil compaction into consideration. The effects of climate change on the characteristics of the wind induced surge along the Dutch coastline has been investigated and no evidence is found for significant changes (Sterl *et al.*, 2009), and hence it can be assumed that the characteristics are not influenced by climate change.

Although there are still inherent uncertainties in the prediction of climate change on the hydraulic boundary conditions within climate change scenario studies, it can be assumed that the future changes in high water level frequencies can be assessed by applying an appropriate climate change scenario.

In this thesis, estimates of mean sea level rise and increases of peak Rhine discharge in the future scenario of 2050 are included to assess the future high water level frequencies. The mean sea level rise is assumed to be 0.35 m (van den Hurk et al., 2006) and the peak Rhine discharge increases by 10% compared to the year of 2000 (Jacobs et al., 2000).

In a second set of the Monte Carlo simulations, the input boundary conditions valid for scenario 2050 are generated by simply re-scaling the present boundary variables. The results can assist in adapting the operational water management system to better control negative effects of climate change in the Lower Rhine Delta.

2.5 Discussions

A large number of scenarios of extreme hydraulic boundary conditions are generated based on the joint probability distributions estimated from available historical records. In the process of estimation of the joint probability distributions, some assumptions may overestimate or underestimate the results. Further research on improving these assumptions is necessary, for example incorporating the non-accurate historical flood information in the previous centuries into distribution estimation, uncertainty in dependence of the North

Sea storm surge and extreme Rhine river discharge, statistical uncertainty in parameters of distributions, etc.

2.5.1 Interaction between astronomical tide and wind induced storm surge

For the sake of convenience, stochastically sampling of the storm surge scenarios assumed that the wind induced surge is independent of the astronomical tides. The wind induced surge component and the astronomical tide component are statistically independent and then were linearly superimposed. The non-linear interaction between two components was ignored, which might result in large uncertainties on the time evolution of the storm surge.

Although quantifying the nonlinear effect is beyond the scope of this study, a stochastic storm surge model, which can take the sea water level as a whole parameter and avoids the non-linear interaction between two components, is preferred to avoid the nonlinear effect.

The alternative stochastic storm surge model used was first introduced by (Wahl et al., 2010; 2011) to simulate a large number of storm surge scenarios at the mouth of the Elbe River and for a tide gauge in the Northern German Bight. The advantages of this model can be summarized: first of all, this model can generate a large number of storm surge scenarios efficiently compared to the numerical hydrodynamic model and the empirical approach. Secondly, instead of the stochastic model in Section 2.2.3, this model takes the storm surge water level as a total parameter, and therefore, can avoid the non-linear interaction between the astronomical tide component and the wind induced surge component. Last but not the least, this model takes into account not only the water level peak height but also the water level temporal evolution in a storm surge. The application of this model is illustrated in Chapter 5.

2.5.2 Statistical uncertainty in parameters of distributions

The statistical uncertainty may exist in the distributions in terms of all variables of the joint probability distributions. Mainly the statistical uncertainty is derived from estimating the relevant distributions from a limited number of selected events (Yevjevich et al., 1972; Roscoe and Diermanse, 2011). It is expected that the statistical uncertainty in the relevant distributions results in the increase of the occurrence probability of the extreme events in terms of storm surges and high Rhine river flows.

The nonparametric bootstrap method (Efron, 1979; Davison and Hinkley, 1997) can be employed to quantify the statistical uncertainty in the distributions as it is simple to present and easy to implement.

The statistical uncertainty can further be incorporated into the original marginal distributions in order to estimate its effect on the high water level frequency. Further research will be introduced in Chapter 7.

2.5.3 Incorporating information of rare floods in previous centuries

It is difficult for the estimated probability distributions to accurately estimate the values with extreme low exceedance probabilities due to the short available gauged records. For example, the return period of the design Rhine discharge are relatively high, up to 1/1250 year at Lobith, and with 110 years of observed discharge data available, statistical extrapolation may leads to large uncertainties (Klemeš, 2000a; 2000b).

Discrete historical extreme flood events in previous centuries will improve the probabilistic analysis. Historical data of extreme sea level and extreme Rhine flow in previous centuries have been studied (Glaser and Stangl, 1999; de Kraker, 2000; 2005; 2006; Baart et al., 2011). The historical information could be gathered from personal diaries, public documents, paintings, drawings, written records, shell deposits that have recently appeared, and signs of flood levels on historic buildings, etc.

The investigated rare events in previous centuries have to be taken as an indication, not as accurate data points. (van Gelder, 1996) classified the historical extreme sea floods before 1880 into 4 classes: Class A for very severe floods; B for heavy floods; C for less heavy floods and D for light floods. Each class of sea floods can be described with a water level and uncertainty level, and modeled to be realizations from a normal distribution.

Although in this thesis the historical events before 1887 have not yet been taken into account, it is still expected that the information of rare events in previous centuries would, if properly included in the estimation procedure, improve the estimation of the probability distributions (Hosking and Wallis, 1986; Bayliss and Reed, 2001).

2.5.4 Dependence between North Sea storm surge and high Rhine river discharge

This chapter investigates the joint probability of Rhine flow, tide and surge on the frequency of extreme water levels in the Lower Rhine Delta. In the joint probability distributions, it is commonly assumed that the magnitude of the Rhine flow is independent of the magnitude of North Sea storm surge (Dantzig

et al., 1960; Jorigny et al., 2002; Zhong et al., 2013). The assumption of independence is estimated by the available gauged data.

The simultaneous occurrence of a storm surge and a Rhine flood is very rare, and has only occurred 9 times in the last 70 years. The limited data result in difficulties in the estimation of the independence between North Sea storm surges and Rhine floods. A probabilistic approach traditionally involves an assumption of independence between these primary hydrological variables, which may lead to the underestimation of the level of risk (White, 2013). In future study, it is suggested that the bivariate logistic threshold-excess model introduced by Zheng et al., (2013) will be applied to detect the dependence with a few joint exceedance points.

Recent research explores the simultaneous threats of North Sea storm surges and extreme Rhine river discharge for the current and future climate in a large 17-member global climate model ensemble (Kew et al., 2013). The results indicate that for the present climate condition, compared to the previous assumption of treating extreme surge and Rhine discharge probabilities as independent, the probability of extreme surge conditions following extreme 20-day precipitation sums is around 3 times higher.

It should be noted that a large uncertainty exists in the simultaneous occurrence probability of North Sea storm surges and extreme Rhine river discharge. Although this thesis accepts the assumption of independence, the uncertainty needs to be assessed in future studies.

2.6 Conclusions

This chapter mainly introduces the joint probability approach to re-sample the stochastic scenarios of the present and future hydrodynamic boundary conditions of the Lower Rhine Delta. Three categories of the hydrodynamic boundary conditions are divided by three different flood resources. A large number of scenarios for each flood source are stochastically generated and used to drive the deterministic model to result in water levels at locations of interest in the following chapter. The resulting peak water levels as well as the accompanying occurrence probability can be transformed into the high water level frequency.

Chapter 3. High water level frequency assessment with a conceptual model

3.1 Introduction

The hydrodynamic characteristics of the Lower Rhine Delta are mainly governed by the discharge of the rivers Rhine, Meuse and by North Sea water level at the mouth of the delta. The joint probability approach introduced in Chapter 2 is used to re-sample the stochastic scenarios of the hydrodynamic boundary conditions. There are three categories of the hydrodynamic boundary conditions divided by three different flood sources. A large number of scenarios for each flood source are generated with the importance sampling Monte Carlo simulation. Then the hydraulic models are required to simulate these scenarios into water levels at locations of interest in the delta.

The traditional approach applied only a very limited number of sampling scenarios (Mantz and Wakeling, 1979; Samuels and Burt, 2002) to the high water level frequency estimation with a detailed model. The computational burden for the usage of the detailed 1-D model strongly limits the number of sampling scenarios.

To model the water system, a detailed 1-D hydrodynamic model of the delta that is calibrated every five years exists. However, a large number of stochastic scenarios are not only necessary for the statistical uncertainty reduction, but also for the validation of the present operational water management system controlling different flood sources. The large number of scenarios require much longer computational time with the application of the detailed model. Therefore, a simplified model which is based on the detailed 1-D hydrodynamic model is required for simulating the large number of stochastic scenarios.

This chapter introduces a conceptual model, so-called “Equal Level Curves” model (Vrijling and Gelder, 1996), as sketched in Figure 3-1, 3-2 and 3-3. Considering that the Lower Rhine Delta can be closed when storm surges occur, two versions of Equal Level Curves are introduced: one for the open delta, and the other for the closable delta. In Equal Level Curves, the operation of the existing structures in the delta can be assumed and simplified as the operation of the Maeslant Storm Surge Barrier.

This model can examine the interaction of sea level, fluvial flows and infrastructure operations to produce water levels at locations in the delta. Lobith (Rhine flow) and Hook of Holland (North Sea water level) are selected as the upstream and downstream model boundaries.

This model has advantages: firstly requiring less information and offers a very fast calculation; secondly convenient to combine with the operational water management in the delta.

Therefore, a large number of boundary stochastic scenarios (Chapter 2) can drive the model, and the outputs are the same number of peak water levels at locations of interest. The resulting series of peak water levels as well as the accompanying occurrence probabilities can be transformed into the high water level frequency curves in the delta.

This chapter is organized as follows: Section 3.2 presents the conceptual model; followed by the high water level frequency results in Section 3.3; discussion in Section 3.4; and conclusions and recommendations are presented in Section 3.5.

3.2 The conceptual model: Equal Level Curves

The Rhine flow discharges into the delta at Lobith in the East and out at Hook of Holland in the West, and where the sea water can flow into the delta when the sea level is higher than the water level in the delta. The distance from Lobith to Hook of Holland is approximately 170 kilometers. The delta can be closed when storm surges occur. The schematization of the water system for the conceptual model is shown in Figure 3-1.

Considering the above characteristics of the Lower Rhine Delta, the conceptual model is illustrated in Figure 3-2 and 3-3. Two versions of Equal Level Curves are introduced: one for the open delta, and the other for the closable delta. The closable delta can be open to the sea except that the delta can be closed with the help of hydraulic structures during extreme weather conditions (storm surges).

In the Equal Level Curves, just only the city of Rotterdam is taken into account for the high water level frequency assessment.

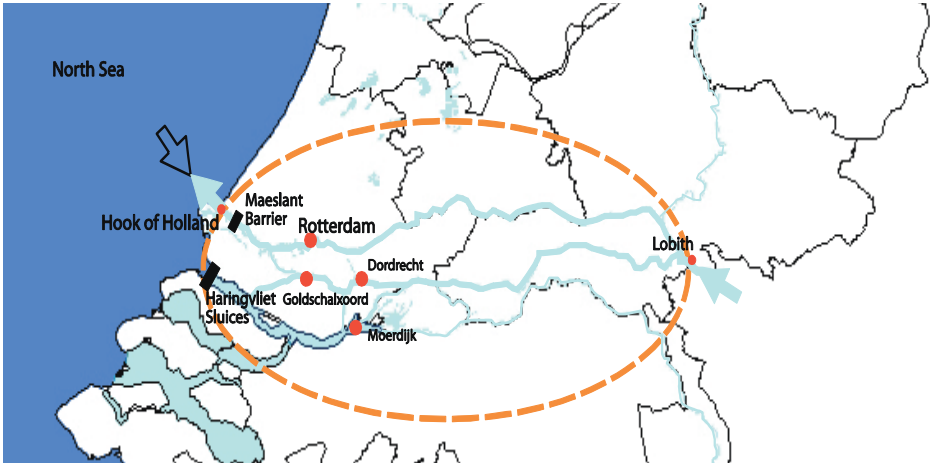


Figure 3-1: The schematization of the water system for the conceptual model

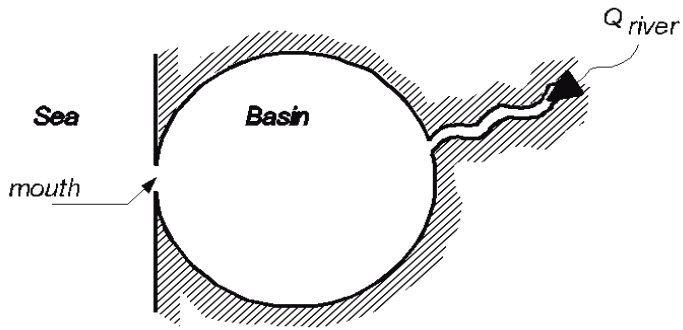


Figure 3-2: The conceptual model of the open delta

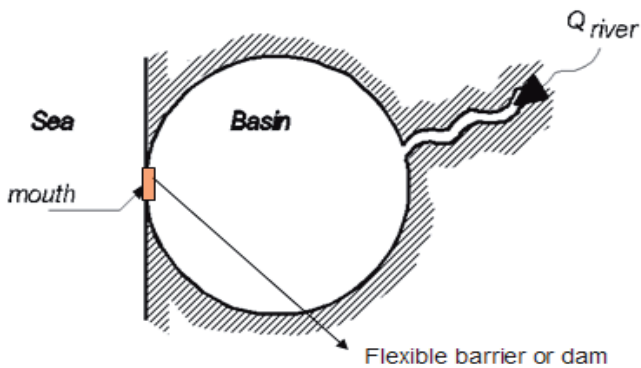


Figure 3-3: The conceptual model of the closable delta

3.2.1 Equal Level Curves with the open delta

Equal Level Curves are a simple steady state function, which can simulate the highest water level at Rotterdam by up-down boundary conditions during one tidal period. For the open delta, Rotterdam water levels can be modeled by the Equal Level Curves with the boundary conditions of the Rhine flow at Lobith and the sea level at Hook of Holland, see Eqn. (3.1):

$$h_R = h_{hvh} + \left(\frac{Q_r}{\mu A}\right)^2 \cdot \frac{1}{2 \cdot g} \quad (3.1)$$

here h_R is the water level at Rotterdam; while h_{hvh} stands for the sea water level at Hook of Holland. Q_r is the Rhine flow at Lobith. μ is the discharge coefficient, A stands for the surface area of the cross section in Hook of Holland and g is the gravitational acceleration.

The parameters of μ and A in Eqn. (3.1) are estimated with selected historical flood events. These flood events are selected from annual maximum sea levels at Hook of Holland and the annual maximum Rhine flows at Lobith from 1940 to 2009, amounting to 137 events in total. If Rotterdam is taken as the location of interest, the parameters can be estimated by the linear regression method and therefore $\mu \cdot A$ is estimated as 3620 m^2 . Equal Level Curves with the open delta are shown in Figure 3-4.

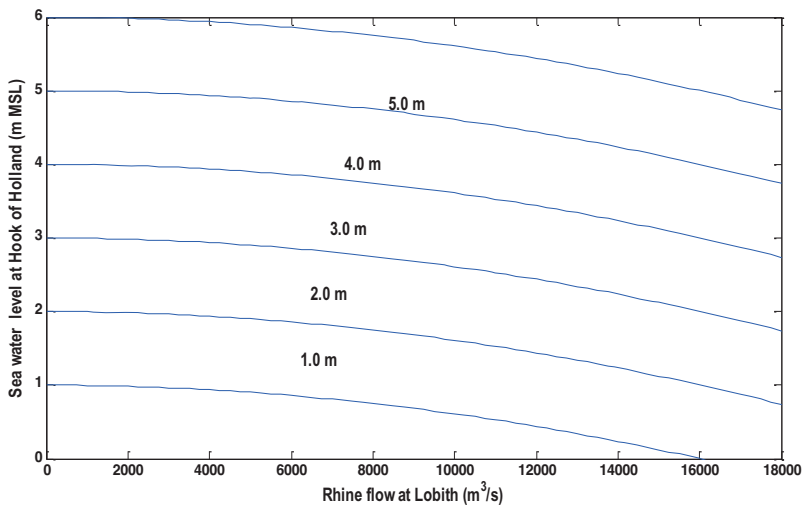


Figure 3-4: Equal Level Curves with the open delta at Rotterdam

In addition, from Figure 3-4 and 3-5 it can be concluded that Rotterdam water level is mostly influenced by sea water level and to a lesser extent by Rhine discharge.

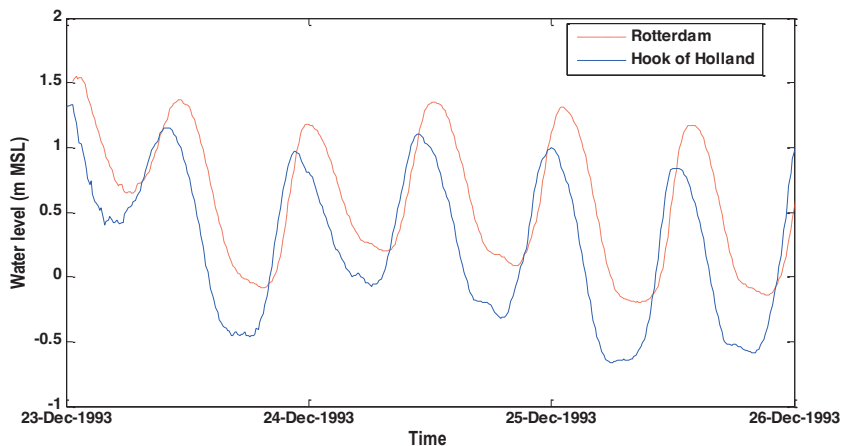


Figure 3-5: Observation of water levels at Rotterdam and Hook of Holland

To validate the estimation of the parameters, the calculated water levels derived from Eqn. (3.1) are compared to the observed water levels for the selected 137 flood events in Rotterdam as seen in Figure 3-6.

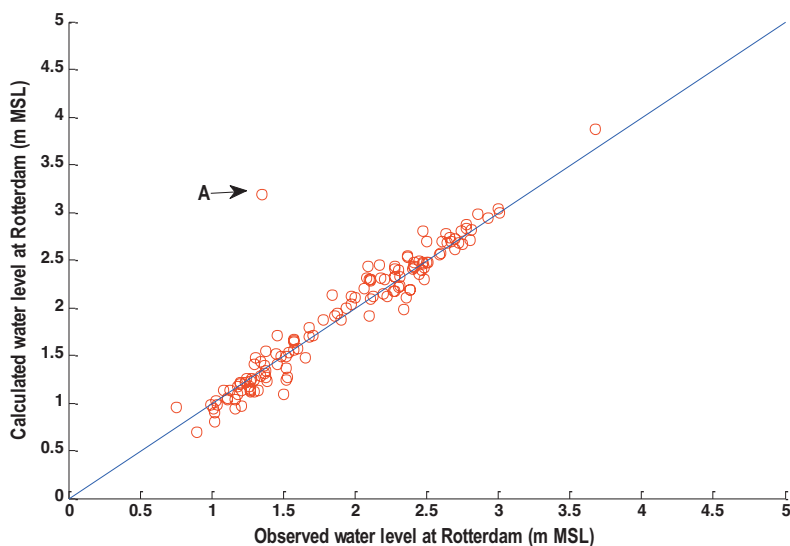


Figure 3-6: Comparison of the calculated and observed water levels at Rotterdam; ‘A’ is the first closure of the Maeslant barrier

In Figure 3-6, the simulated water levels agree with the observed water levels except for the ‘A’ point which means the storm surge ‘Tilo’ induced flood event at November 9th 2007. During this flood event, the Maeslant barrier was closed for the first time after its completion to stop the severe storm ‘Tilo’. The closure of the delta stopped the storm surge from propagating into the delta, and as a result the water level at Rotterdam was lowered to 1.5 m MSL instead

of 3.2 m MSL that was simulated in the condition of the open delta. However, on the other hand, the closure event in 2007 gives a valuable measurement which can be used to model the delta's behavior during closure.

3.2.2 Equal Level Curves with the closable delta

After the big storm surge flooding in 1953, to protect the Rhine delta from sea flooding, large dams and controllable storm surge barriers/gates and pumps have been designed and constructed to close off the delta in order to stop the storm surges. At present, the Rhine delta can be kept open always via the New Waterway and be closed by closing the Maeslant Barrier and the Haringvliet dams when facing extreme weather conditions, for example, storm surges.

Being a closable delta, Rotterdam water level can also be modeled by the Equal Level Curves with the boundary conditions of the Rhine flow at Lobith and the sea level at Hook of Holland. There are two states for the Equal Level Curves: the state of open can be described by Eqn. (3.1) which has been introduced in the former section relating the open delta, the state of closure can be described by Eqn. (3.2).

Eqn. (3.2) shows that after the closure of the delta, the water level behind the barrier rises because the Rhine flow cannot be discharged into the North Sea and will accumulate. In this process the heights of the surrounding dikes are assumed to be infinite high and no dike breaches occur.

$$h_R = h_{R,c} + \frac{Q_r \cdot \Delta T}{B} \quad (3.2)$$

where h_R is Rotterdam water level after the closure duration ΔT ; $h_{R,c}$ is the average water level behind the Maeslant barrier at the closure time; Q_r is the Rhine flow at Lobith; B is the surface area of the delta where water can be stored.

$h_{R,c}$ can be estimated from the average water level of four locations (Rotterdam, Goidschalxoord, Dordrecht, and Moerdijk) at the moment of the Maeslant barrier closing.

$$h_R^t = 0.9735 \cdot h_{hvh}^{t-1} + 7.781 \cdot 10^{-9} \cdot (Q_r^{t-24})^2 \quad (3.3)$$

$$h_G^t = 0.7335 \cdot h_{hvh}^{t-1} + 1.013 \cdot 10^{-8} \cdot (Q_r^{t-24})^2 \quad (3.4)$$

$$h_D^t = 0.6065 \cdot h_{hvh}^{t-2} + 1.737 \cdot 10^{-8} \cdot (Q_r^{t-24})^2 \quad (3.5)$$

$$h_M^t = 0.3753 \cdot h_{nh}^{t-3} + 1.458 \cdot 10^{-8} \cdot (Q_r^{t-24})^2 \quad (3.6)$$

The water levels at these locations at time t depend on the sea water level of amount of hours ago at Hook of Holland and on the Rhine discharge of 24 hours ago at Lobith, because the propagation of the flood waves need travel time. The parameters of the above equations are estimated by system identification of historical measurements. The time unit of t is an hour.

The parameter B can be estimated by inverting Eqn. (3.2) into:

$$B = \frac{Q_r \cdot \Delta T}{h_R - h_{R,c}} = \frac{\left(\frac{8}{9}Q_r + Q_m\right) \cdot \Delta T}{\Delta h} \quad (3.7)$$

The factor $8/9$ comes from the distribution of the Rhine River inflow of which $1/9$ flows north towards the IJsselmeer. The water level can rise by Δh after the closure time ΔT . In the closure event of 2007, the Rhine discharge Q_r was $1171 \text{ m}^3/\text{s}$, the Meuse discharge Q_m was $148 \text{ m}^3/\text{s}$ and the water level at Rotterdam rose from 0.70 to 1.12 m after 15 hours closure. In Figure 3-7, the derivative is constant and the value of B is estimated to be $152,000,000 \text{ m}^2$.

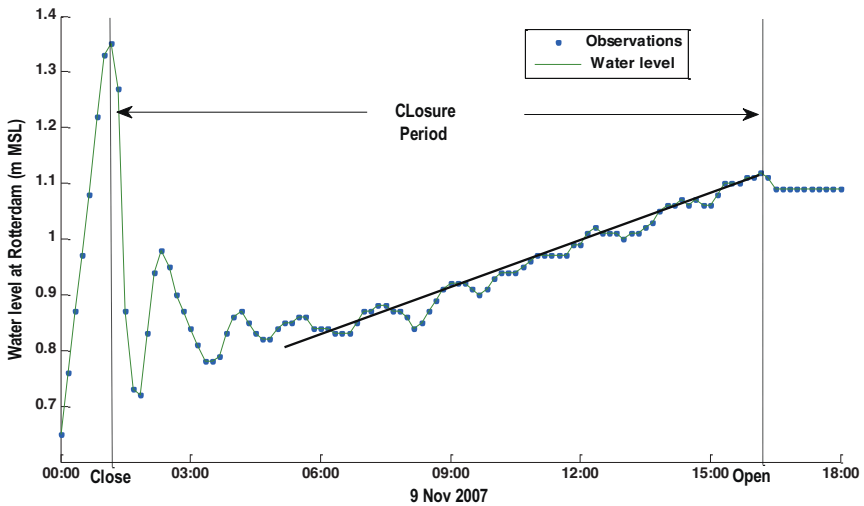


Figure 3-7: Rotterdam water level during the first closure event of November 9, 2007

The closure duration ΔT depends on the operational control of closing and opening of the delta. Two hydraulic structures: the Maeslant storm surge barrier and the Haringvliet dams are mainly responsible for closing the Rhine delta, see Figure 3-1. The present operational control of the Haringvliet dams fully depends on the Rhine discharge at Lobith, see Figure 4-8. And the

operational control of the Maeslant Barrier was introduced in Figure 4-9. In the closure event of 2007, the Rhine delta was fully closed off from the North Sea. Then the Haringvliet dams were kept fully closed because of the low Rhine flow in Lobith ($1171 \text{ m}^3/\text{s}$), and the Maeslant Barrier was also kept closed for about 15 hours.

When a high Rhine flow coincides with a storm surge, the present operational control of the Haringvliet dams keep the Rhine delta partly open, depending on the quantity of the Rhine flow in Lobith. However, to keep the analysis simple, it is assumed that when the Maeslant Barrier closes, the Haringvliet dams fully close. This assumption will overestimate the water level when a storm surge coinciding with a high Rhine flow occurs. Therefore, the closure duration ΔT depends on the operational control of the Maeslant Barrier responding to the hydraulic boundary conditions.

The control system of the Maeslant Barrier (named BOS, in Dutch: *Beslissing & Ondersteunend Systeem*; in English, Decision and Support System) has the responsibility to close the barrier completely autonomously (Bol, 2005). To keep the analysis simple, it is assumed that only one control parameter is considered: the closing decision level H_{ds} in the operational control of the barrier. When the water level in Rotterdam is predicted to exceed the closing decision level H_d (3.0 m MSL in Rotterdam) at the time of t , the barrier closes at the time when the lowest water level at Hook of Holland occurs between $t-7$ and t . The water level in Hook of Holland drops after the storm surge, and when the water level in Rotterdam is higher than the water level in Hook of Holland, the barrier re-opens to make the delta open again. Considering the time the procedure of close and re-open takes, the minimum closure duration is 6 hours.

Equal Level Curves with the closable delta are shown in Figure 3-8 in which Equal Level Curves in the shadow area are presented in Figure 3-9.

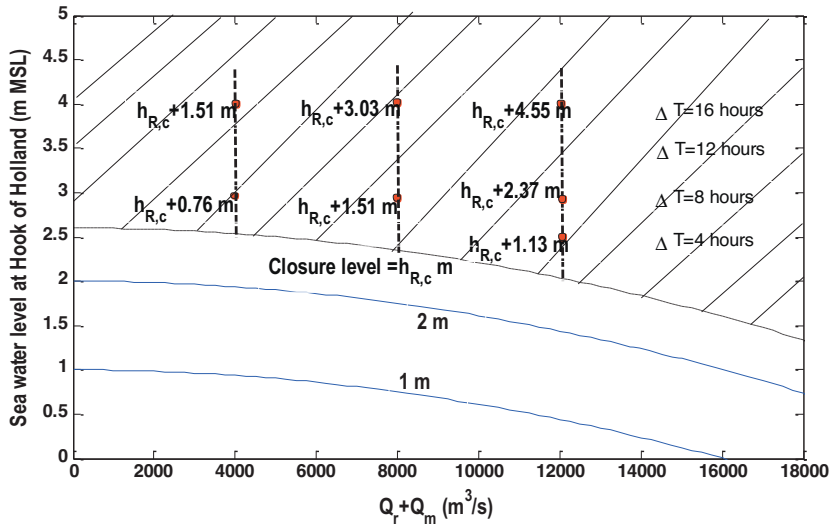


Figure 3-8: Equal Level Curves with the closable delta at Rotterdam

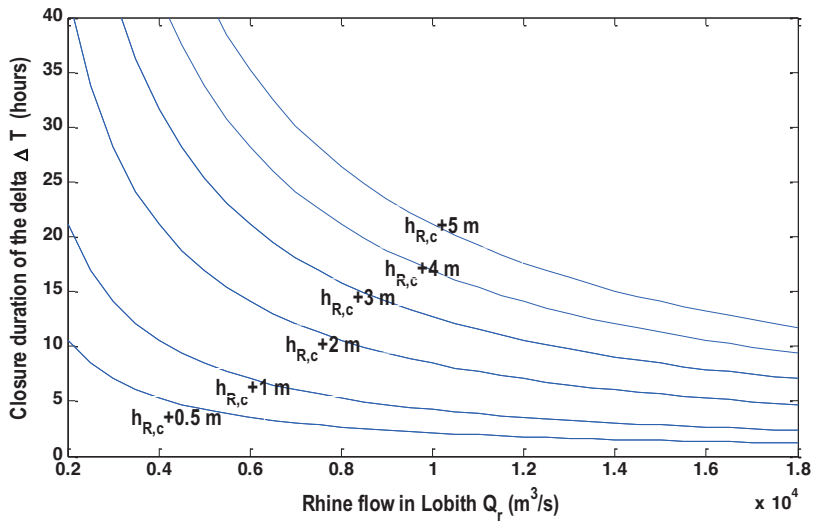


Figure 3-9: Equal Level Curves with the closable delta at Rotterdam after the delta closes at $h_{R,c}$

It is assumed that when 5.0 m MSL water level is exceeded at Hook of Holland, the operational control of the Maeslant Barrier fails to close the delta. Equal Level Curves which consider the failure of the closure of the delta are shown in Figure 3-10. In the following step, the failure operation of the Maeslant Barrier is out of the scope of this study, and has not been taken into account in this thesis.

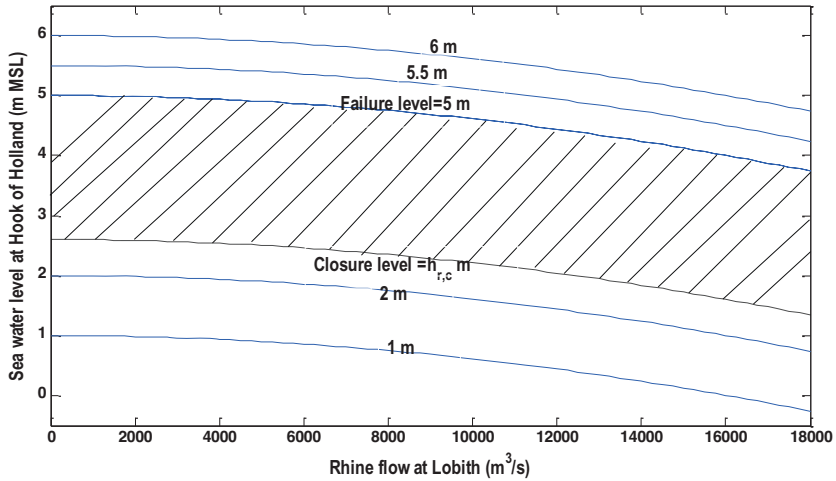


Figure 3-10: Equal Level Curves in the closable delta at Rotterdam considering the failure of the closure.

In conclusion, the conceptual model: Equal Level Curves, with the values of the hydraulic boundary conditions, is able to calculate the peak Rotterdam water level.

3.3 Results

Three categories of hydraulic boundary conditions have been divided: Category I storm surge and normal Rhine flow; Category II high Rhine flow and normal sea water level; Category III storm surge and high Rhine flow. A total of 100,000 stochastic scenarios derived from each category are used to drive Equal Level Curves models presented above in order to estimate the high water level frequency at the city of Rotterdam. In order to test whether 100,000 simulations are enough to get stable results, another two groups of 100,000 simulations are generated to compare the difference. The differences are found negligible.

The two high water level frequency curves are separated: one in the open delta and the other in the closable delta. The Maeslant storm surge barrier is designed to be able to withstand sea level rise until 2050. The high water level frequency in 2050 can also be assessed.

The high water level frequency results will be presented here. This section is organized as follows: the high water level frequency assessed with Equal Level Curves with the open delta is presented in sub section 3.3.1; the high water level frequency assessed with Equal Level Curves with the closable delta is shown in sub section 3.3.2.

3.3.1 High water level frequency in the open Rhine delta

From Figure 3-12, high Rhine flow has very limited influence on extreme water levels of the downstream part of the delta. The high water level frequency curves of Category II are significantly lower. In the present, the exceedance probability of 3.0 m MSL is lower than 10^{-7} ; and in the scenario of 2050, the exceedance probability of 3.0 m MSL is about 10^{-4} .

From Figure 3-11 and 3-13, storm surges in the mouth of the Rhine delta dominate high water levels of Rotterdam. According to the Dutch law, the present design water level in Rotterdam is 3.6 m MSL for Rotterdam (Ministerie van Verkeer and Waterstaat, 2007). In the present, the exceedance probability of 3.6 m MSL is about 10^{-2} in Category I; and 2.0×10^{-3} in Category III. Both values are much larger than 10^{-4} which is regarded as the design exceedance probability value for the design water level.

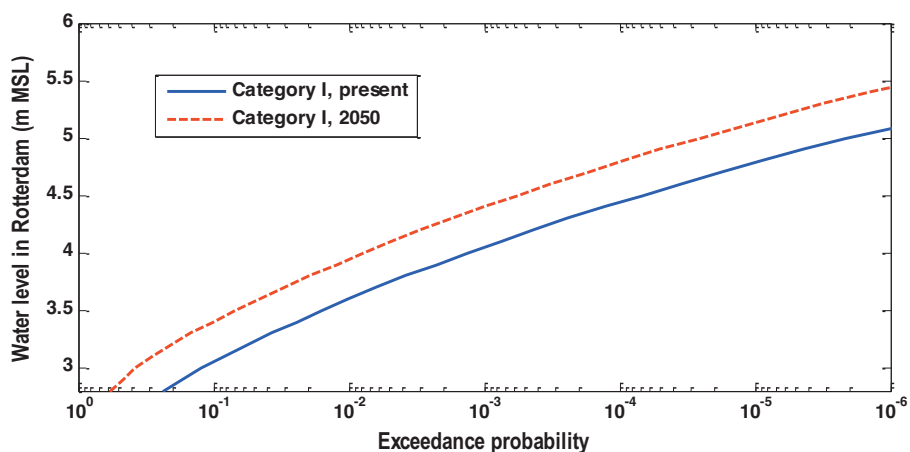


Figure 3-11: High water level frequency curves in the open Rhine delta conditioned on Category I

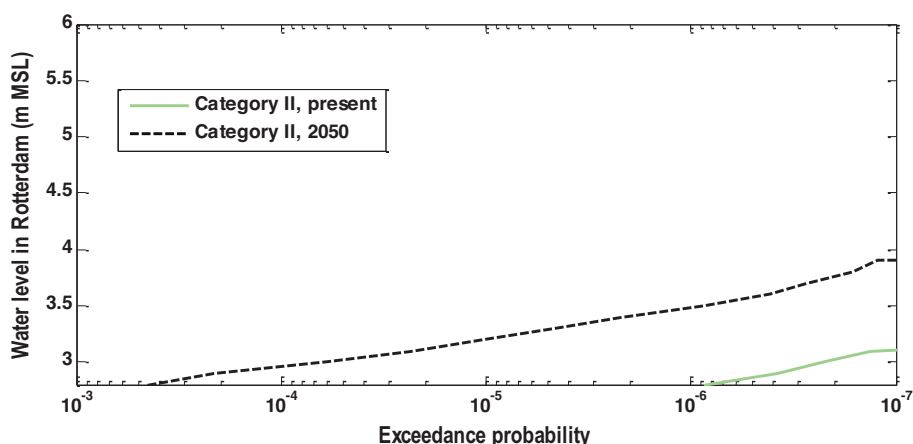


Figure 3-12: High water level frequency curves in the open Rhine delta conditioned on Category II

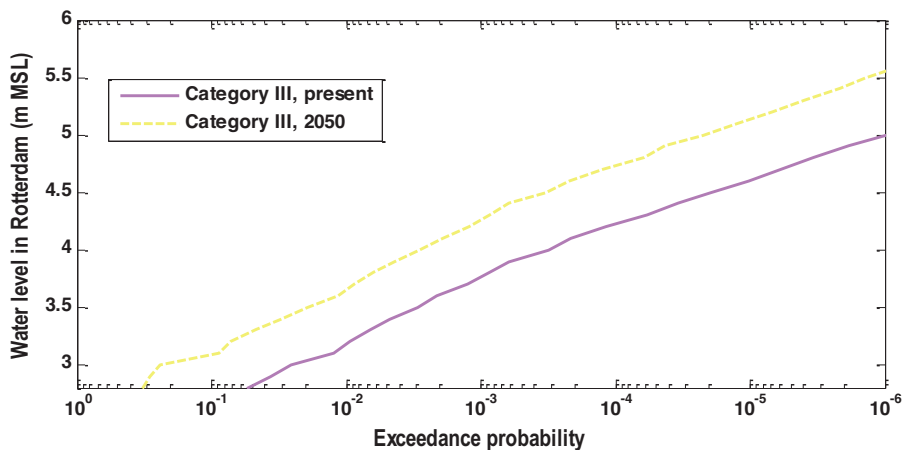


Figure 3-13: High water level frequency curves in the open Rhine delta conditioned on Category III

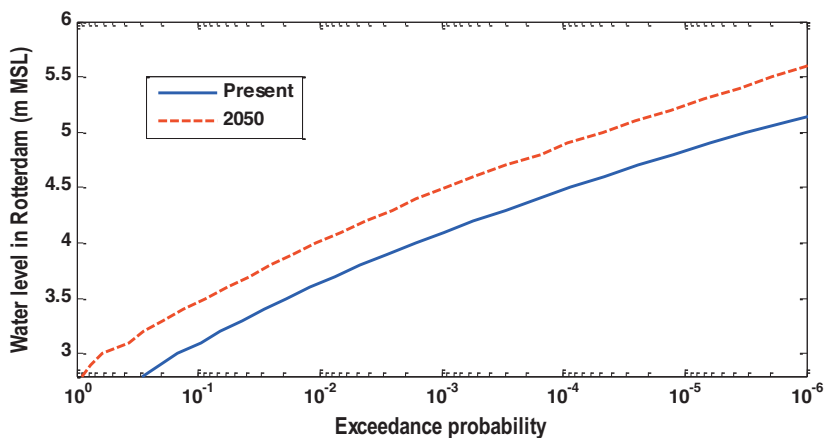


Figure 3-14: The total high water level frequency curves in the open Rhine delta

In Figure 3-14, the flood frequencies derived from three categories are summed up. In the present, for 3.0 m MSL of Rotterdam water level, the exceedance probability is about 10^{-1} ; for 3.6 m MSL the exceedance probability is 10^{-2} ; and for 4.5 m MSL the exceedance probability is 10^{-4} . The high high water level frequency curve in the open Rhine delta further suggests that measures in terms of hydraulic structures and protection strategies are needed.

Climate change will increase the high water level frequency significantly for three categories and the total sum. For example, in Figure 3-12 the exceedance probability of 3.0 m MSL will increase from 10^{-1} to 5.0×10^{-1} in 2050; and the exceedance probability of 3.6 m MSL will increase from about 10^{-2} to 6.0×10^{-2} in the total high water level frequency curves.

3.3.2 High water level frequency in the closable Rhine delta

The closable Rhine delta can significantly reduce the high water level frequency derived from Category I. In Figure 3-15, due to the fact that the Rhine delta can be closed against storm surges, at present, in Category I the exceedance probability of 3.0 m MSL of Rotterdam water level drastically drops from 10^{-1} in the open delta to less than 10^{-7} in the closable delta; the exceedance probability of 3.6 m MSL drops notably from 10^{-2} to 0. It can be concluded that the flood source of Category I has been well protected by the closing action.

As seen in Fig. 3-16, for the time being, high Rhine discharge has very limited influence on extreme water levels of the downstream part of the delta. But due to sea level rise in future, the frequency of the high sea water level increases in the future, and therefore the high water level frequency curve of Rotterdam conditioned on Category II increases in 2050 in the open delta. The Rhine delta can be closed against more frequent high sea water levels and significantly lower the high water level frequency curve of the future.

The closable Rhine delta can reduce the high water level frequency derived from Category III. In Figure 3-17, at present, in Category III the exceedance probability of 3.0 m MSL drops from 3.0×10^{-2} in the open delta to 2.0×10^{-2} in the closable delta; the exceedance probability of 3.6 m MSL drops from 2.0×10^{-3} to 4.0×10^{-5} .

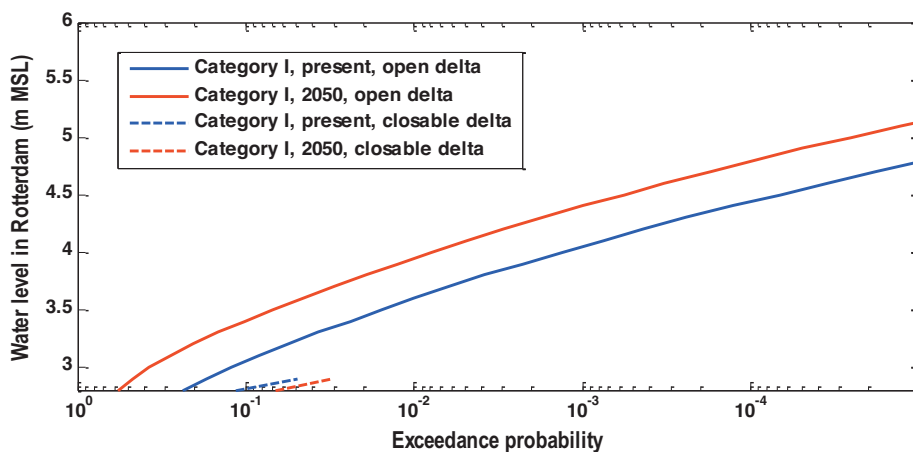


Figure 3-15: High water level frequency curves in the closable Rhine delta conditioned on Category I

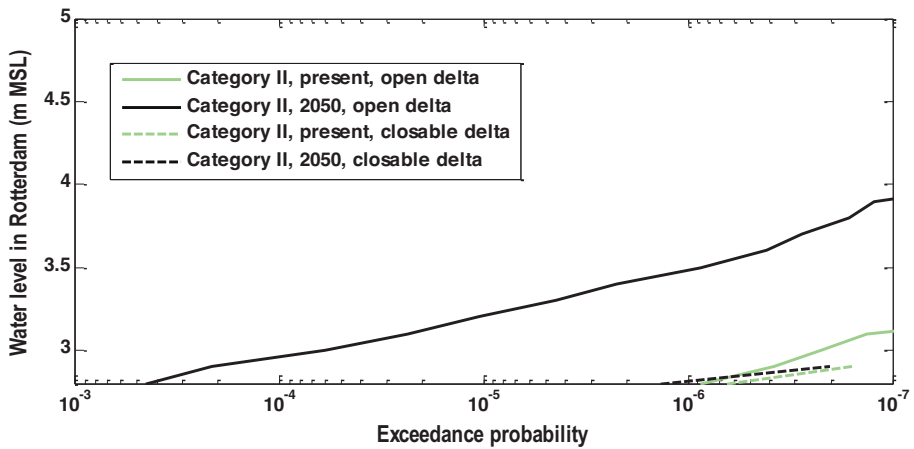


Figure 3-16: High water level frequency curves in the closable Rhine delta conditioned on Category II

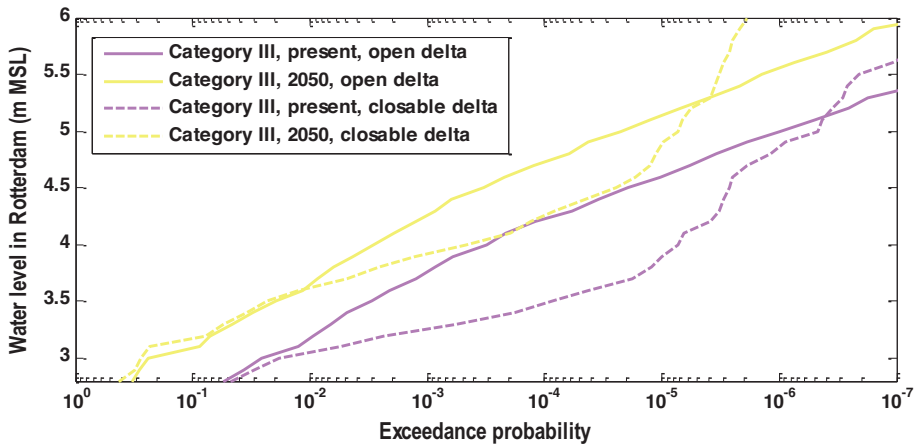


Figure 3-17: High water level frequency curves in the closable Rhine delta conditioned on Category III

However, in Figure 3-17, it is interesting to see that in the tail of the high water level frequency curves of Category III, the high water level frequency is higher in the closable Rhine delta (the dashed pink and yellow line) than in the open Rhine delta (the solid pink and yellow line). It can be explained that, when a long duration storm surge coincides with a high Rhine flow, accumulation of high Rhine flow in a long closure duration of the delta can result in extreme high water level in Rotterdam.

Climate change will significantly increase the high water level frequency. For example, in the total sum high water level frequency in Figure 3-18, the exceedance probability of 3.0 m MSL will increase from 10^{-2} to more than 2.0×10^{-1} in 2050; and the exceedance probability of 3.6 m MSL will increase from about 10^{-4} to 10^{-2} . Although the closable delta can partly compensate the

negative effect of climate change, it is of vital importance to update the flood control measures to make the Rhine delta climate proof.

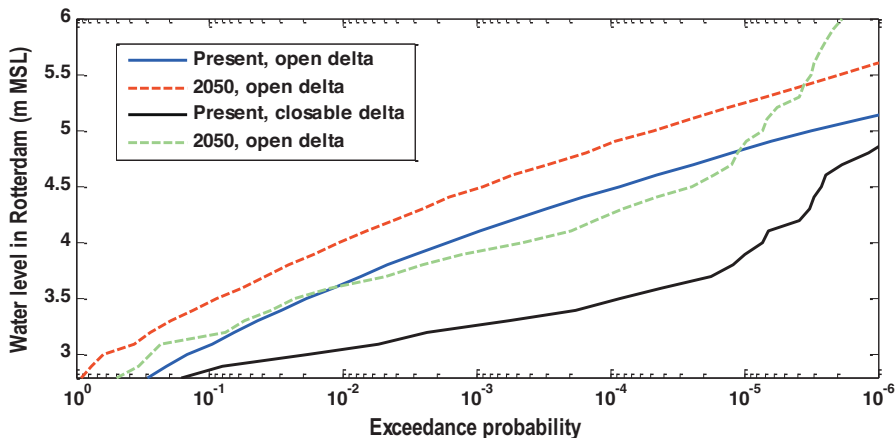


Figure 3-18: The total sum high water level frequency curves in the closable Rhine delta

3.4 Discussion

When a storm surge is approaching, it is of vital importance to decide whether and when to close the delta in advance. However, in the case of Rotterdam as a major port with considerable shipping traffic, the delta should be closed only when absolutely necessary. An unnecessary closure will cause the loss of millions because of the restricted ship traffic, while there is also the danger of flooding through the Rhine when its water is blocked.

The operation of the closure process depends on one parameter: the closing decision water level at Rotterdam H_d (in present 3.0 m MSL). The control parameter is such that the levees in Rotterdam correspond to the flood safety standards and that the Maeslant Barrier closes as seldom as possible.

To find out an optimized value for the closing decision water level H_d , a sensitivity test for this parameter is required. The above results show that the high water level frequency in Category I and II can be ignored in the closable Rhine delta, while Category III is much higher. Therefore, the focus is on the sensitivity test of H_d on Category III. The result is shown in Figure 3-19.

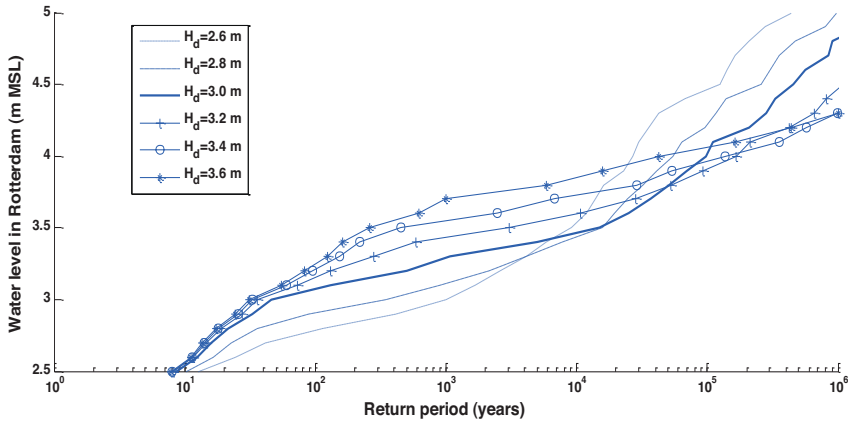


Figure 3-19: Return periods for different values of H_d in Category III.

In Figure 3-19, it can be seen that a changing H_d does influence the return periods of water levels. For the event of a storm surge coinciding with a high Rhine flow, a lower value of H_d leads to close the delta earlier, and therefore in most cases, it can increase the return period. However, a lower value of H_d results in lower return period in the tail. This is due to the fact that when a long duration storm surge coincides with extreme Rhine flow, the lower value of H_d will be decisive to close the delta earlier and result in a longer duration of closure ΔT . The longer ΔT multiplies the extreme Rhine flow, the larger the amount accumulation that dramatically raises the water level in Rotterdam.

A higher value of H_d leads to a later closure of the delta. For the levels which are lower than H_d , their return periods are higher in a higher value of H_d than in a lower value of H_d . This is due to the fact that H_d is the only parameter on which to base the closing decision.

A high value of H_d is beneficial for navigation as it lowers the frequency of the closure events. But flood safety is a primary concern, and therefore H_d should be determined in a conservative way. From the point of view of the high water level frequency, it seems that 3.0 m MSL is a reasonable value for H_d .

3.5 Conclusions and recommendations

This chapter introduces Equal Level Curves for simulating the water system in the Lower Rhine Delta. Two versions of Equal Level Curves are introduced: one for the open delta, and the other for the closable delta. The closable delta can be open to the sea except at times when the delta needs to be closed when facing extreme weather conditions (storm surges). A total number of 100,000 stochastic scenarios derived from each of three categories are used to drive Equal Level Curves models presented above in order to estimate the high water level frequency at the city of Rotterdam.

Conclusions:

1. A high Rhine flow has very limited influence on extreme water levels of the downstream part of the delta, while storm surges in the mouth of the Rhine delta dominate high water levels of Rotterdam.
2. The closable Rhine delta can significantly reduce the high water level frequency in Rotterdam. However, when a long duration storm surge coincides with a high Rhine flow, accumulation of high Rhine flow in a long closure duration of the delta can still result in extreme high water levels in Rotterdam.
3. Climate change will significantly increase the high water level frequency, no matter if the open Rhine delta or the closable Rhine delta is considered.
4. H_d does influence the high water level frequency curves in the closable Rhine delta. The sensitivity analysis shows that 3.0 m MSL is a proper value for H_d .

Recommendations:

1. In the closable Rhine delta, when a high Rhine flow coincides with a storm surge, the present operational control of the Haringvliet dams may keep the Rhine delta partly open, depending on the quantity of the Rhine flow at Lobith. However, to simplify, it was assumed that the Haringvliet dams are fully closed in the above conditions. This assumption can overestimate the high water level frequency in Rotterdam. In the following chapter, a simplified 1-D model will be introduced, which can take into account the operational control of the Haringvliet dams.
2. Instead of Equal Level Curves, a simplified 1-D model is recommended to simulate the delta water system consisting of inter-connected rivers, canals, reservoirs and adjustable structures, as can be seen in Figures 1-3 and 1-4, and within the context of different changes, for example changes in climate and human interventions (the operational water management system). In addition, it has to run very fast in order to be coupled with Monte Carlo Simulation.
3. The closing decision water level H_d not only affects the high water level frequency of the Rhine delta, but also influences the navigation of the harbor of Rotterdam. Although 3.0 m MSL is a reasonable value for H_d from the point of view of the high water level frequency, further research needs to optimize the value of H_d .

Chapter 4 High water level frequency assessment with a simplified 1-D hydrodynamic model

4.1 Introduction

A strongly simplified 1-D hydrodynamic model, derived from a detailed 1-D hydrodynamic model of the delta that is calibrated every five years, has been developed to reduce the computational burden (van Overloop, 2011). The simplified 1-D model is able to simulate the delta water system, consisting of inter-connected rivers, canals, reservoirs and adjustable structures, (as can be seen in Figures 1-3 and 1-4) in the context of different changes in climate and human interventions (the operational water management system). The simplified 1-D model can take the operation of all existing structures into account.

The joint probability approach introduced in Chapter 2 is used to re-sample the stochastic scenarios of the present and future hydrodynamic boundary conditions. There are three categories of the hydrodynamic boundary conditions divided by three different flood sources. A total number of 10,000 scenarios for each category are generated with the importance sampling Monte Carlo simulation. These scenarios can be used as inputs to the simplified 1-D hydrodynamic model in order to estimate the high water level frequency curves at the locations of interest. The resulting series of peak water levels as well as the accompanying occurrence probabilities can be transformed into the high water level frequency curves in the delta.

The results present the exceedance probability of the present design water level for the economically important cities of Rotterdam and Dordrecht. The calculated exceedance probability is evaluated and compared to the governmental norm. Moreover, the impact of climate change on the high water level frequency curves is quantified for the year 2050 in order to assist in decisions regarding the adaptation of the operational water management system and the flood defense system.

This chapter is organized as follows: the simplified 1-D model is described in Section 4.2; followed by the present operational water management system in Section 4.3. The results of the high water level frequency assessment are presented in Section 4.4, and the conclusions and the recommendations are given in Section 4.5.

4.2 The simplified 1-D hydrodynamic model

In addition to the Equal Level Curves, a simplified 1-D numerical hydrodynamic model has been developed for this study. The simplified 1-D model is described in this section. Different operational control algorithms of the man-made structures including storm surge barriers, dams and floodgates, have been modeled within the simplified 1-D model. The water system of the Netherlands and the present structures are shown in Figure 1-4.

4.2.1 Introduction of the simplified 1-D model

The simplified De Saint-Venant equations have been widely used for 1-D simulation of river flows (Chow, 1959; Cunge et al., 1980). The equations consist of a mass balance and a momentum balance as seen in Eqn. (4.1) and in Eqn. (4.2). The mass balance ensures the conservation of water volume, while the momentum balance is a summation of the descriptions for inertia, advection, gravitational force, and friction force:

$$\frac{\partial Q}{\partial x} + \frac{\partial A_f}{\partial t} = q_{lat} \quad (4.1)$$

$$\frac{\partial Q}{\partial t} + \frac{\partial}{\partial x} \left(\frac{Q^2}{A_f} \right) + g \cdot A_f \cdot \frac{\partial h}{\partial x} + \frac{g \cdot Q |Q|}{C^2 \cdot R_f \cdot A_f} = 0 \quad (4.2)$$

where Q represents the flow (m^3/s); t is the time (s); x is the distance (m); A_f is the wetted area (i.e., the cross sectional area that is wet) of the flow (m^2); q_{lat} is the lateral inflow per unit length (m^2/s), g is the gravitational acceleration and its value is 9.81 m/s^2 ; h is the water level (m MSL); C is the Chézy friction coefficient ($\text{m}^{1/2}/\text{s}$) and R_f is the hydraulic radius (m). R_f is calculated as $R_f = A_f / P_f$, where P_f is the wetted perimeter (m) (i.e., the perimeter of the cross sectional area that is wet). Figure 4-1 gives a schematic representation of a typical open canal with its parameters (van Overloop, 2006).

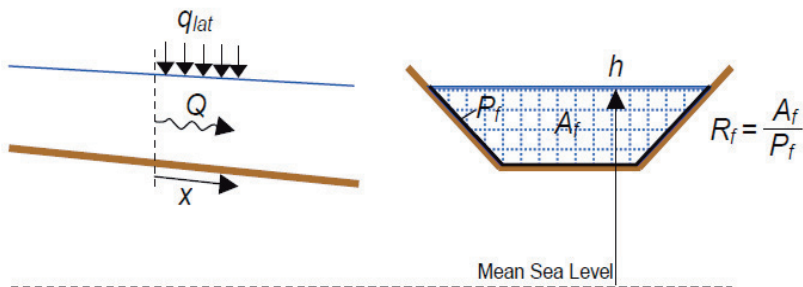


Figure 4-1: Open-water canal variables and parameters (van Overloop, 2006)

To use the above equations in a numerical model of a water system, the partial differential equations are discretized in time (Δt) and in space (Δx). If these discretized equations are simulated, the model results in time series values of water levels and flow discharges at discrete locations along the channels.

Several schemes for discretizing the De Saint-Venant equations exist (Cunge et al., 1980; Stelling and Duinmeijer, 2003). The scheme of a staggered grid with wind-up implementation is preferred in the 1-D model used, because it is more robust and it can deal with super-critical flow (Stelling and Duinmeijer, 2003).

The discretized 1-D model needs calibration from actual measurements. A calibration procedure of a model requires adjusting the values of the parameters to get the outputs of the model as similar as possible to the real system outputs while using the same input data for both. This is an optimization procedure in which the deviation between the model and the real system should be minimized. The least square of the difference is commonly used in model calibration.

A detailed 1-D numerical hydrodynamic model has been developed to simulate flood routing in the water system of the Netherlands based on SOBEK (Delft Hydraulics, 2005). In the SOBEK model cross sections every 500 m, dike locations, dike heights and detention areas currently existing in the water system of the Netherlands, are schematized, shown in Figure 4-2 (van Overloop, 2011).

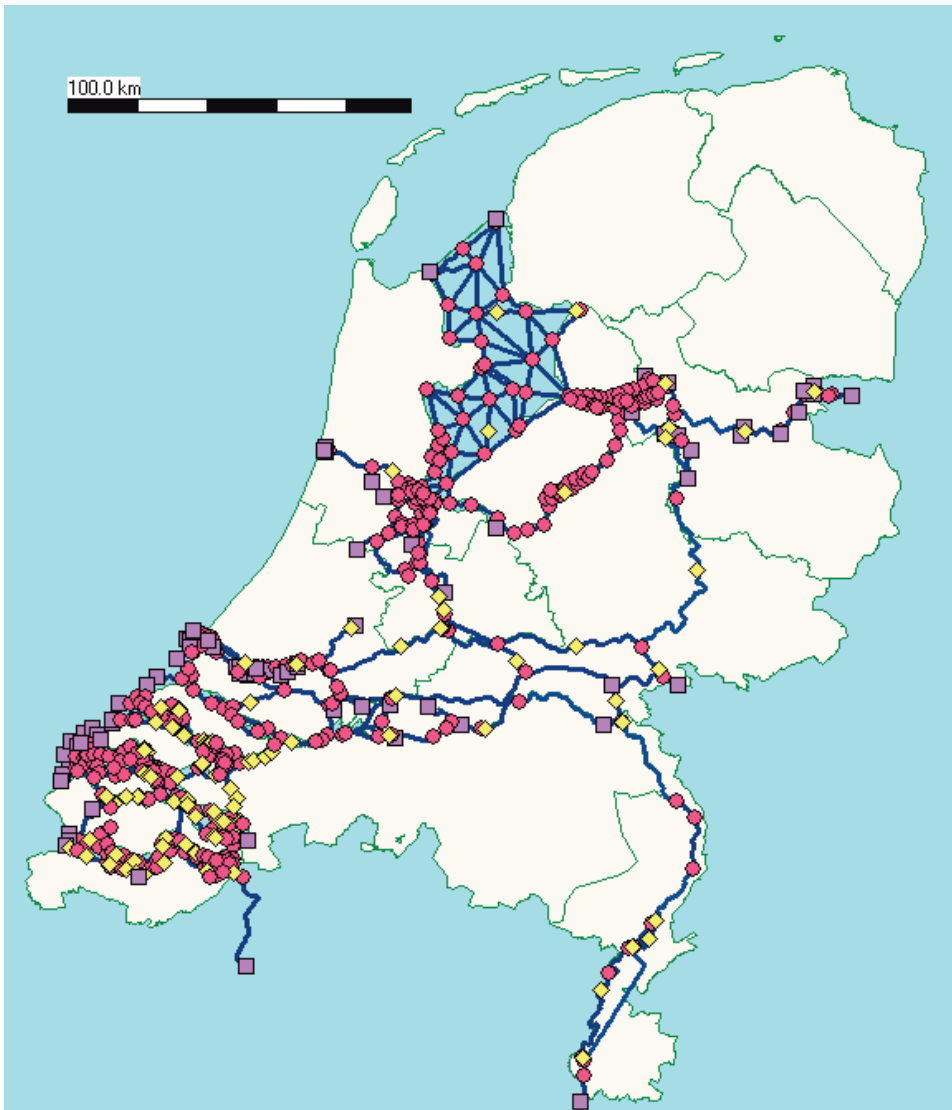


Figure 4-2: Overview of the detailed 1-D detailed model of the water system of the Netherlands

The detailed model is accurate enough to be used as a representation of the real water system. It should be noted that when the discretization is done with a smaller grid size Δx and a smaller time step Δt , the discretized model can more accurately simulate the water levels and water flows in an open water system. However, the smaller grid size also results in a longer computation time. Therefore, the detailed SOBEK model takes longer time than is acceptable, and this makes it difficult to apply in this study. Since a large number of scenarios generated from Monte Carlo simulation needs to be executed, the 1-D model needs to be very fast. Therefore, a simplified 1-D model is required.

A strongly simplified 1-D hydrodynamic model, derived from a detailed 1-D hydrodynamic model, has been developed to reduce the computational burden (van Overloop, 2011). This simplified 1-D model uses a large grid size of 20 km. The total number of water level nodes, including the extra grid points on reaches longer than 20 km is 56. Figure 4-3 presents 36 nodes of the total 56 nodes and the total 40 reaches in the model. A constant bed slope and cross section are assumed for every reach.

Many parameters in the simplified 1-D model are given as fixed values that are supposed to be accurate. As can be seen in Eqn. (4.2), the bed friction, which can be seen as a damping that works against the flow, is mainly determined by the flow Q , the Chézy friction coefficient C , the wetted area A_f and the hydraulic radius R_f . The bed friction coefficient cannot be measured, and therefore tuning the Chézy coefficient value is commonly used in the De Saint-Venant equations in order to adjust the bed friction of the reaches. It is important to note that a higher Chézy friction coefficient means a lower bed friction. In the model the same bed friction coefficients are assumed in all reaches.

The water depth in the model can be adjusted by tuning the bottom level values of the reaches. A good adjustment of the bed levels at reaches around Pannerdensch Kop (node 15) and IJsselkop (node 16) is quite important because they play a significant role on the bifurcation fractions and the water distribution in the water system. As very limited control is possible in this zone, the bifurcation fractions are mainly depending on the dimensions of the rivers (bed levels and Chézy coefficient values).



Figure 4-3: Overview of the simplified 1-D hydrodynamic model derived from the SOBEK model (van Overloop, 2011)

In the simplified 1-D model fixed ratios of water distribution in the bifurcation points of the Bovenrijn and the Pannerdensche canal are considered. The Waal-Pannerden Canal bifurcation is presented in Figure 4-4. In Figure 4-5, 2/3 of the Rhine river discharge goes to the Waal towards the West via the Bovenrijn river and 1/3 to the Pannerdensche canal towards the North. 2/3 of the discharge in the Pannerdensche canal flows through the Nederrijn river towards the West and the other 1/3 flows to the IJsselmeer through the IJssel canal.



Figure 4-4: The Waal-Pannerden Canal bifurcation

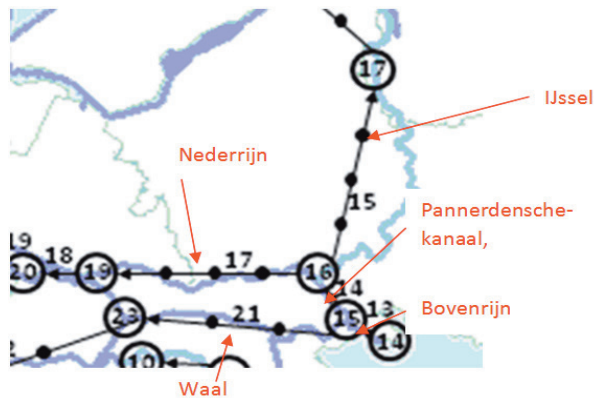


Figure 4-5: The bifurcation points in the Rhine Delta

The present man-made structures, operated in the model, are indicated in red in Figure 1-4. These structures are under the present operational control of the National Water Board. The flow discharge through these structures is modeled by their discharge-water level relation. The information of these structures and their operation will be illustrated in Section 4.3.

Large water bodies, such as the IJsselmeer, are modeled as reservoirs with the relation between stage and surface area. In addition, there are two assumptions in the model process. First, the dike heights along the rivers are assumed to be high enough and no overflowing or breaching occurs. Second, the operational control of these hydraulic structures based on the national code is assumed not to fail in this study.

Tortosa (2012) calibrated and validated this simplified 1-D model using simulation results of the high-order numerical SOBEK model over the period 1970 to 2003. The accuracy of this simplified 1-D model is sufficient to

incorporate into the joint probability approach for the high water level frequency assessment.

The hydrodynamic characteristics of the delta are mainly determined by the discharge of the rivers Rhine (Lobith: node 14 in Figure 4-3) and Meuse (Borgharen: node 1), and by the water level at the sea boundaries (Hook of Holland: node 36, and Haringvliet: node 29). In the model calculations, the sea level at the Haringvliet is assumed to be the same as at Hook of Holland.

As the focus of the research is on the Lower Rhine Delta surrounding the cities of Rotterdam and Dordrecht, the other sea level boundaries in the North (node 30, 33, 35) which do not affect Rotterdam and Dordrecht, are set to 0 m MSL during the running of the model. Rotterdam (node 24) and Dordrecht (node 22) are the locations of interest where the high water level frequency is estimated.

4.2.2 Assumptions in the simplified 1-D model

Assumptions in the simplified 1-D model may lead to uncertainties in the model simulation. A brief introduction of the uncertainties derived from the assumptions is given, while the quantification of uncertainties is not pursued in this thesis.

4.2.2.1. Rhine river discharge distribution at the bifurcation points

In the simplified 1-D model, fixed ratios of water distribution in the bifurcation points of the Bovenrijn and the Pannerdensche canal are considered. The distribution for the Rhine discharge at Lobith is presented in Figure 4-6 (Winkelhorst, 2013).

Obviously, these ratios are not fixed for different Rhine floods (Schielen et al., 2008). The assumption of the fixed ratios may lead to uncertainty in the high water level frequency assessment.

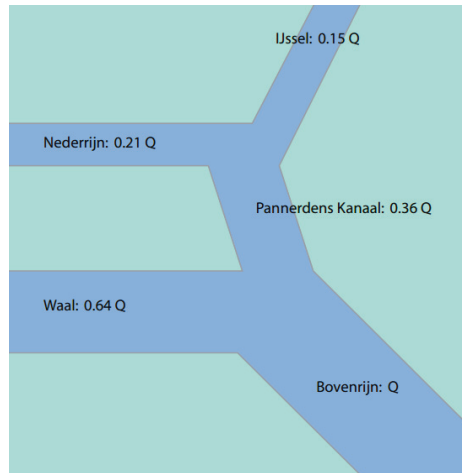


Figure 4-6: Discharge distribution of the Rhine discharge at the bifurcation points

4.2.2.2 Bathymetry and roughness

Once the hydraulic properties (bathymetry and roughness) of the river stretches are subject to changes, adaptation of the stage-discharge relationships is required.

The hydraulic roughness is an important sensitive parameter. However, the roughness is affected by many factors and is difficult to estimate accurately. In the simplified 1-D model, hydraulic roughness of all channels is assumed to be the same, which may lead to uncertainty in the model calculation.

The bed level at the delta increases as the mean sea level increases in the context of climate change. The mechanism of sediment transportation and fluvial processes can be predicted by a mathematical model (Vries, 1965). Therefore, to assess high water level frequency in future scenarios, the changes in the bathymetry need to be taken into account.

It should be noted that this thesis only considers the effect of climate change on the mean sea level and Rhine flow, thus the bathymetry is retained when assessing the high water level frequency in the future.

4.3 The present operational water management system

To protect the delta from storm surges, the Lower Rhine Delta can be closed off from the sea by large dams and controllable gates, storm surge barriers, and

pumps. Controllable structures along the Rhine branches can regulate high Rhine flow, although this influence is limited.

The present operational control rules of these structures are under the supervision of the National Water Board. The operational water management system of the Netherlands refers to these structures and their present operational control rules.

The main objective of this system is to be able to control the water levels and flows within the delta as protection against overtopping of dikes (due to high river flows or high sea water level or the combination of both), as a freshwater supply during dry periods, and for navigation (van Overloop, 2009). In this thesis, the focus is on the effect of the present operational water management system on the high water level frequency reduction. This section introduces detailed information of the present operational water management system of the Netherlands.

4.3.1 Man-made structures

In the Lower Rhine Delta, the existing hydraulic structures are indicated in Figure 1-4. The flood risk map of the Netherlands indicated the urbanized areas Rotterdam and Dordrecht are more hazardous and vulnerable than the others, and so with the higher fatalities (De Bruijn and Klijn, 2009). As a result, Rotterdam and Dordrecht are taken as the case areas of interesting for the high water level frequency estimation in this chapter. The main structures, including the Maeslant storm surge barrier, the Hartel storm surge barrier, the Haringvliet gates and the Volkerak gates, will effectively influence the water system in Rotterdam and Dordrecht. The detailed information of these structures is listed in Figure 4-6 and Table 4-1.

The Haringvliet sluices are located between the estuary of the Haringvliet and the North Sea. The Haringvliet consists of seventeen discharge sluices (each 56.5 m wide), located at the mouth of the former Haringvliet-estuary. Each discharge sluice has two gates. Therefore it can turn away water from the seaside as well as from the riverside. The gate can be partially lifted making different discharges through the sluices possible. It prevents the rise of the water levels in the Rhine-Meuse delta due to high water levels in the North Sea by closing off the mouth of the Haringvliet estuary. It keeps the Haringvliet fresh by preventing salt water flowing into the Haringvliet from the North Sea and it keeps the water level at Moerdijk at 0 m MSL;



The Volkerak sluices are between the Hollandsch Diep and the Volkerak. Water can be discharged from the Hollandsch Diep to the Volkerak by means of 4 discharge gates each of 30 m width. The crest of these gates is at -4.25 m MSL, while the maximum opening is 1.50 m MSL;



The Maeslant storm surge barrier is between the New Waterway (“Nieuwe Waterweg”) and the North Sea. The Maeslant barrier is capable of closing off the New Waterway. The structure consists of two gates that, when it has to close off the New Waterway, are floated out of their dry docks and sunk down to the bottom of the canal. The Maeslant barrier therefore prevents the rising of the water levels in the lower Dutch Rhine delta behind the barrier, due to high water levels in the North Sea, by closing off the New Waterway;



The Hartel storm surge barrier is also between the New Waterway and the North Sea. It has two gates, which can be lowered to close off the Hartel canal. Similar to the Maeslant barrier, the Hartel barrier prevents an increase in the water levels of the lower Dutch Rhine delta area caused by high water levels in the North Sea;



Figure 4-7: The main existing structures within the delta (van Overloop, 2011).

Table 4-1: Summary of controllable structures (van Overloop, 2009)

Structure	Type	Width (m)	Contractions coefficient μ	Crest level (m MSL)	Max level gate (m MSL)	Gate velocity (mm/s)
Haringvliet dam	17 undershot gates	960.5	0.8	-5.50	0.75	5
Maeslant Barrier	Completely opened or closed gate	NA	NA	NA	NA	closing time: 2h
Hartel Barrier	Completely opened or closed gate	NA	NA	NA	NA	closing time: 1h
the Volkerak gates	4 undershot gates	120	0.9 to Volkerak 0.8 to Haringvliet	-4.25	1.50	

4.3.2 The present operational control rule

One main aim of the operational water management system is to prevent high water levels at Rotterdam and Dordrecht in the conditions of extreme hydrodynamic boundary conditions.

The present operational control of these structures is similar to the feedback control method, which is characterized as single objective, local and non anticipatory. It serves a single objective: safety, for the area in its neighborhood and bases its actions on local measurements. The structure of feedback control of an actual system is shown in Figure 4-8.

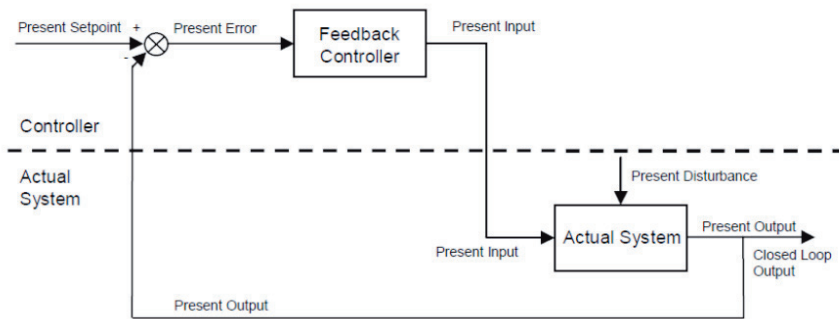


Figure 4-8: Structure of feedback control of an actual system

In the real water system, the measured water level is compared to the target level, and the deviation is computed. Once the pre-determined deviation is exceeded, the man-made structures are operated to control the water level in the actual system in order to reduce the deviation.

This procedure constantly corrects the differences between measured water levels and the target level in a repetitive loop. The above deviations result from disturbances such as high Rhine discharges or storm surge events.

The present control is straightforward and very robust. It is approved by the National Water Board. The detail of the present operational water management system of the Netherlands is available (van Overloop, 2009; 2011), and here a brief introduction is given.

Note that the procedure of the present operational control is complex, and simplified control rules are hence derived and incorporated in the model.

The operational control of the Haringvliet dam is called LPH'84 in which the discharge of the Rhine River determines the discharge through the sluices. The discharge sluices are opened only when the water pressure at the riverside is higher than the water pressure at the seaside. Figure 4-9 shows the relation between the surface under the gates and the discharge of the Rhine River measured at Lobith. When the discharge sluices are open and the water pressure at the seaside is becoming higher than the water pressure at the riverside, the gates are closed. As a consequence the scouring sluices are closed almost every high tide. To open or close the gates does not take more than 20 minutes.

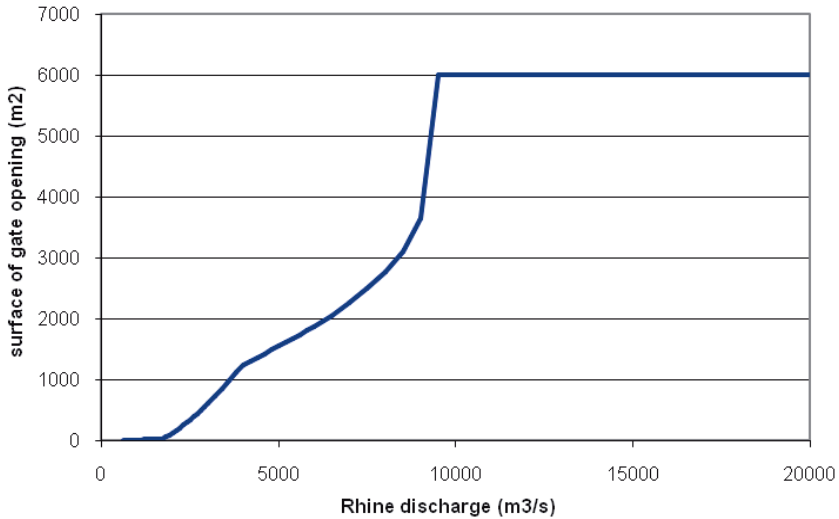


Figure 4-9: Operational control of the Haringvliet gates: LPH'84

The Maeslant Storm Surge Barrier is a storm surge barrier capable of closing off the New Waterway, through which the Rhine flow is discharged into the North Sea.

The control system of the Maeslant barrier (named BOS, in Dutch: Beslissing & Ondersteunend Systeem; in English, Decision and Support System) has the responsibility to close the barrier completely autonomously (Bol, 2005). For simplicity, only one control parameter is considered: the closing decision level H_d , in the operational control of the barrier. When the water level in Rotterdam is predicted to exceed the closing decision level H_d (3.0 m MSL in Rotterdam or 2.7 m MSL in Dordrecht) at the time of t , the barrier closes at the time when the lowest water level at Hook of Holland occurs between $t-7$ and t . The water level in Hook of Holland drops after the storm surge, and at the time when the water level in Rotterdam is higher than the water level in Hook of Holland, the barrier re-opens to make the delta open again. The operational control rule is presented in Figure 4-10. Here h_R is the water level in Rotterdam; h_D is the water level in Dordrecht; and h_{HH} is the water level in Hook of Holland.

Considering the time the procedure of close and re-open takes, the minimum closure duration is 6 hours. The closure process is assumed to be completed in one time step in the 1-D model, so is the re-open process.

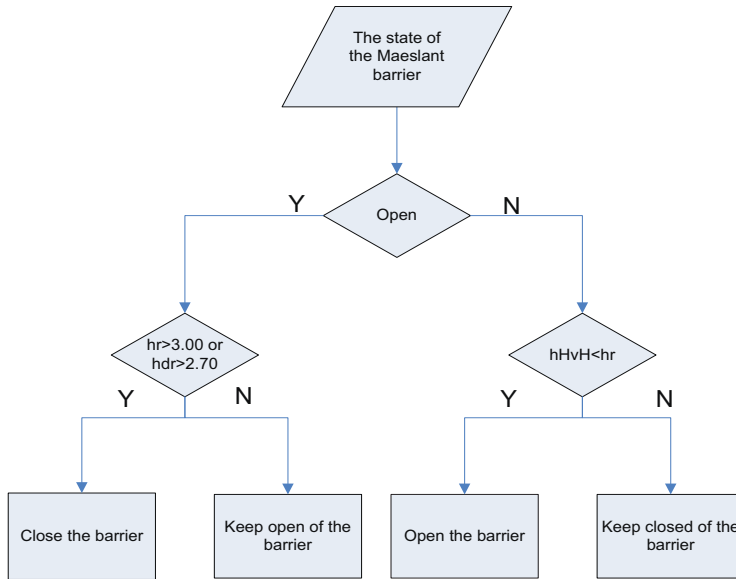


Figure 4-10: The closure decision making of the Maeslant Barrier

The Hartel Storm Surge Barrier prevents the storm surges in the North Sea from propagating into the Lower Rhine Delta. The operational control of the Hartel Storm Surge Barrier is the same as the Maeslant Storm Surge Barrier's.

Water can be discharged from the Haringvliet to the Volkerak by the Volkerak gates. The flow through the Volkerak gates depends on the difference between water levels at two sides. The crest of these gates is at -4.25 m MSL, while the maximum opening is 1.50 m MSL. The contraction coefficient when water flows from the Haringvliet (at that location called Hollands Diep) to the Volkerak is 0.9, while in the other direction this coefficient is calibrated as 0.8.

4.4 Results

A large number of scenarios of each category of hydrodynamic boundary conditions are used as inputs to the simplified 1-D hydrodynamic model in order to estimate the high water level frequency curves in Rotterdam and Dordrecht. The introduced four hydraulic structures with their different operational control rules have been coupled in the 1-D model.

To get the reliable simulation results, 10,000 events are generated with the Importance Sampling method and the model outputs are 10,000 maximum water levels at Rotterdam and Dordrecht for each of the three categories. In order to test whether 10,000 simulations are enough to get stable results,

another two groups of 10,000 simulations are generated to compare the difference. These differences are found negligible.

4.4.1 Exceedance probabilities of the present design water levels

High water level frequency results show the exceedance probabilities of the present design water levels in Rotterdam and Dordrecht in Table 4-2. Three categories refer to three flood sources in Chapter 2: Category I, storm surge and normal Rhine flow; Category II, high Rhine flow and normal sea water level; Category III, storm surge and high Rhine flow.

The design water level is crucial for the design, construction and maintenance of the flood defense system. According to the Dutch law, the design water level in Rotterdam is regarded as the water level with an exceedance frequency of 1/10,000; the design water level in Dordrecht with an exceedance frequency of 1/2,000. The present design water level is 3.6 m MSL for Rotterdam and 3.0 m MSL for Dordrecht (Ministerie van Verkeer and Waterstaat , 2007).

Table 4-2: Exceedance probability of the present design water levels in Rotterdam and Dordrecht

	Year	Annual exceedance frequency		
		Category I	Category II	Category III
Rotterdam (3.6 m MSL)	2010	$\ll 10^{-6}$	$\ll 10^{-6}$	$\ll 10^{-6}$
	2050	$\ll 10^{-6}$	$\ll 10^{-6}$	2.0×10^{-6}
Dordrecht (3.0 m MSL)	2010	$\ll 10^{-6}$	$\ll 10^{-6}$	2.0×10^{-5}
	2050	10^{-6}	$\ll 10^{-6}$	4.0×10^{-4}

The results show that Rotterdam and Dordrecht can be protected from storm surges until the year of 2050, with the help of the present operational water management system. The exceedance probability of the present design water level is far lower than 10^{-6} for Rotterdam and Dordrecht in Category I. In addition, the exceedance probability in the year of 2050 is far lower than 10^{-6} for Rotterdam and 2.1×10^{-6} for Dordrecht in Category I.

The exceedance probability in Category II is also far lower than 10^{-6} for Rotterdam for both the current and the year of 2050. The exceedance probability for Dordrecht in Category II is lower than 10^{-6} in the year of 2050. This is because high Rhine and Meuse flows have very limited influence on extreme water levels downstream of the delta. However, high fluvial flow could easily result in the breaching or overflowing in the Dutch Upper Rhine Delta, which agrees with the near-catastrophic floods of 1993 and 1995 (Engel, 1997).

The exceedance probabilities in Category III are still far lower than the official standard 10^{-4} in Rotterdam for present and the year of 2050, while the

exceedance probability in Dordrecht is higher than the official standard 1/2000 for the year of 2050.

Moreover, the sum of the exceedance probability in three categories shows that the exceedance probabilities of the present design water levels are much lower than the official standard in Rotterdam and Dordrecht. The Lower Rhine Delta complies with the required norm for flood safety, except the Dordrecht in the future climate scenario of 2050.

The results depend on the assumption that the operation of the storm surge barriers and the Haringvliet dams at the mouth of the delta never fail. However, it is believed that taking the failure of the operational water management system into consideration could result in a much higher high water level frequency for Rotterdam and Dordrecht in all three Categories. Therefore, further research on the failure of the operational water manage system is required.

4.4.2 High water level frequency curves in Rotterdam and Dordrecht

The above results show that the exceedance probability of the design water level is much higher in Category III than in Category I and Category II. It indicates that a combination of a storm surge and a high Rhine flow becomes the main source of flooding for Rotterdam and Dordrecht. The high water level frequency curves derived from Category III are drawn for Rotterdam and Dordrecht in Figure 4-10.

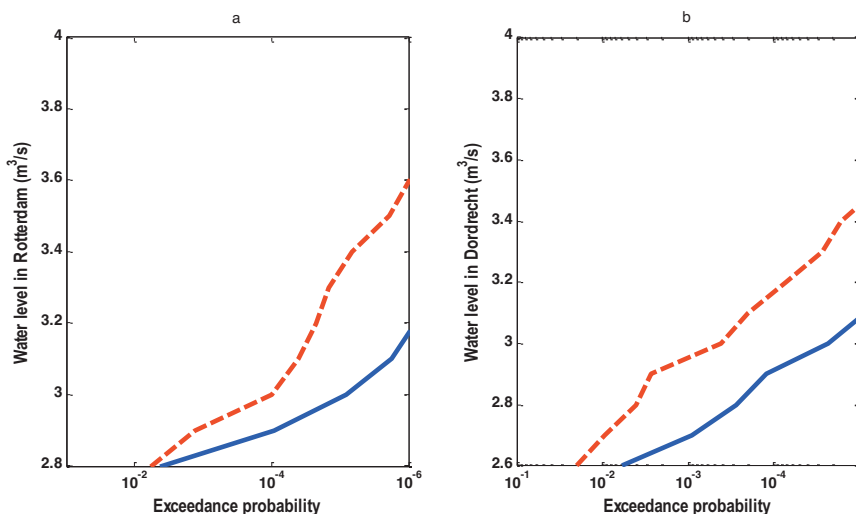


Figure 4-11: The high water level frequency curves conditioned on Category III in a. Rotterdam. b. Dordrecht

The present high water level frequency curve in Rotterdam shows that the exceedance probability of 3.0 m MSL is below 10^{-5} . It is attributed to the operational water management system. Facing the combination of a storm surge and a high Rhine flow, the Maeslant storm surge barrier and the Haringvliet sluices are closed in order to prevent the storm surge water from propagating into the delta; after the closure of the delta, the water level in Rotterdam and Dordrecht will increase due to the Rhine and the Meuse flows coming into the delta. The mouth of the delta is opened again to discharge fluvial water into the sea after the storm. The closing decision level is 3.0 m MSL in Rotterdam and 2.7 m MSL in Dordrecht.

The future high water level frequency curves (the dashed lines in Figure 4-11) are about 0.2 to 0.4 m higher than the present curves (the solid lines in Figure 4-11) in Rotterdam and Dordrecht. It indicates that climate change will lead to more extreme events which increase the high water level frequency in the future.

Climate change will increase the magnitude of storm surges and high Rhine flows at the same occurrence probability. Therefore, the Rhine delta closure duration and the magnitude of Rhine flow which accumulates in the delta will increase, finally resulting in a higher water level in Rotterdam and Dordrecht compared to the present situation.

On the one hand, climate change will increase the high water level frequency in Rotterdam and Dordrecht. On the other hand, the development of local economy and urbanization will increase flood damage when floods occur (Linde et al., 2011). Therefore adaption measures are needed.

To avoid high water levels in Rotterdam and Dordrecht triggered by the flood source in Category III, construction of new structures in upstream area is required in order to protect extreme Rhine flow from coming into the Lower Rhine Delta when the delta is closed. The quantified high water level frequency curves in the present and future can provide an indication for further construction of new structures.

4.4.3 Comparison of high water level frequency curves between the conceptual model and the simplified 1-D model

High water level frequency assessments with the conceptual model and with the simplified 1-D model both show that the high water level frequency derived from Category III is much higher than from the other two Categories. Attention has been paid on Category III. The high water level frequency curves comparison between the conceptual model and the simplified 1-D model is presented in Figure 4-12.

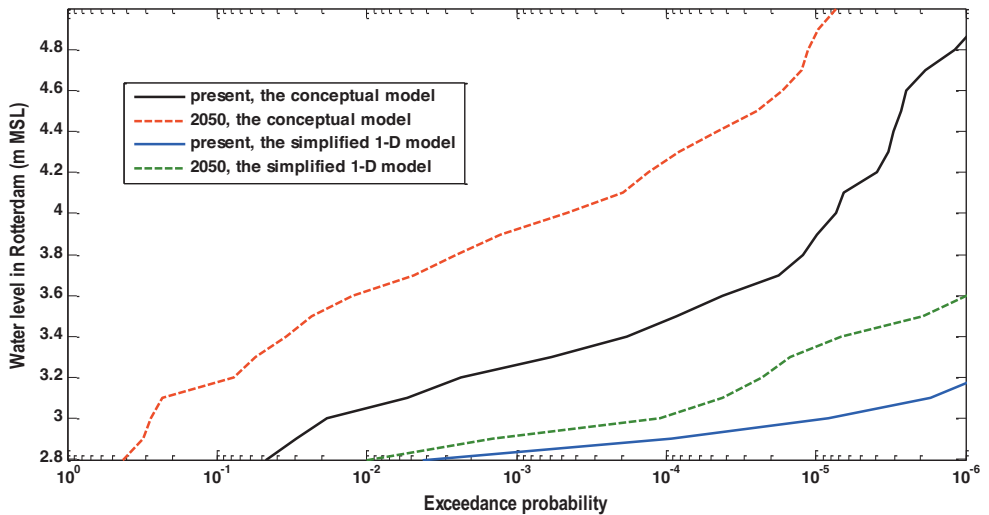


Figure 4-12: Comparison of the high water level frequency curves assessed in the conceptual model and the simplified 1-D model conditioned on Category III

In Figure 4-12, a large difference in the high water level frequency curves exists between the conceptual model and the simplified 1-D model. The conceptual model results in a much higher high water level frequency curve in Rotterdam than the simplified 1-D model. For the exceedance probability of 10^{-4} , in the present the conceptual model corresponds to 3.5 m MSL while the 1-D model corresponds to less than 3.0 m MSL. In the year of 2050, for the exceedance probability of 10^{-4} , the conceptual model corresponds to 4.2 m MSL while the 1-D model corresponds to less than 3.1 m MSL.

It is because that the conceptual model assumes that the Haringvliet dams fully close when the Maeslant barrier closes. However, when a high Rhine flow coincides with a storm surge, the present operational control of the Haringvliet dams keep the Rhine delta partly open, depending on the quantity of the Rhine flow in Lobith, see Figure 4-9. This assumption overestimates the water level when a storm surge coinciding with a high Rhine flow occurs. In the simplified 1-D model, the operational control of the Haringvliet dams is fully based on Figure 4-9. Therefore, the simplified 1-D model results in more accurate high water level frequency curves.

4.5 Conclusions and recommendations

This chapter presents the application of the joint probability sampling approach coupled with a simplified 1-D hydrodynamic model to assess the exceedance probability of the present design water level in Rotterdam and in Dordrecht. The high water level frequency complies with the required norm for safety in the present. The threat of water levels exceeding the design water level still

exists for both cities at a low probability mainly due to the combination events of storm surges in the North Sea and high Rhine discharge in Lobith. In the future, climate change will lead to more extreme events and increase the high water level frequency in the Lower Rhine Delta.

Recommendations:

1. The simplified 1-D model enables assessment of the flood frequencies in a changing environment with associated effects from climate change and the operation of the infrastructures. The model uncertainties that arise from the assumptions need to be quantified and further reduced through research and /or data collection.
2. Taking the failure of the operational water management system into consideration may result in a significantly increase in the high water level frequency curve for Rotterdam and Dordrecht in the three Categories considered here. Therefore, further research on the failure probabilities of the operation of these structures is required.
3. The present operational control algorithm is straightforward and very robust, but does not take advantage of modern information technology in order to achieve a higher level of the control for the delta as a whole. A centralized Model Predictive Control algorithm which uses the information of forecasting and better meteorological, hydrological and hydrodynamic models has been available (van Overloop et al., 2010). It is expected that the application of the advanced operational control algorithm will further lower the high water level frequency in the delta. It is an interesting topic that assessing the high water level frequency of the delta under the new operational water management system which applies the centralized Model Predictive Control algorithm.
4. To avoid high water levels in Rotterdam and Dordrecht driven by storm surges coinciding high Rhine flows, construction of new structures in upstream area is under consideration. These structures can be operated to protect extreme Rhine flow from coming into the Lower Rhine Delta when the delta is closed.

Chapter 5. An alternative stochastic storm surge model

5.1 Introduction

Presently, against storm surges from the North Sea, the delta can be closed off by large dams, controllable storm surge barriers, gates and pumps, as can be seen in Figure 1-4. These hydraulic structures and their operational control algorithms have been introduced in the operational water management system of the Netherlands (van Overloop, 2009; 2011). However, when a storm surge from the North Sea simultaneously coincide with a high Rhine flow in the upstream basin, the delta has to be closed, and an extreme high water level may still occur due to accumulation of high Rhine and Meuse flows (Zhong et al., 2012; 2013).

It is important to estimate the high water level frequency derived from these combined events; first for the flood risk estimation, and second, for the design of the flood defense system. The high water level frequency was assessed by a fully-probabilistic approach using a 1-D hydrodynamic model (Zhong et al., 2013). In the approach, a sufficient large number of storm surge scenarios are generated for driving the hydrodynamic model to estimate the high water level frequency in the delta.

The alternative stochastic storm surge model used in this chapter was first introduced by Wahl et al., (2010; 2011) and applied to Cuxhaven at the mouth of the Elbe river and to Hörnum further North in the German Bight area. The term “storm surge” refers to the extreme still water levels (i.e. waves not included) that arise from the combination of astronomical tides and a meteorologically induced surge component.

There are advantages in the application of this model. First, it takes the sea water level as a total parameter, which avoids the non-linear interaction between the astronomical tide component and the wind induced surge component. Second, this model can efficiently generate a large number of storm surge scenarios. Although a numerical hydrodynamic model (Gerritsen et al., 1995; Verlaan et al., 2005) or an empirical approach (Gönnert et al., 2010) can be applied, due to the computational time, there are restrictions in applying them in a scenario-based risk assessment method. Finally, this model takes into account not only the water level peak height but also the dynamics of the water level temporal evolution in a storm surge, and the latter is necessary when considering the operational control of the existing hydraulic structures.

The derived storm surge scenarios and the scenarios of the Rhine, Meuse flow are imposed on a deterministic 1-D hydrodynamic model to estimate the high

water level frequency in Rotterdam. A large enough number of scenarios is necessary to reduce the stochastic uncertainty. However, the 1-D hydrodynamic model (van Overloop, 2011) in combination with so many combined scenarios takes too much computational time. Therefore, the importance sampling Monte Carlo simulation is applied to reduce the number of scenarios (Glynn and Iglehart, 1989).

In addition to the stochastic storm surge model in Chapter 2, the alternative stochastic storm surge model is applied in this chapter. Compared to the results in Chapter 4, the high water level frequency is estimated with the alternative storm surge model to deeply understand on its effect on the high water level frequency assessment.

This chapter is organized as follows: the methodology is presented in Section 5.2. The application of the alternative stochastic storm surge model in Hook of Holland is given in Section 5.3, followed by the high water level frequency assessment with the alternative stochastic storm surge model in Section 5.4. Discussions and Conclusions are presented in Section 5.5 and Section 5.6.

5.2 Methodology

The gauge station of Hook of Holland (tide gauge location: 51°58'34''N, 4°7'56''E) is located at the mouth of the Lower Rhine Delta. The astronomical tide is a semi-diurnal tide, and the tide range is 1.72 m, derived from the data between 1976 and 2003.

Hourly data is available since 1971, 10-minute data since 1987, and high\low tidal water level data with their occurring time stamps since 1887. Note that a gradual increase of 0.20 m mean sea level rise per century was detected (Dantzig et al., 1960; van Gelder, 1996; Zhong et al., 2012), and a linear trend was estimated and then used to correct the observed water level time series to account for long-term sea level rise. The daily average discharge time series of River Rhine and Meuse start in 1901 and 1911, respectively. Table 5-1 lists the detailed data information:

Table 5-1: The observation data in the boundary gauge stations of the Lower Rhine Delta

Gauge station	Data	Length	Description
Hook of Holland	High tide water level (HW) (m MSL)	1887-2009	The highest water level observation per tidal cycle
	Low tide water level (LW) (m MSL)	1887-2009	The lowest water level observation per tidal cycle
	Observed sea level (m MSL)	1971-2009	Water level observation per hour since 1971, water level observation per 10 minutes since 1987
Lobith	Rhine discharge (m^3/s)	1901-2009	Daily-average discharge
Borgharen	Meuse discharge (m^3/s)	1911-2009	Daily-average discharge

The high water level frequency in Rotterdam is calculated with the following procedure:

1. The application of the stochastic storm surge model at Hook of Holland:
 - The peak over threshold (POT) method is applied to detect the storm surge events in the series of high tidal water level (HW) data.
 - The hydrograph parameters of the storm surge are introduced (Wahl et al., 2010; 2011). From the selected storm surges, the samples of these design parameters are determined and fitted to appropriate probability distributions.
 - These parameters are re-sampled from their probability distributions with a Monte-Carlo Simulation, except the storm surge peak water level, which is sampled with the Importance Sampling Monte-Carlo Simulation. These generated parameters are converted into storm surge hydrographs using an appropriate interpolation method.
 - A filter function assist in avoiding strongly deformed storm surge hydrographs by smoothing the values. The generated storm surge scenarios are further validated.
2. The high water level frequency assessment with the validated stochastic storm surge scenarios:

- The stochastic scenarios of storm surges as well as the stochastic scenarios of the high Rhine, Meuse flows are forced into the 1-D hydrodynamic model to assess the high water level frequency in Rotterdam.

5.2.1 Detect storm surge events

The POT method is applied to identify the storm surge events from the time series of tidal high water level (HW). This study used the threshold value above mean tidal high water level (MHW) to select the storm surges used in this study. MHW at Hook of Holland is 1.08 m MSL. The pure statistical method is applied to detect an appropriate threshold. Figure 5-1 shows the result of the Stability Method (STM). An appropriate threshold is assumed where the shape parameter is approximately constant. Although the threshold can be chosen from 0.30 m to 1.07 m, considering that storm surges with high water levels are relevant for the following high water level frequency, the threshold of 1.07 m above MHW is chosen for the present study. The threshold of 2.15 m MSL (1.07 m threshold + 1.08 m MHW) is then used to detect the storm surges in the HW time series of Hook of Holland. Figure 5-2 shows the available HW time series from 1887 to 2009 and the threshold line.

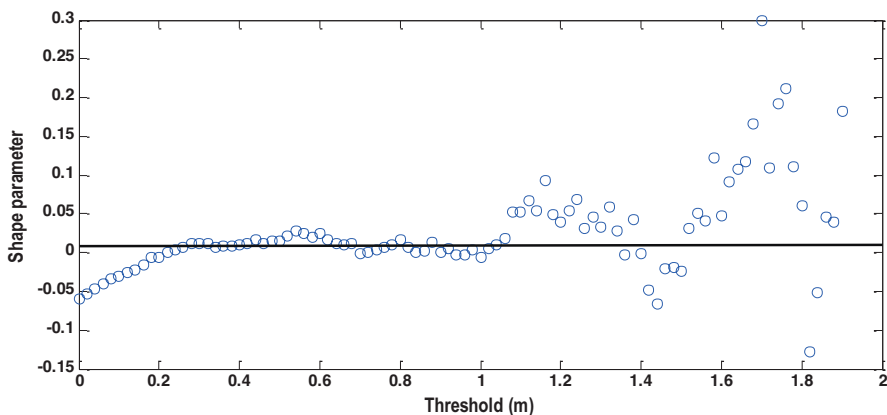


Figure 5-1: Result of the Stability Method to identify appropriate threshold

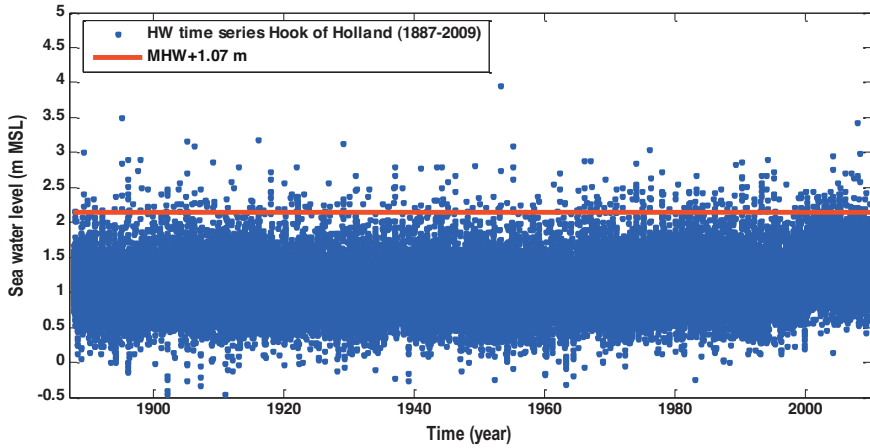


Figure 5-2: Tidal high water (HW) time series for Hook of Holland and the estimated threshold

The number of storm surge events in which at least a fixed number of successive high tides exceeded the threshold is shown in Fig. 4. The storm surge at Hook of Holland usually lasts from a few hours to a few days. In a storm surge event, the longer duration results in more successive high tides exceeding the threshold. Three tides of the observed storm surge events are considered for the storm surge hydrograph. To assure independency, two storm surge events have to be at least 30 hours apart from each other (Wahl et al., 2011). In total 320 storm surges are selected from 1887 to 2009.

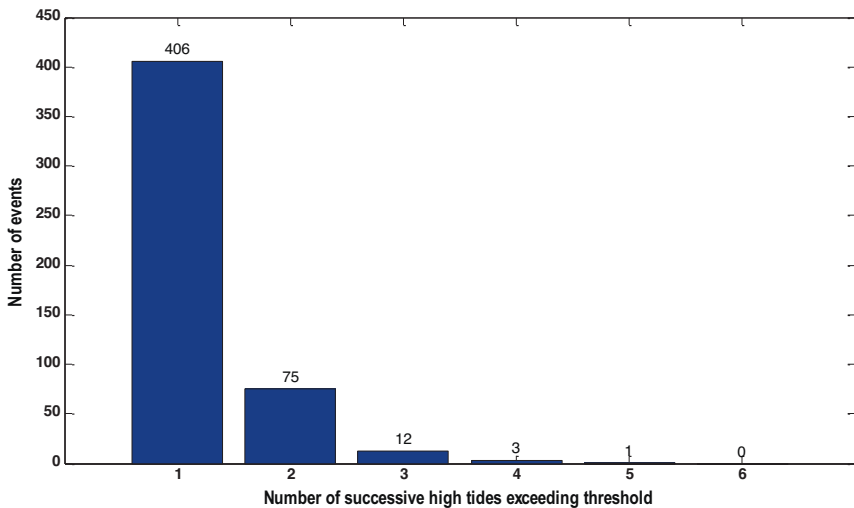


Figure 5-3. The number of the storm surge events in which at least a fixed number successive high tides exceeded the threshold

5.2.2 Parameterization

The stochastic storm surge model considers three tides including 25 parameters to detect the main characteristics of a storm surge event, as is illustrated in Figure 5-4 and Table 5-2. For each parameter, there are 320 sample values according to 320 selected storm surge events. Five tides with 41 parameters are also considered in the model.

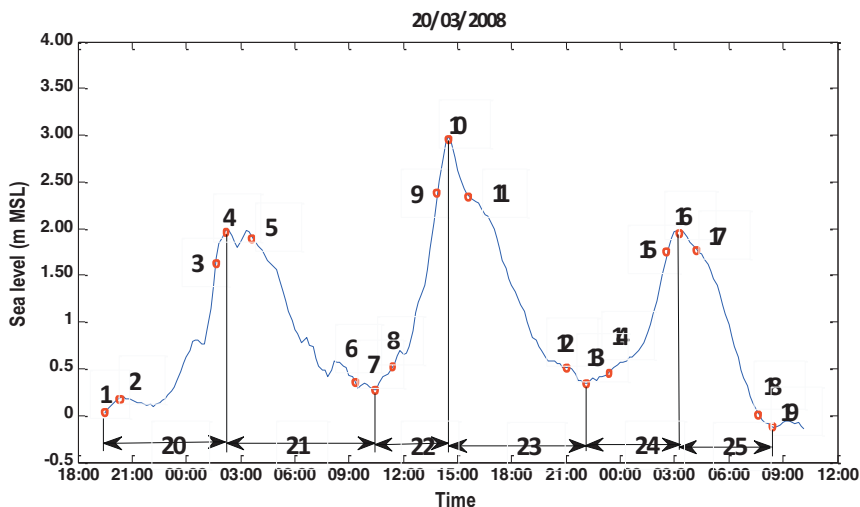


Figure 5-4. Parameterization scheme used to parameterize the observed storm surge hydrograph (20/March/2008) consisting of three tides

Table 5-2: Description of the 25 parameters in the stochastic storm surge model considering three tides (Wahl et al., 2010; 2011)

Parameter	Location	Description
P ₁₀	The maximum high tide of the three tides	The peak height of the storm surge (m MSL)
P ₁ P ₄ P ₇ P ₁₃ P ₁₆ P ₁₉	The tidal high and low waters of the three tides	The absolute difference between the observed water level and P ₁₀ (m)
P ₂ P ₃ P ₅ P ₆ P ₈ P ₉ P ₁₁ P ₁₂ P ₁₄ P ₁₅ P ₁₇ P ₁₈	One hour before and one hour after the high and low waters	The absolute difference between the observed water level and the near high or low waters (m)
P ₂₀ P ₂₁ P ₂₂ P ₂₃ P ₂₄ P ₂₅		The time periods between two adjacent high and low waters (hours)

Note that there is always either a single low water or a double low water in Hook of Holland and only the first low water in case of double low water is chosen.

Present research demonstrates that the storm climate has not undergone significant systematic changes during the 20th century at the mouth of the Lower Rhine Delta (WASA-Group, 1998; Alexandersson et al., 1998; 2000) and no discernible long term trend in storm activity has been detected (Barring and von Storch, 2004). Therefore, it is reasonable to assume that the 320 sample values of each parameter are independent and identically distributed random variables with a common distribution function.

The parameterization of the storm surge time revolution requires high frequent storm surge level data (at least hourly data). However, the hourly data is only available since 1971. As a result, only 143 storm surges which occurred between 1971 and 2009, from the selected 320 storm surge events since 1887, are available for parameterization. According to Figure 5-4 and Table 5-2, each parameter has a total number of 143 samples.

Widely used parametric distributions in Hydrology including the normal, log-normal, generalized Pareto and Weibull distribution are employed to fit the samples of each parameter. The best fit distribution can be identified by the smallest Root-Mean-Square Error (RMSE). The RMSE r can be computed by Eqns. (5.1) and (5.2), where x_i is the empirical cumulative probability, while x'_i is the theoretical cumulative probability derived from the fitted distribution. The results can be seen in Figure 5-5.

$$r = \sqrt{\frac{\sum_{i=1}^n (x_i - x'_i)^2}{n}} \quad (5.1)$$

$$x_i = \frac{i}{n+1} \quad i = 1 \dots n, \quad (5.2)$$

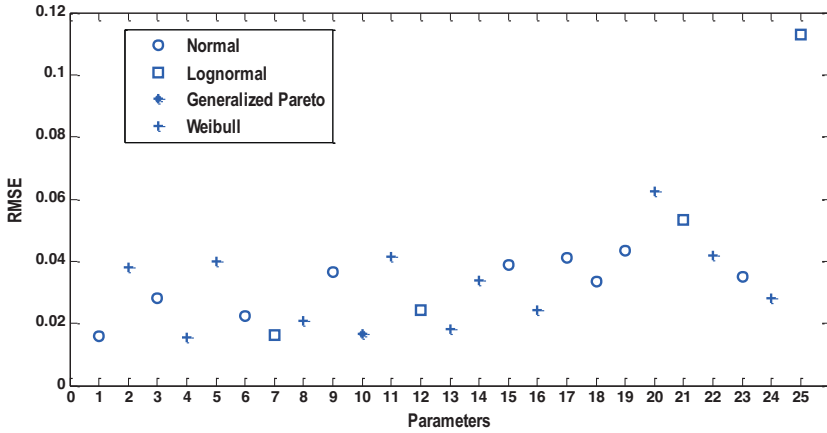


Figure 5-5: The best fit distribution functions of the 25 parameters (1971-2009) based on the lowest RMSE

The 320 storm surges detected from the long-term high/low tide water level data from 1887 to 2009 are available to improve the distribution functions in terms of the sea level parameters ($P_1, P_4, P_7, P_{10}, P_{13}, P_{16}, P_{19}$) and the parameters of time period ($P_{20}, P_{21}, P_{22}, P_{23}, P_{24}, P_{25}$). These modified distribution functions are shown in Figure 5-6. Taking P_{10} as an example, as seen in Figure 5-7 the modified distribution (the red dashed line) corresponds to much higher peak heights at high return periods and therefore can estimate the magnitudes of extreme storm surges more appropriately. For the sea level parameters ($P_1, P_4, P_7, P_{10}, P_{13}, P_{16}, P_{19}$) and the parameters of time period ($P_{20}, P_{21}, P_{22}, P_{23}, P_{24}, P_{25}$), the modified distribution functions are employed instead.

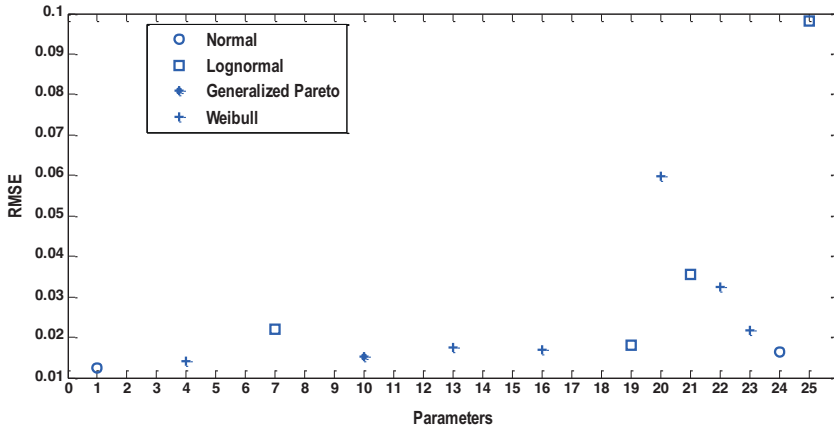


Figure 5-6: The best fit distribution functions of the 13 parameters (1887-2009) at Hook of Holland based on the lowest RMSE

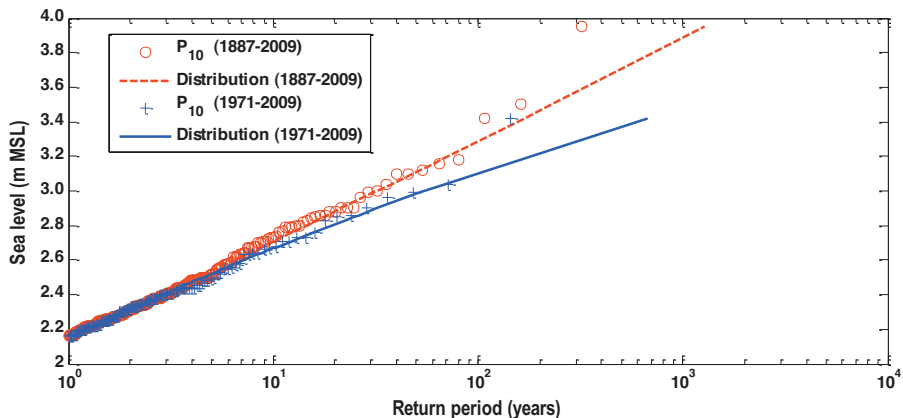


Figure 5-7: Two distributions of P_{10}

The interdependences between the sea level parameters including P_1 , P_4 , P_7 , P_{13} , P_{16} , P_{19} and P_{10} , are addressed in the upper right triangle in Table 5-3, 5-4, 5-5. A threshold of 0.60 is chosen for the linear correlation coefficient, the Kendall's rank correlation coefficient and the Spearman rank correlation coefficient. Values exceeding this threshold are highlighted in the pairs of P_1 and P_4 , P_4 and P_7 , P_{16} and P_{19} in the linear correlation. The rank correlation coefficient in the above three pairs are high, although some of them do not exceed the threshold.

Table 5-3: Linear correlation matrices for the 7 sea level parameters from the 320 observations

Linear correlation	P_1	P_4	P_7	P_{10}	P_{13}	P_{16}	P_{19}
P_1		0.66	0.26	0.51	0.09	0.21	0.24
P_4			0.63	0.42	-0.23	0.21	0.19
P_7				0.29	-0.16	-0.05	0.18
P_{10}					0.13	0.41	0.52
P_{13}						0.47	0.39
P_{16}							0.71
P_{19}							

Table 5-4: Spearman rank correlation matrices for the 7 sea level parameters from the 320 observations

Spearman rank correlation	P ₁	P ₄	P ₇	P ₁₀	P ₁₃	P ₁₆	P ₁₉
P ₁		0.64	0.21	0.42	0.11	0.15	0.15
P ₄			0.57	0.29	-0.22	0.13	0.10
P ₇				0.14	-0.17	-0.10	0.11
P ₁₀					0.13	0.33	0.39
P ₁₃						0.47	0.37
P ₁₆							0.67
P ₁₉							

Table 5-5: Kendall rank correlation matrices for the 7 sea level parameters from the 320 observations

Kendall's rank correlation	P ₁	P ₄	P ₇	P ₁₀	P ₁₃	P ₁₆	P ₁₉
P ₁		0.47	0.14	0.30	0.07	0.10	0.10
P ₄			0.41	0.20	-0.15	0.09	0.07
P ₇				0.09	-0.11	-0.07	0.08
P ₁₀					0.09	0.22	0.27
P ₁₃						0.33	0.26
P ₁₆							0.49
P ₁₉							

The significant linear correlation in these pairs should be taken into account in the stochastic storm surge model by using linear functions to model the dependence in the pairs, as can be seen in Eqn. (5.3).

$$y = a \cdot x + b + \varepsilon \quad (5.3)$$

where a and b are the linear function parameters which are estimated by a linear regression method; ε is a random value which fits a normal distribution estimated from the residuals between observations and predictions of the linear function.

5.2.3 Monte Carlo Simulation

A three-tide storm surge hydrograph can be converted from the 25 parameters shown in Figure 5-4 by a piecewise cubic hermite interpolation method (Wahl et al., 2011), and hence a large number of storm surge scenarios are converted from the 25 parameters' samples derived from the corresponding probability distribution functions.

10,000 P_{10} samples are generated with the Importance Sampling Monte Carlo simulation. For the other 24 parameters, the same number of samples is generated with the crude Monte Carlo simulation. The reason for the difference is that P_{10} , the peak water level height of a storm surge, is the most important parameter to estimate the magnitude of a storm surge, and the other sea level parameters are all related to P_{10} directly or indirectly. The Importance Sampling method is applied to reduce the number of samples in the Monte Carlo simulation but still get sufficiently accurate estimations (Glynn and Iglehart, 1989; Roscoe and Diermanse, 2011).

In order to avoid inconsistencies in these interpolated storm surge hydrographs, filter rules as indicated in Table 5-6 are considered. Empirical threshold values based on the historical data are employed. For example, the threshold (historical highest value) of peak-steepness is 1.34 m MSL and the threshold of peak-skewness is 1.00 m MSL based on the selected storm surge events. In statistics, when a large number of extreme storm surge scenarios are considered, the highest values of peak-steepness and peak-skewness may exceed the thresholds. Thus, in the filter procedure the two thresholds can increase by 10%.

On the one hand the thresholds on surrounding peaks, low water evolution and peak-flatness can make the hydrograph smooth and avoid small disturbances; on the other hand the thresholds on peak-steepness and peak-skewness can avoid very strange or unrealistic hydrographs. Note that these filter rules do not affect the statistics of these storm surge scenarios (Wahl et al., 2011).

Table 5-6: Filter rules considered to avoid inconsistencies in the simulation storm surge hydrographs

Abbreviation	Description	Threshold
Surrounding peaks	First and third high tide are higher than second one; the second low tide is lower than the first one; the third low tide is lower than the fourth one	0 m
Peak-flatness	Difference of the water level one hour before/after a peak (high or low water) and the peak water level itself is very small (i.e. almost a flat line)	0.01 m
Peak-steepness	Difference of the water level one hour before/ after a peak (high or low water) and the peak water level itself is very large	$1.34 \times (1+0.1)$ m
Peak-skewness	Water level one hour before a peak shows a much larger/ smaller difference compared to the peak water level than the water level one hour after the peak	$1.00 \times (1+0.1)$ m
Low water evolution	Second low water is smaller than the first low water or third low water is smaller than the fourth low water	0 m

5.2.4 High water level frequency assessment with the alternative stochastic storm surge model

The fully probability approach using a deterministic 1-D model was introduced and applied to estimate the high water level frequency in the Lower Rhine Delta (Zhong et al., 2013). The water level in Rotterdam is derived from the scenario hydrograph of the storm surge, River Rhine flow and River Meuse flow using the simplified 1-D hydrodynamic model. The simplified 1-D hydrodynamic model of the Netherlands was introduced by van Overloop (2011) and Tortosa (2012).

The hydraulic structures (in Figure 1-4) including storm surge barriers, dams and pump stations can be operated against North Sea storm surges (van Overloop, 2009; 2011). Any extreme storm surges which will result in Rotterdam water level exceeding 3.0 m MSL can trigger the closure of the delta. The failure of the closure is not taken into account. The operation of the present hydraulic structures has been incorporated in the simplified 1-D model.

It is concluded in Chapter 4 that under the present operation of these hydraulic structures, the simultaneous occurrence of the storm surge from the North Sea and the high Rhine flow in the upper Rhine basin becomes the main flood source resulting in extreme water levels in Rotterdam. During this combination event, the present hydraulic structures close the delta, and afterwards Rhine flow accumulates in the delta. Therefore, the focus of the high water level frequency is on this kind of flood source.

Thresholds of storm surge peak level and high Rhine flow (both occur at the same day) are used to identify this flood source. The threshold of storm surge peak level is 2.15 m MSL in Hook of Holland, and the threshold of high Rhine discharge is 6000 m³/s at Lobith according to Section 2.2.2. In Figure 5-8, there are only 3 events exceeding the thresholds of peaks of storm surges and Rhine flows from 1901 to 2009. Due to this lack of data, the occurrence probability of the flood event is difficult to estimate. Based on the historical observations this occurrence probability can be assumed to be 3/109 per year.

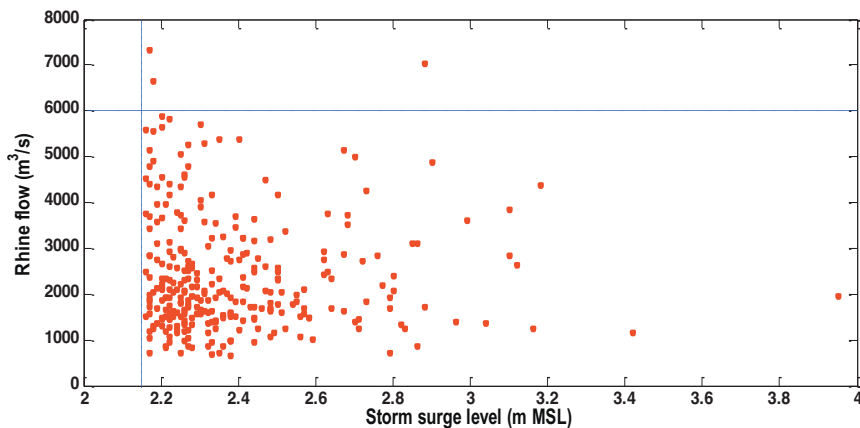


Figure 5-8: The storm surge peak levels and corresponding Rhine discharges

The high water level frequency conditioned on the combination event is estimated. The exceedance probability of Rotterdam water level h_r^* in one year is calculated with Eqn (5.4):

$$P(h_R^*) = \alpha \cdot \iiint I(*)f(h_{P_{10}})f(Q_r, Q_m)dh_{P_{10}} dQ_r dQ_m$$

$$I = 1: h_R(h_{P_{10}}, Q_r, Q_m) \geq h_R^* \quad (5.4)$$

$$I = 0: h_R(h_{P_{10}}, Q_r, Q_m) < h_R^*$$

where α is the occurrence probability of the combination flood event in one year which is 3/109. I is an indicator function and h_R is the Rotterdam water level which is derived from the scenario of the storm surge, River Rhine flow and River Meuse flow using the simplified 1-D hydrodynamic model. $f(h_{P_{10}})$ is the probability density function of the storm surge peak level height P_{10} , see Eqn. (5.5). $f(Q_r, Q_m)$ is the joint probability density function of high Rhine flow and high Meuse flow where the generalized Pareto distribution (Eqn. (2.12)) and the Lognormal distribution (Eqn. (2.13)) fit the high Rhine and Meuse flows and the Gumbel copula function (Eqn. (2.15)) describes their dependency.

$$f(h_{P_{10}}) = \frac{1}{\sigma} \left(1 + \xi \frac{h_{P_{10}} - \mu}{\sigma}\right)^{-\left(\frac{1}{\xi} + 1\right)} \quad (5.5)$$

In this equation the shape parameter ξ is 0.0143; the scale parameter σ is 0.2390 m; the location parameter μ is 2.15 m.

In the combination events, the magnitude of high Rhine flow is independent of the magnitude of the storm surge (Dantzig et al., 1960; Jorigny et al., 2002). The hydrographs of high Rhine flow and high Meuse flow can be generated by the norm hydrographs (Parmet et al., 2002a; Parmet et al., 2002b) multiplied by the ratio between the generated values (sampling values from distributions) and the design peak values. The hydrographs of storm surges are generated by the stochastic storm surge model introduced in this chapter.

5.4 Results

10,000 scenarios of the storm surge, River Rhine flow and River Meuse flow are generated. Top five generated extreme storm surge scenarios are shown in Figure 5-9.

It shows deformed in the storm surge curves in Figure 5-9, as all parameters (shown in Figure 5-4) are generated randomly due to the fitted distribution functions and are independent of each other (except for the pairs of P_1 and P_4 , P_4 and P_7 , P_{16} and P_{19}). Although the deformed curves do not affect the statistical results, they are expected to be improved by new filter rules.

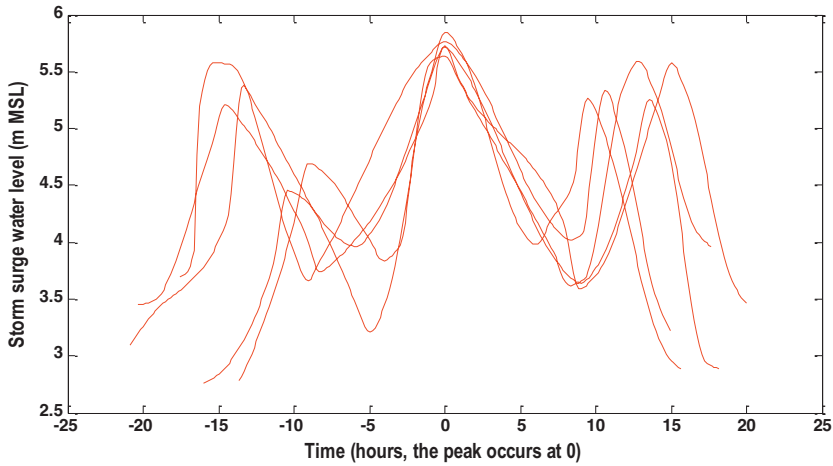


Figure 5-9: Top five generated extreme storm surge scenarios at Hook of Holland

The high water level frequency curve of Rotterdam (the solid line), based on the three-tide length stochastic storm surge model, is shown in Figure 5-10.

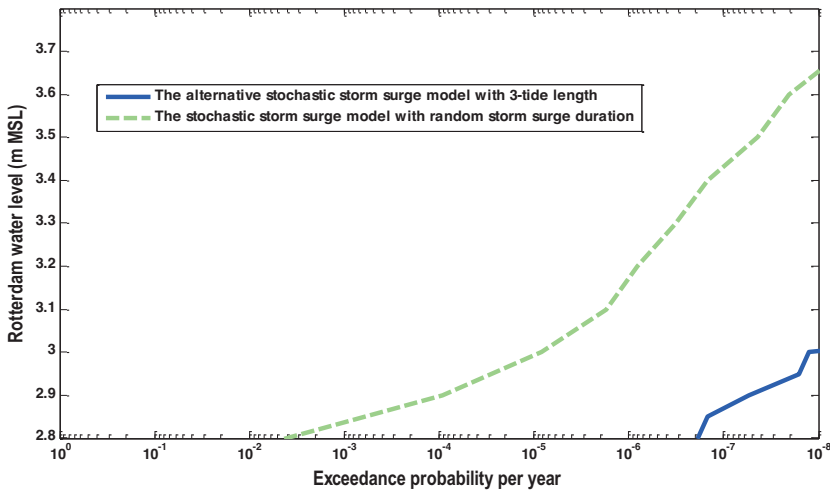


Figure 5-10: High water level frequency curve with the three-tide length stochastic storm surge model conditioned on the combination event

In Figure 5-10, at the exceedance probability of $1/10,000 \text{ year}^{-1}$ the corresponding water level is far below 3.6 m MSL, the present norm water level in Rotterdam. The estimated high water level frequency curve tends to a significantly lower norm water level in Rotterdam. Note that the failure of the closure of the delta against storm surges has not taken into account. Incorporating this failure will shift the high water level frequency curve upwards.

Compared to the high water level frequency curve assessed in section 4.4.2 (the green dashed line in Figure 5-10), unexpectedly, the high water level frequency curve here (the blue solid line) is significantly lower. Two different stochastic storm surge models applied to the same joint probability approach results in two different high water level frequency curves in Rotterdam. The stochastic storm surge model applied solely considers three tides, removing the possibilities of longer durations. On the contrary, random duration can be generated in the previous study (Chapter 2).

The storm surge duration apparently takes an important role in the operational water management system, as it principally determines the closure duration of the Lower Rhine Delta. To estimate the effect of the storm surge duration, the stochastic storm surge model is reconsidered using the length of five tides. Five successive tide peaks exceeding 2.15 m MSL once occurred in history (more than five never occurred), as can be seen in Figure 5-3. More than five tides results in a large number of parameters in the stochastic storm surge model.

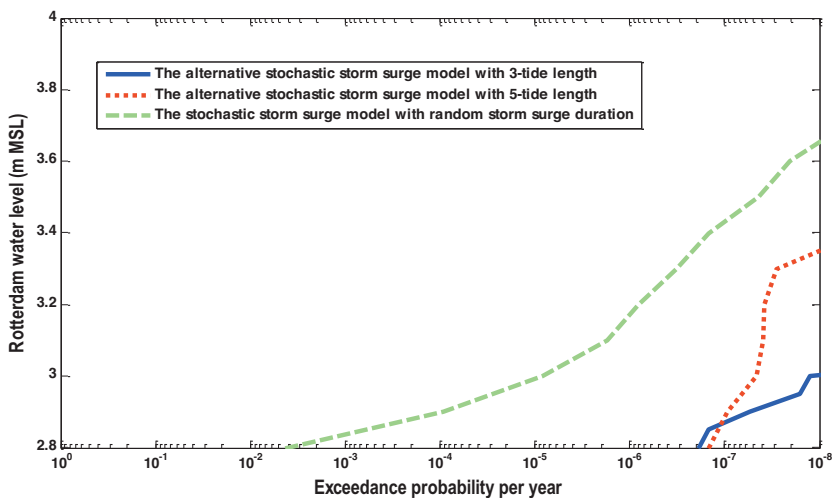


Figure 5-11: High water level frequency curve with the five-tide length stochastic storm surge model conditioned on the combination event

In Figure 5-11, the high water level frequency curve (the red dotted line) estimated with the five-tide length model is higher than the curve (the blue solid line) with the three-tide length model. The five-tide length model allows the occurrence of storm surges with a longer duration. The curve estimated with the five-tide length model (the red dotted line) is still lower than the curve (the green dashed line) derived in the previous study, because in the five-tide length model durations longer than five-tide length have not been taken into account.

5.5 Discussion

The difference between the curves in Figure 5-11 highlights the importance of the storm surge duration on the high water level frequency assessment in the Lower Rhine Delta. The high water level frequency curves are conditioned on the combination event of storm surge and Rhine flood. During this combination event, after the delta is closed, the water level in Rotterdam can rise quickly as the Rhine flood stores in the delta (cannot be discharged into the North Sea). The storm surge duration almost completely determines the closure duration of the delta according to the operation rules of the present hydraulic structures (van Overloop, 2011). Therefore, the storm surge duration becomes a critical parameter to significantly affect how long the delta needs to be kept closed and how much Rhine flood will be stored in the delta. Given the same condition, the longer the storm surge duration is, the higher the high water level frequency is. As seen in Figure 5-11, once the number of tides (duration) in the stochastic storm surge model increases (from three to five), the high water level frequency curve increases.

The previous model in Chapter 2 considered a probability distribution of the storm surge duration, which is preferred. The previous study assumed that the astronomical tide component and the wind induced surge component were statistically independent and then were linearly superimposed. The non-linear interaction between two components was ignored, which might result in large uncertainties on the time evolution of the storm surge.

The storm surge model applied in this article can take the sea water level as a total variable and avoid the non-linear interaction between two components. But a fixed number of tides considered in the model limit the possibilities for long storm surge durations. Therefore, further effort is required for the development of the stochastic storm surge model for the aim of high water level assessment in the Lower Rhine Delta.

5.6 Conclusions

In this chapter, a new stochastic storm surge model has been applied to the mouth of the Lower Rhine Delta. In this model, storm surge lengths of three and five tides have been taken into consideration. A sufficient number of storm surge scenarios have been generated and used to drive a simplified 1-D hydrodynamic model to result in the high water level frequency in Rotterdam. The estimated high water level frequency curve tends to a significantly lower norm water level in Rotterdam. Moreover, it is highlighted that the storm surge duration takes an important role on the high water level frequency assessment in the Lower Rhine Delta. The fixed number of tides considered in the stochastic storm surge model limits the possibilities for longer storm surge durations to occur.

Chapter 6. The effect of four new floodgates on the high water level frequency reduction

6.1 Introduction

To protect the Lower Rhine Delta from storm surges in the North Sea, the delta can be closed off from the sea by the Haringvliet Dams and the Maeslant Storm Surge Barrier and the Hartel Storm Surge Barrier. However, the highly urbanized cities of Rotterdam and Dordrecht in the Lower Rhine Delta are still at risk of being confronted with high water levels.

The high water level frequency assessment is based on a joint probability approach using a deterministic 1-D hydrodynamic model in Chapter 4, including three flooding sources: Category I, storm surges; Category II, Rhine floods; Category III, the combination of both. The results indicate that the simultaneous occurrence of storm surges and high Rhine flows (Category III) becomes the main flood source, see Table 4-2 and Figure 4-10. It is emphasized that the threat of water levels exceeding the design water level still exists for both cities, although with a low probability. It is also highlighted that this probability will increase significantly in the context of climate change.

When a simultaneous extreme event occurs, the Haringvliet Dams and the Maeslant Storm Surge Barrier and the Hartel Storm Surge Barrier should be closed in time under the present water operational management system. Therefore, the extreme Rhine flow that accumulates during the closure would result in a very high water level within the delta area.

The Dutch water board maintains the high-level design water level for design, construction and maintenance of the flood defence systems. The design water level corresponds to a fixed low exceedance probability. For example, the design water level in Rotterdam is 3.6 m MSL corresponding to the exceedance probability 10^{-4} , which also means a flood event with a peak water level exceeding 3.6 m MSL occurs on average 10^{-4} times per year (Ministerie van Verkeer and Waterstaat, 2007).

The flood defence system has to cope with the design water level. However, climate change increases the high water level frequency curve. The potential threat of exceeding the design water level requires adaption measures for the flood defence system. In addition measures will have to be taken to protect possible new housing projects, business districts, etc., from high water levels.

In the past, attention was on the improvement of the strength of the dikes or levees to upgrade the flood defence system. Recently the development of active hydraulic structures like storm surge barriers and floodgates trigger the

investigation of new adjustable structures as a key adaption measure for the flood defence system (Second Delta Commission, 2008).

As a suggested adaptation measure, adjustable floodgates are suggested to be designed in Pannerdensch Canal and the other three floodgates in Merwede, Drechtse Kil and Spui are designed east of Rotterdam and Dordrecht (Second Delta Commission, 2008). These floodgates are expected to decrease the potential extreme water levels which are driven by the simultaneous extreme events. The new structures will be operated with the existing ones to regulate the flood water in a proper way. The main function of the system is to decrease the potential extreme water levels and then to keep the delta flood-proof.

This chapter will focus on the simultaneous occurrence of storm surges and Rhine floods (Category III) and will explore a suggested adaption measure to protect the most important economic center, Rotterdam and Dordrecht in the delta. In the adaption measure four adjustable floodgates are designed and coupled with the present operational water management system. The operational management of these floodgates is to deal with the above flood source, and therefore its effect on the high water level frequency will be quantified. The result will assist the policy decision making in the adaptation measures in the delta.

6.2 The adaptation of the operational water management system

Four new flood gates are proposed along the Rhine river branches in the Rhine delta. One active floodgate is proposed in the Pannerdensch Canal. The costs for the fourth gate are estimated at 800 million euro (de Jong, R, 2010). Three new active floodgates in Merwede, Drechtse Kil and Spui are designed on the South and East of the cities Rotterdam and Dordrecht. These new three structures are inspired by the research of Delft University of Technology on 'Open and Closed Rhine' which also is referred as 'Geregelde Rijnmond' in Dutch. The estimate for the cost of these three gates is 500 million euro each (estimate from 'Open and Closed Rhine'). These structures are designed as floodgates instead of barriers, and therefore these controllable gates can take on any level instead of completely open or closed. These new flood gates as well as the existing ones are shown in Figure 6-1.

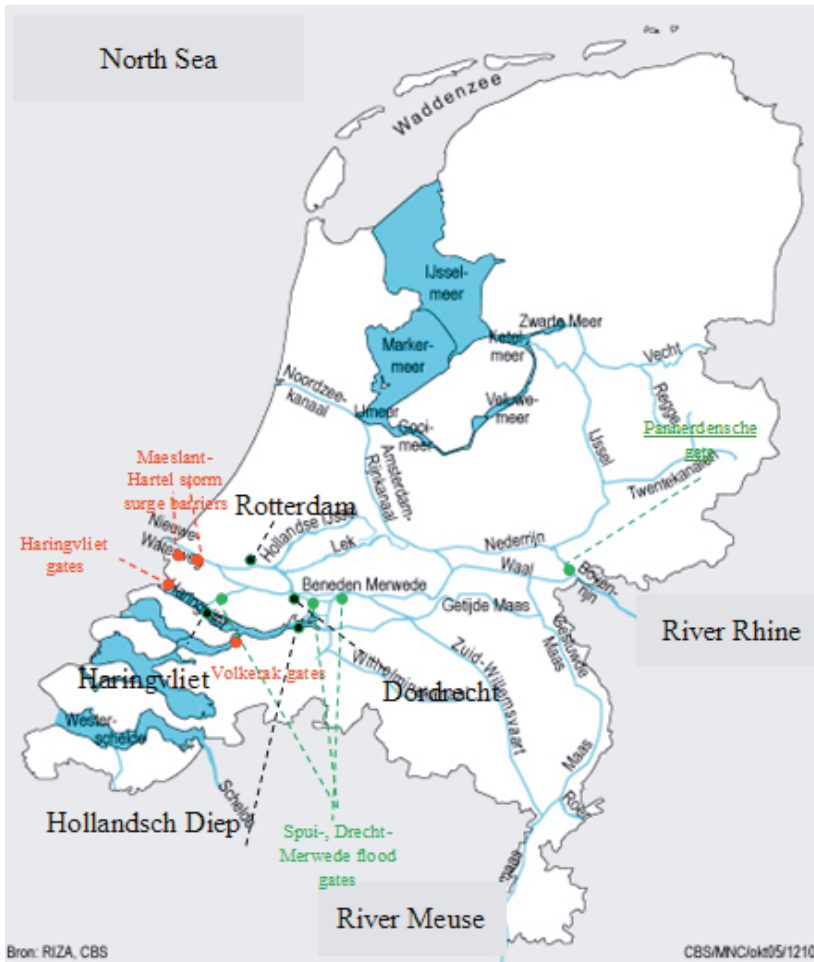


Figure 6-1: The Rhine delta with four new floodgates (in green) (van Overloop, 2011).

These four new flood gates are expected to lower the potential extreme water levels resulted from Category III of flood resource in Rotterdam and Dordrecht. Three floodgates at the South and East of Rotterdam and Dordrecht are designed to close when the water level in Rotterdam and Dordrecht exceeds a reference water level and the water level in Rotterdam and Dordrecht is lower than the water level in Hollandsch Diep and Haringvliet. During the simultaneous occurrence of storm surges and Rhine floods, these three floodgates work together with the Maeslant barrier and Hartel barrier as a surrounding dike to protect Rotterdam and Dordrecht from the threat of extreme water levels. But the Rhine flow water can still flow into this area via the Lek-Nederrijn branch. The designed Pannerdenschegate aims to direct water towards the Waal instead of the Lek-Nederrijn branch. It is expected that the water level in Rotterdam and Dordrecht can be kept low by the operation of these four flood gates mentioned above.

The operation of the new four floodgates is very similar to the present control of the other existing structures. The operational control logic is shown in Figure 6-2. The operational control of the four new flood gates has been incorporated into the present operational water management system.

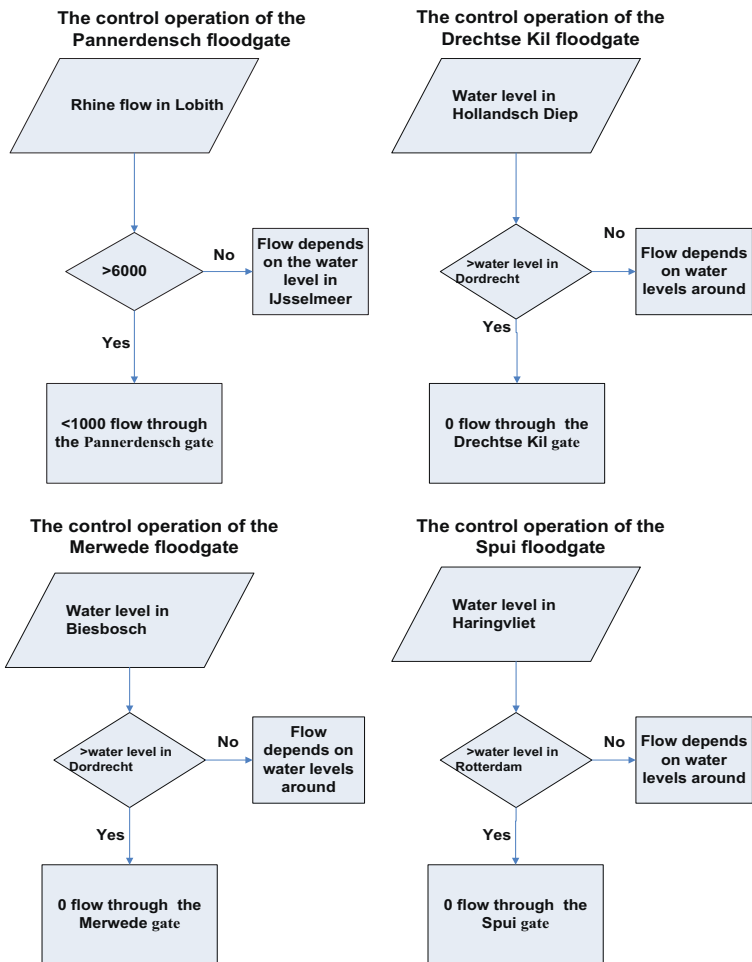


Figure 6-2: The operational control method for 1. Pannerdensch floodgate; 2. Merwede floodgate; 3. Drechtse Kil floodgate; 4. Spui floodgate

6.3 Results

The procedure of the high water level frequency assessment has been illustrated in Chapter 2 and 4. In Chapter 2, a large number of stochastic scenarios of Category III of flood source have been generated for the aim of the high water level frequency assessment in Rotterdam and Dordrecht. In Chapter 4, these stochastic scenarios are used to drive the simplified 1-D hydrodynamic model

associated with the operational water management system. The model is able to convert these scenarios into the peak water levels associated with hydrographs in target locations within the delta. These peak water levels are statistically analyzed and converted to the high water level frequency curves.

To investigate the effect of each floodgate and distinguish the importance for each floodgate, the operational water management system changes with four situations: 1. the present; 2. the present with the Pannerdensch floodgate; 3. the present with Merwede, Drechtse Kil and Spui floodgates; 4. The present with the above four floodgates. For each situation the frequency results are shown in Figure 6-3, 6-4, 6-5 and 6-6 for each target location.

In addition, the effect of the future climate change scenario under different situations will be assessed. In 2050, it is predicted that the mean sea level rise is 0.35 m (van den Hurk et al., 2006) and the peak Rhine discharge increases by 10% relative to the year of 2000 (Jacobs et al., 2000).

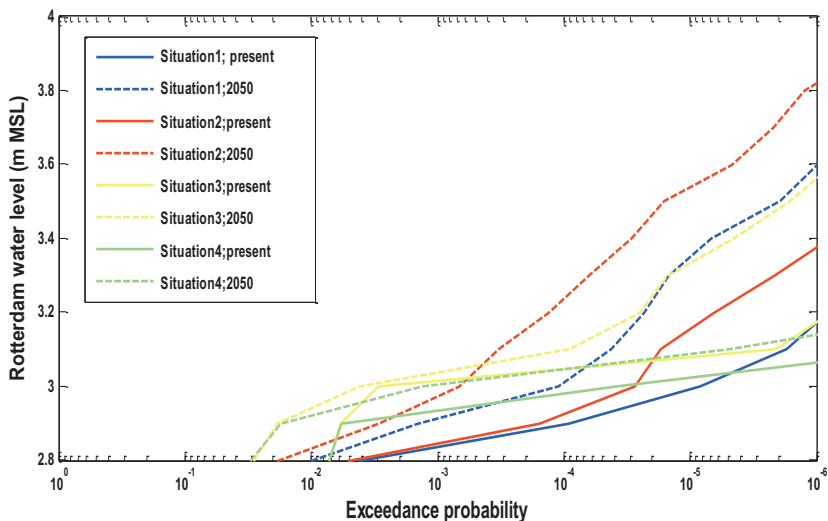


Figure 6-3: The high water level frequency curves conditioned on the simultaneous occurrence of storm surges and Rhine floods in Rotterdam

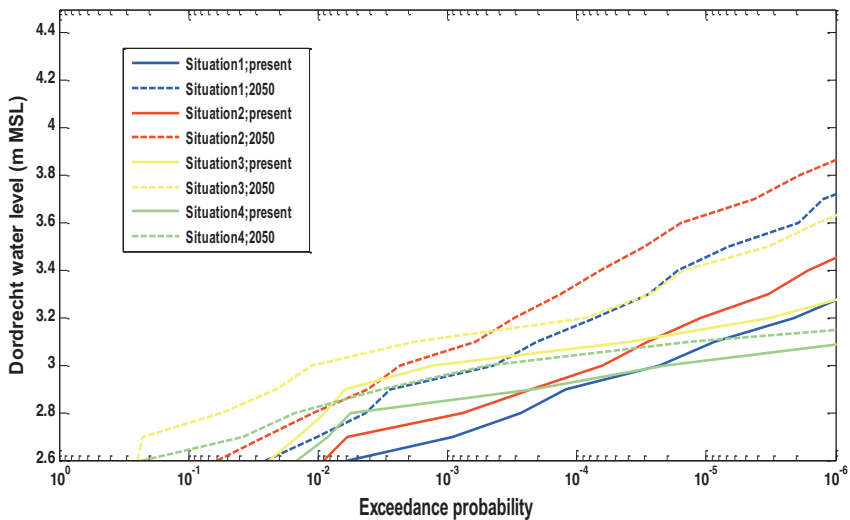


Figure 6-4: The high water level frequency curves due to the simultaneous occurrence of storm surges and Rhine floods in Dordrecht

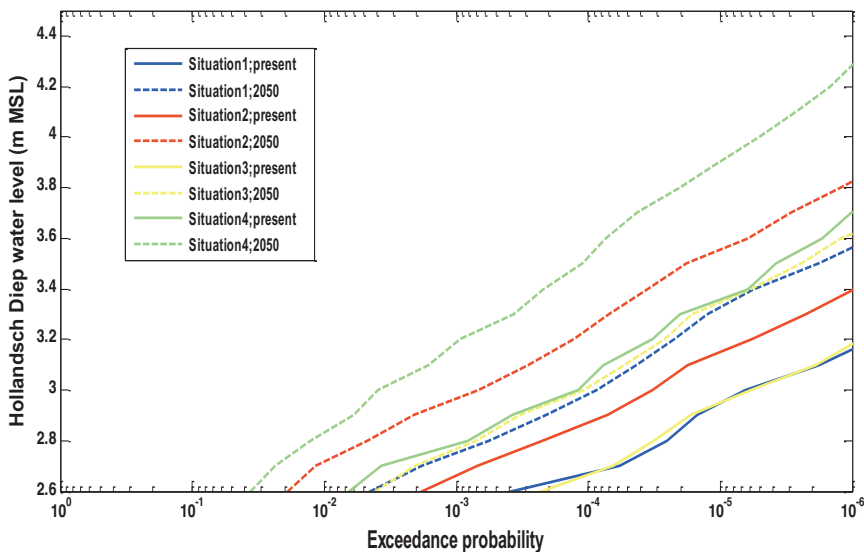


Figure 6-5: The high water level frequency curves due to the simultaneous occurrence of storm surges and Rhine floods in Hollandsch Diep

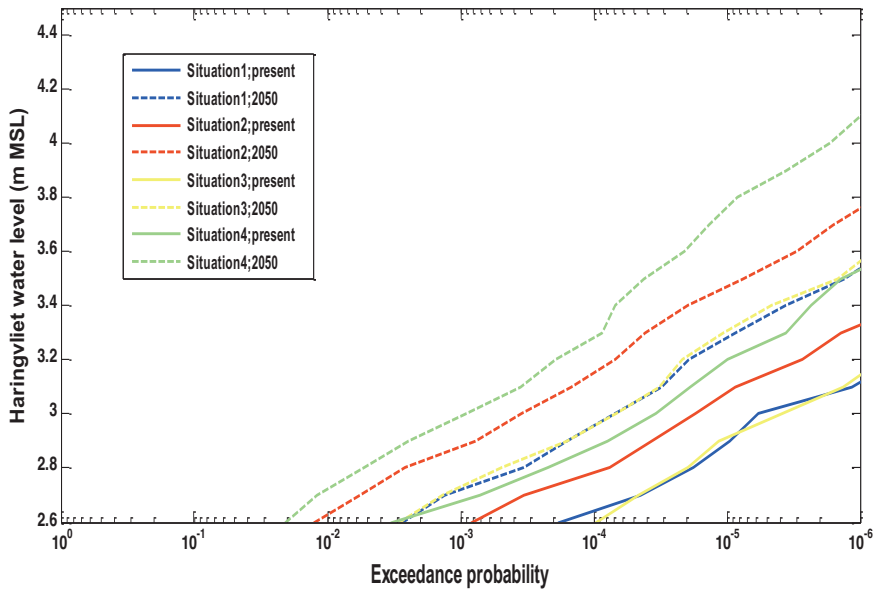


Figure 6-6: The high water level frequency curves due to the simultaneous occurrence of storm surges and Rhine floods in Haringvliet

The present design water levels for the investigated locations are taken from the recent publication by Ministry of Infrastructure and the Environment of the Netherlands (Ministerie van Verkeer and Waterstaat, 2007) in Table 6-1.

Table 6-1: The present design water levels for Rotterdam, Dordrecht, Haringvliet, Hollandsch Diep

Location	The present design water level (m MSL)	Associated with the frequency
Rotterdam	3.6	1/10,000
Dordrecht	3.0	1/2,000
Haringvliet	2.7	1/4,000
Hollandsch Diep	2.8	1/4,000

From Figure 6-3 and 6-4, the future high water level frequency curves are much higher than the present curves. In 2050, the exceedance probability of the present design water level in Dordrecht will be 8.0×10^{-4} , which is higher than the design value of 5.0×10^{-4} . The high exceedance probability indicates that the present system cannot keep the present design water level for the future flood safety. In other words, the present norm water level needs to be increased. This will result in adaption of the present flood defence system.

The present operational water management system still needs adaptations for the future climate proofing. The effect of four new flood gates on the high water level frequency reduction needs quantification.

In 2050, the operation of the Pannerdensch floodgate cannot reduce the high water level frequency curve in Rotterdam and Dordrecht; on the contrast it will increase the high water level frequency curve largely in all investigated locations. In Figure 6-4, 6-5, 6-6 and 6-7, the high water level frequency curves in 2050 in situation 2 (the red dashed line) are much higher than in other situations.

The operation of the three floodgates in Merwede, Drechtse Kil and Spui can reduce the high water level frequency curve slightly in Rotterdam and Dordrecht, but will increase the curve a little in Hollandsch Diep and Haringvliet. The high water level frequency curves in situation 3 (the yellow lines) are slightly lower than in situation 1 (the blue lines) in Figure 6-4 and 6-5, but a little higher in Figure 6-6 and 6-7.

From Figure 6-3 and 6-4, the operation of the above four floodgates reduces the high water level frequency in Rotterdam and Dordrecht. The water level with the frequency of 10^{-4} is far lower than 3.6 m MSL in Rotterdam, and the water level with the frequency of $2 \cdot 10^{-3}$ is lower than 3.0 m MSL in Dordrecht. But it definitely increases the high water level frequency in Hollandsch Diep and Haringvliet as seen in Figure 6-5 and 6-6, as most flooding water is delivered to these places.

To look into the climate scenario of 2050, the increase in the mean sea level and the peak Rhine discharge will increase the high water level frequency in all four situations. The adaption measure of four new flood gates, consequently, make Rotterdam and Dordrecht cope with the expected climate change.

6.4 Conclusions and recommendations

This chapter suggests that adaptations in the present operational water management system will be required for the future climate proof of Rotterdam and Dordrecht. It also explores the operational management of four new floodgates to be established in the delta, and further estimates the high water level frequency reduction in the cities of Rotterdam and Dordrecht.

The results indicate that the joint operation of the four floodgates can reduce the high water level frequency significantly in Rotterdam and Dordrecht. The water level in Rotterdam and Dordrecht can be kept drastically lower than the present design water level, even for the most serious simultaneous extreme events in the future. However, this joint operation increases the high water level frequency in Hollandsch Diep and Haringvliet significantly, as most fresh flooding water is delivered to these places. The operational control of the four flood gates avoids extreme water levels in the highly urbanized Rotterdam and Dordrecht by allowing high water levels in Hollandsch Diep and Haringvliet where farmlands are located. The benefit comes from the reality that damage

induced by flooding in the low value area is much lower than the high value area.

Recommendations are suggested for future research:

1. The feedback control rule applied to the four flood gates is straightforward and the control parameters are chosen arbitrarily. Although the feedback control measure can decrease the high water level frequency significantly in Rotterdam and Dordrecht, control parameters still need to be optimized for the sake of navigation.
2. Modern technologies in terms of better meteorological, hydrological and hydrodynamic models, real-time measuring and forecasting of water levels and discharges, advanced optimal operational control algorithm, etc, have not been applied to the present operational water management system. A centralized Model Predictive Control which uses the information of forecasting and better meteorological, hydrological and hydrodynamic models is available (van Overloop et al., 2010). It is an interesting topic to assess the high water level frequency of the delta under the new operational water management system which applies the centralized Model Predictive Control algorithm.
3. The operation of the Pannerdensch floodgate allows most of Rhine flood flow in Lobith to go to the Waal River and therefore the capacity of Waal River is vital for the new operational water management system. This chapter assumes the capacity of the Waal is kept as the present and ignores the important linkage between the operational rules of the Pannerdensch floodgate and the capacity of the Waal River. These will be taken into consideration in further study. Turning to the capacity of the Waal River, the present project 'Room for the Rhine' aims to increase the capacity of the Waal River for the high Rhine discharge.
4. The four new flood gates avoid extreme water levels in the highly urbanized Rotterdam and Dordrecht by allowing high water levels in Hollandsch Diep and Haringvliet where farmlands are located. The benefit comes from the reality that damage induced by flooding in the low value area is much lower than the high value area. Given good forecasting technology and evacuation measures, it is expected that the human loss can be avoided. However, more information on the damage analysis is required for the support of this new flood gates.

Chapter 7. Effect of statistical uncertainty in the hydraulic boundary conditions on the high water level frequency

7.1 Introduction

The hydrodynamic characteristics of the Lower Rhine Delta are mainly governed by discharge of the Rhine and Meuse and the water level at the North Sea boundaries. The joint probability approach using a deterministic hydrodynamic model was applied to assess the high water level frequency in the Lower Rhine Delta. In the joint probability approach the relevant extreme hydrodynamic loading variables at boundaries, namely astronomical tides, wind induced storm surge, and Rhine and Meuse flow, were jointly investigated and their joint probability distribution was estimated from historical flood events.

The high water level frequency computation consisted of two steps: firstly a large number of stochastic scenarios of extreme hydraulic boundary conditions were sampled from the joint probability distributions with Importance Sampling Monte Carlo simulation; secondly these scenarios were used as inputs to drive a simplified deterministic 1-D hydrodynamic model to result in the corresponding peak water levels at transition locations of interest. The resulting peak water levels as well as their occurrence probabilities were converted to the high water level frequency.

As a result the high water level frequency may be critically influenced by the estimated joint probability distributions, the chosen design hydrograph curves of the relevant hydrodynamic loading variables and the accuracy of the 1-D model.

This chapter aims at investigating insight in the statistical uncertainty of the joint probability distributions and the impact of the statistical uncertainty on the flood frequency.

Statistical uncertainty exists in the marginal distributions of the joint probability distribution, which refers to the uncertainty in the parameters of the marginal distributions caused by estimating them from a limited number of flood events.

The nonparametric bootstrap method (Efron, 1979; Davison and Hinkley, 1997) is employed to quantify the statistical uncertainty in the marginal distributions as it is simple to present and easy to implement. This bootstrap method relies on re-sampling with replacements from the given samples and providing estimates of uncertainty of distribution variables and quantiles in the frequency

analysis. Recently this method is popular in the uncertainty analysis relating to extreme climatological and hydrological events (Dunn, 2001; Kysely, 2010; Roscoe and Diermanse, 2011).

The statistical uncertainty can be further incorporated in the marginal distributions to form new marginal distributions. It is expected that the new distributions will increase the probability of extreme load values because of the uncertainty in the low quantiles of the marginal distributions. In the joint probability distribution, the marginal distributions with/without incorporating the statistical uncertainty are applied to probabilistically compute the high water level frequency. By this, the impact of the statistical uncertainty of the marginal distributions on the high water level frequency can be investigated and quantified.

According to the results from Chapter 3 and 4, of three kinds of flood sources it should be highlighted the most critical one: namely the simultaneous occurrence of a storm surge and a high Rhine flow (Category III). This kind of flood event has become the major flood threat for the Lower Rhine Delta (Zhong et al., 2012; 2013). Note that the present operational water management system, as can be seen in Figure 1-4, has been incorporated in the hydrodynamic model to avoid high water level in the Lower Rhine Delta. During this kind of flood event, the delta can be closed to prevent the high sea level from propagating into the delta (Bol, 2005; van Overloop, 2009). Yet, the simultaneous high Rhine flow coinciding with a long closure duration can still accumulate a large volume freshwater and may result in overtopping/overflowing into the delta.

In the joint probability distribution (Category III, see Eqn. (2.16)), the wind induced surge peak, the wind surge duration and the Rhine discharge are three important variables to influence the high water level frequency in the Lower Rhine Delta. It is assumed that the magnitude of the Rhine flow is independent of the magnitude of the storm surge at the mouth of the delta (Dantzig et al., 1960; Jorigny et al., 2002). The critical marginal distributions were estimated from the selected values (Peak over Threshold values) with the parametric distributions (generalized Pareto distribution, Weibull distribution). All parameters in the marginal distribution were estimated by the Maximum Likelihood Method. The joint probability distribution was shown in Eqn. (2.16) and its marginal distributions were shown in Eqn. (2.2) for the distribution of the wind induced surge peak (h_{smax}), in Eqn. (2.5) for the distribution of the wind induced surge duration (T_s), in Eqn. (2.12) for the distribution of high Rhine discharge (Q_r).

In this chapter the statistical uncertainty of these three important marginal distributions will be quantified. The flood risk map of the Netherlands indicated the urbanized areas of Rotterdam are more hazardous and vulnerable

than the others, and so with the higher fatalities (De Bruijn and Klijn, 2009). As a result, Rotterdam is taken as the case.

This chapter is organized as follows: Methodology is presented in Section 7.2; Results are given in Section 7.3; followed by Conclusions and Recommendations in Section 7.4.

7.2 Methodology

The outline of the method is illustrated in Figure 7-1. First, the bootstrap method is applied to investigate the statistical uncertainty of the marginal distributions. Second, the uncertainty-incorporated marginal distributions are estimated.

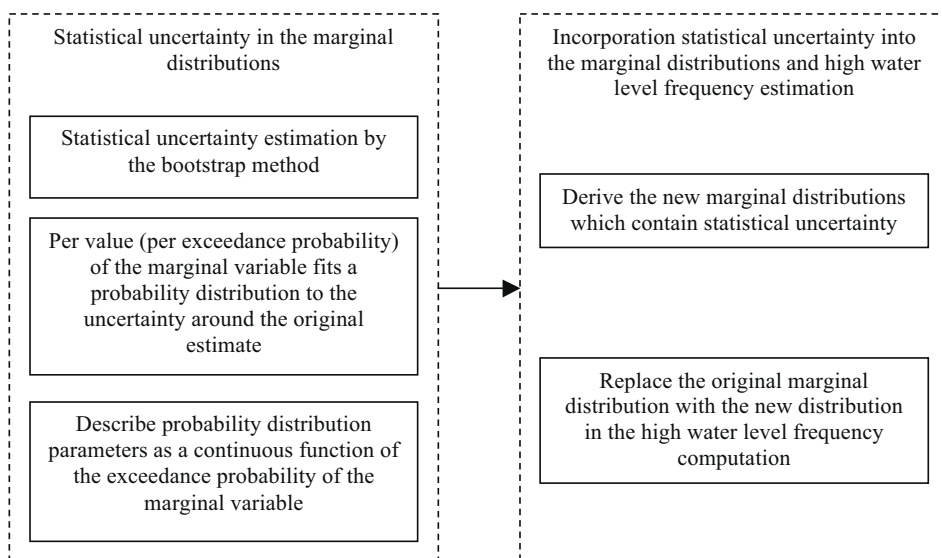


Figure 7-1: Outline of the method

7.2.1 Statistical uncertainty in the marginal distributions

Statistical uncertainty in a marginal distribution can be estimated using the nonparametric bootstrap method, and subsequently is parameterized as a function of the exceedance probability of the marginal variable.

The nonparametric bootstrap method generates a predetermined N times of marginal variable sample which have the same size as the observation by a random re-sampling with replacements from the observation. Every new sample fits to the same distribution type. As a result there are N new distributions in which, for a given exceedance probability, the bootstrap

method returns N values close to the original estimate. For a given exceedance probability of the marginal variable, N discrete bootstrap values can well fit to a Log-normal distribution, a simple skewed distribution.

The probability density function of the Log-normal distribution is:

$$f_x(x; u, \sigma) = \frac{1}{x\sigma\sqrt{2\pi}} e^{-\frac{(\ln x - u)^2}{2\sigma^2}}. \quad (7.1)$$

On a logarithmic scale, u and σ are the location and the scale parameter.

The parameter σ can be modeled as a function of the exceedance probability of the marginal variable P by fitting a polynomial in a least squares sense.

The mode of the Log-normal distribution is located in the point with the maximum density probability. The original estimate of the marginal variable x is assumed to serve as the mode of the Log-normal distribution see Eqn. (7.2), and therefore the other Log-normal parameter u can be estimated from Eqn. (7.3):

$$x = mode(x) = \exp(u - \sigma^2), \quad (7.2)$$

$$u(P) = \ln(x(P)) + \sigma(P)^2. \quad (7.3)$$

The statistical uncertainty in the marginal distributions can be estimated by the Log-normal distribution: given a value of the marginal variate x , the corresponding log-normal distribution, in terms of the parameters u and σ , around that x is known.

7.2.2 Uncertainty-incorporation marginal distributions

The statistical uncertainty can be incorporated into the marginal distributions by the Monte Carlo Integration method. The new marginal distributions can be computed by Eqn. (7. 4) in which there are two random variables: x is the original marginal variable and x_{um} is the uncertainty incorporated marginal variable, where $x_{um} = x + \varepsilon$.

$$F_2(x_{um}) = \int_x F_u((x_{um}); u(x), \sigma(x)) f_1(x) dx \quad (7.4)$$

here F_2 is the uncertainty-incorporated marginal cumulative distribution; f_1 is the original marginal density distribution; F_u is the Log-normal (statistical uncertainty) cumulative distribution conditioned, on the marginal variate x .

7.2.3 Impact on the high water level frequency

In the joint probability distribution, the marginal distributions with/without incorporating the statistical uncertainty are both applied to compute the high water level frequency. Then the impact of the statistical uncertainty on the high water level frequency can be quantified.

The high water level frequency computation consisted of two steps: first, a large number of stochastic scenarios of extreme boundary conditions are generated from the joint probability distribution; second, these scenarios are used as inputs to drive a deterministic hydrodynamic model to result in the peak water levels at locations of interest in the delta. The resulting peak water levels as well as their accompanying joint probabilities can be converted to the high water level frequency. The probabilistically computed high water level frequency is critically influenced by the joint probability distribution, the design hydrographs of the relevant loading variables and the accuracy of the deterministic model.

To quantify the effect of the statistical uncertainty of three critical marginal distributions on the high water level frequency in Rotterdam, a large number of scenarios will be applied. However, the 1-D model is time consuming. A conceptual model, the so-called “Equal Level Curves” (Vrijling and Gelder, 1996; Zhong et al., 2012) is preferred to be applied to examine the interaction of sea level, fluvial flows and infrastructure operations to produce water levels at locations of interest in the Lower Rhine Delta. This model has advantages: first, requiring less information and offers a very fast calculation; second, convenient to combine with the present operation control of the hydraulic structures in the delta.

Considering the characteristics of the Lower Rhine Delta, the conceptual model is illustrated. Two versions of Equal Level Curves are introduced: one for the open delta, and the other for the closable delta. The closable delta can be open to the sea except the extreme weather conditions (storm surges) when the delta is closed by the present hydraulic structures. The detailed information of the conceptual model is in Chapter 3.

7.3 Results

7.3.1 Statistical uncertainty in the marginal distributions

For each marginal variable, there are 1000 bootstrap sample distributions. From these 1000 bootstrap distributions, the quantiles of the 25th, 50th ...975th as well as 5th and 995th are selected. As can be seen in Figure 7-2, there are 40 selected bootstrap curves. And therefore, 40 discrete bootstrap estimates around

the original estimate are given for an exceedance probability of each marginal variable. For the given exceedance probability of each marginal variable, the discrete bootstrap estimates fit to a Log-normal distribution, can be seen in Figure 7-3. Here the figures related to the wind induced surge peak (h_{smax}) are given for the aim of illustration.

The estimated Log-normal parameter σ for the marginal variable (h_{smax}) is shown in Figure 7-4. The parameter σ can be modeled as a third-degree polynomial of the exceedance probability P of the marginal variable in Eqn. (7.6).

$$\sigma(P) = a_1 \log_{10}(P)^3 + a_2 \log_{10}(P)^2 + a_3 \log_{10}(P) + a_4 \quad (7.6)$$

here P is the exceedance probability of the marginal variable, a_1, a_2, a_3, a_4 are estimated by fitting a polynomial in a least squares sense, which can be seen in Table 7-1.

Table 7-1: The estimations of a_1, a_2, a_3 and a_4 for the exceedance probability of each marginal variable

σ	a_1	a_2	a_3	a_4
$\sigma(P(h_{smax}))$	0.0010	0.011	-0.0078	0.0065
$\sigma(P(T_s))$	-0.0001	-0.0021	-0.0141	0.0189
$\sigma(P(Q_r))$	0.0017	0.0247	0.0069	0.0189

The other log-normal parameter u can be estimated based on Eqn. (7.3). In conclusion, the statistical uncertainty in each marginal distribution can be quantified with the Log-normal distribution: given a value of the marginal variable, the corresponding Log-normal uncertainty distribution as well as their parameters u and σ , is known.

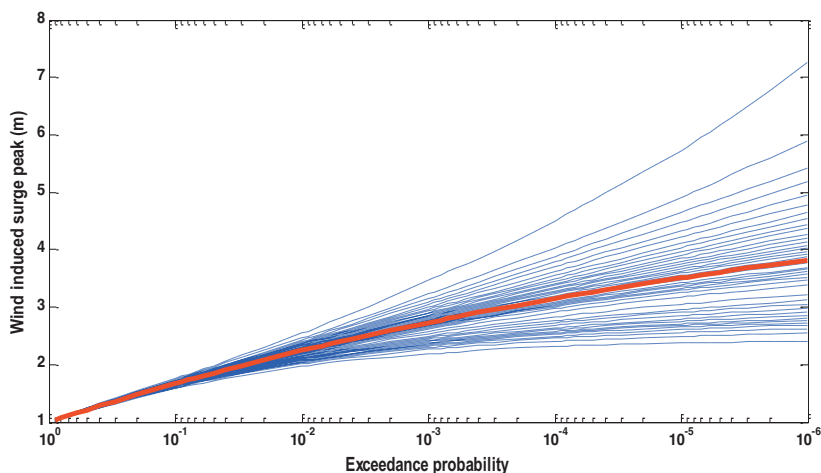


Figure 7-2: Selected bootstrap quantiles for the wind induced surge peak (h_{smax})

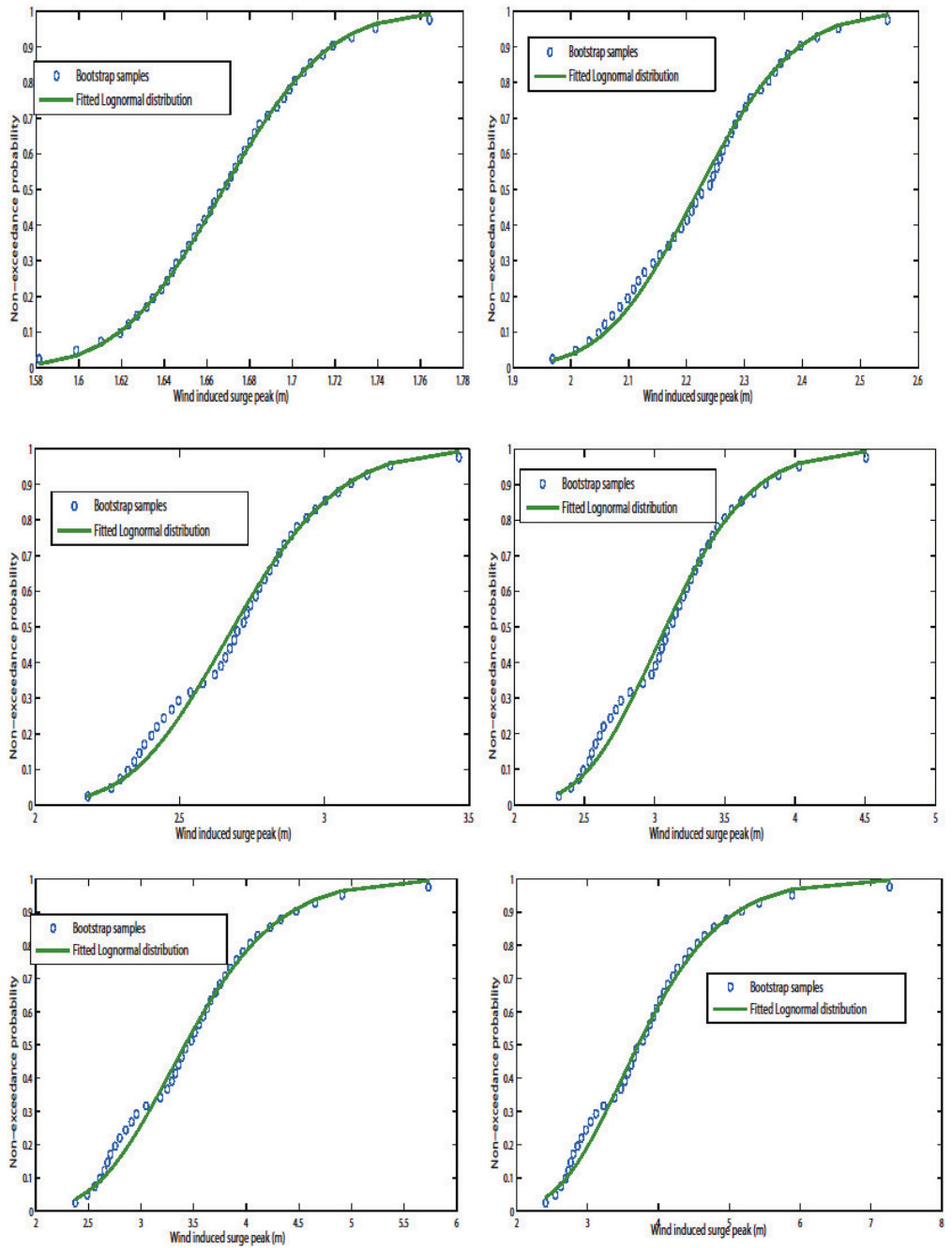


Figure 7-3: The fitted log-normal distributions at the exceedance probability of 10^{-1} , 10^{-2} , 10^{-3} , 10^{-4} , 10^{-5} , 10^{-6} of the wind induced surge peak (h_{smax})

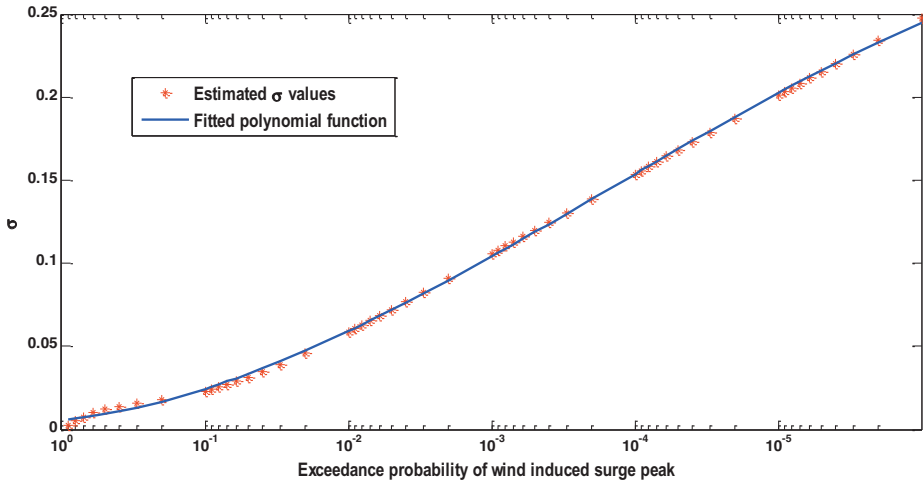


Figure 7-4: The Log-normal distribution's parameter σ is modelled as a function of the exceedance probability of the wind induced surge peak (h_{smax})

7.3.2 Uncertainty-incorporation marginal distributions

According to Eqn. (7.4), the statistical uncertainty can be incorporated into each marginal distribution. The results are shown in Figure 7-5, 7-6 and 7-7.

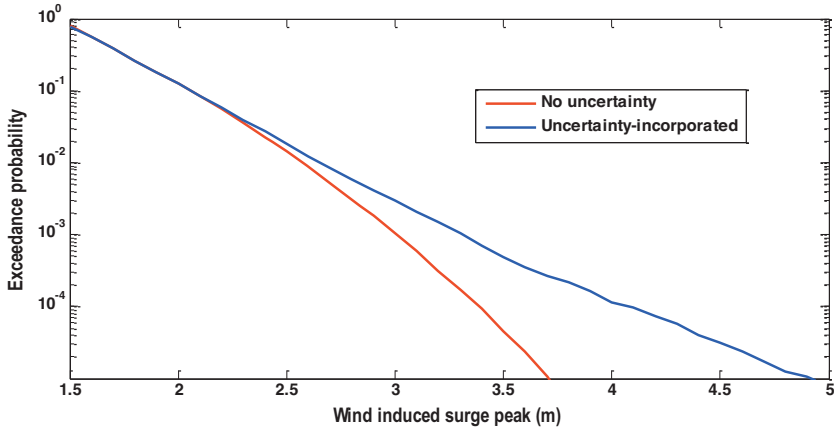


Figure 7-5: The uncertainty-incorporated wind induced surge peak (h_{smax}) distribution

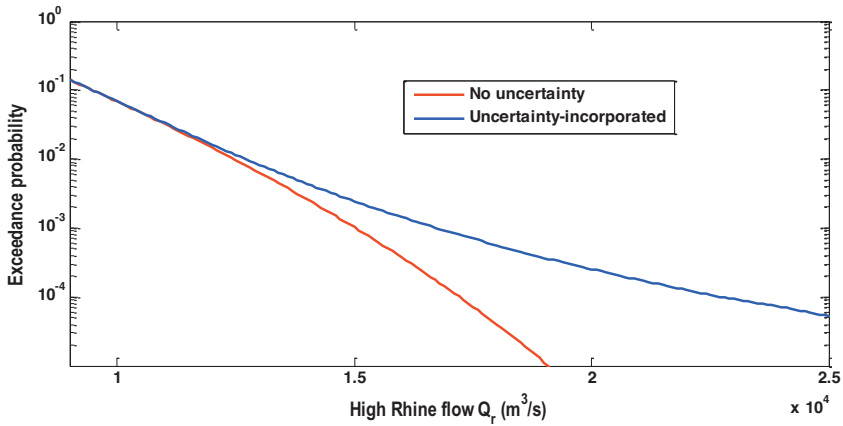


Figure 7-6: The uncertainty-incorporated high Rhine flow (Q_r) distribution

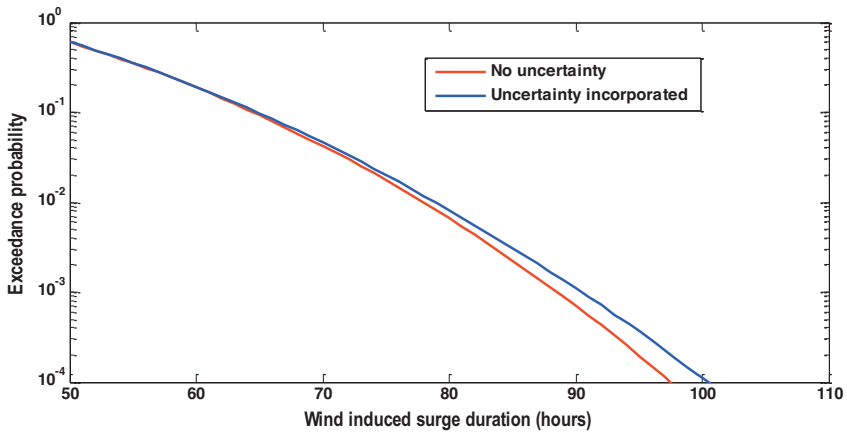


Figure 7-7: The uncertainty-incorporated wind surge duration (T_s) distribution

For higher exceedance probabilities (lower return periods), the uncertainty has a negligible effect on the uncertainty-incorporated distribution, mainly due to the small variance of the uncertainty for higher exceedance probabilities (see Figure 7-4). For lower exceedance probabilities (higher return periods), the variance increases, and the effect on the extreme distribution becomes more substantial.

The results indicate that the uncertainty-incorporated marginal variable's exceedance frequency curve is higher than the original one. In other words, incorporating the statistical uncertainties result in a higher value of the marginal variable at the same low exceedance probability.

However, considering the limitations of the physical conditions the statistical uncertainty in the marginal distributions needs to be constrained at extreme return periods in order to avoid unreal situations. On the other hand, the

relevant knowledge improvement or data extending will assist to reduce the statistical uncertainty.

7.3.3 Impact on the high water level frequency

The influence of the statistical uncertainty on the high water level frequency will be investigated. The impact can be addressed by the differences between the high water level frequency curves derived from two types of marginal distributions, as indicated in Section 7.2.3. The results are shown in Figure 7-8, 7-9, 7-10 and 7-11 respectively.

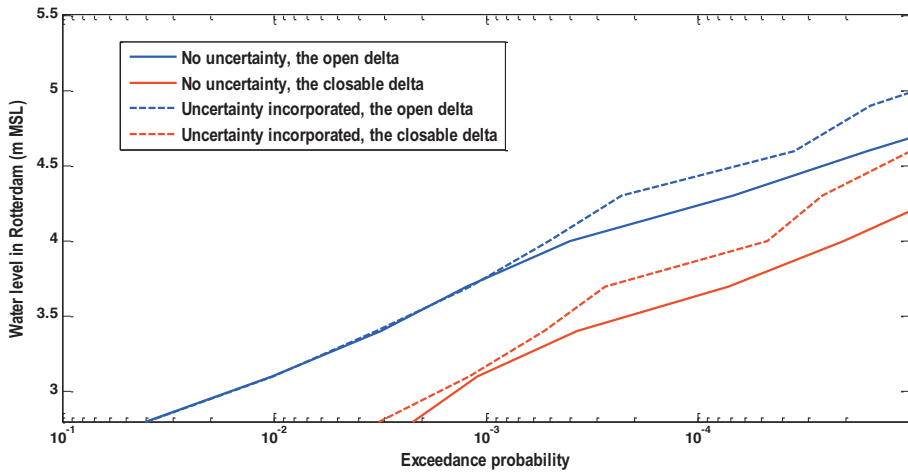


Figure 7-8: The high water level frequency curve considering the statistical uncertainty in the marginal distribution of h_{smax}

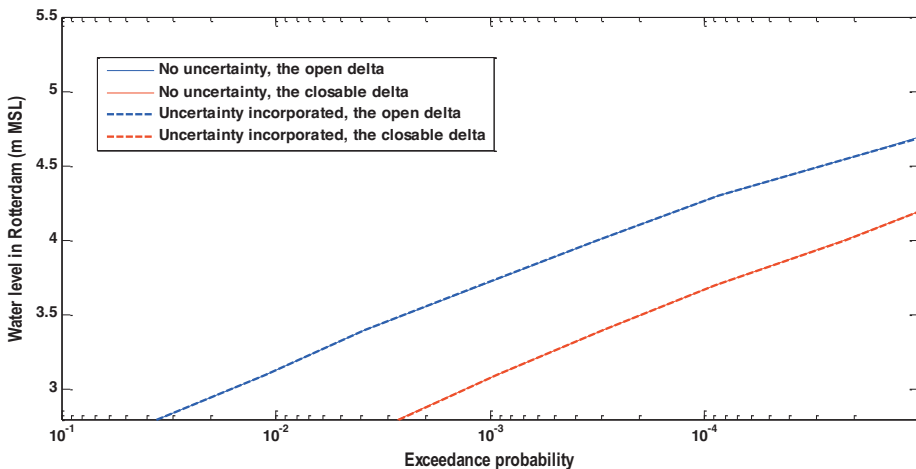


Figure 7-9: The high water level frequency curve considering the statistical uncertainty in the marginal distribution of T_s

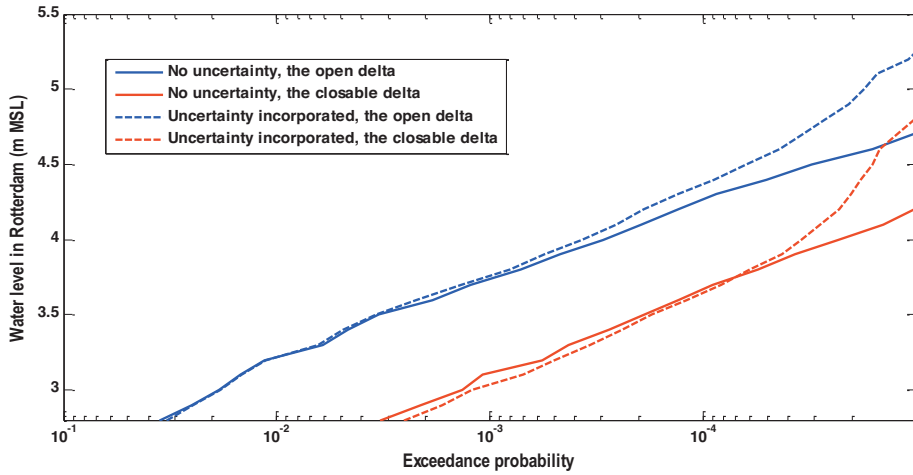


Figure 7-10: The high water level frequency considering the statistical uncertainty in the marginal distribution of Q_r

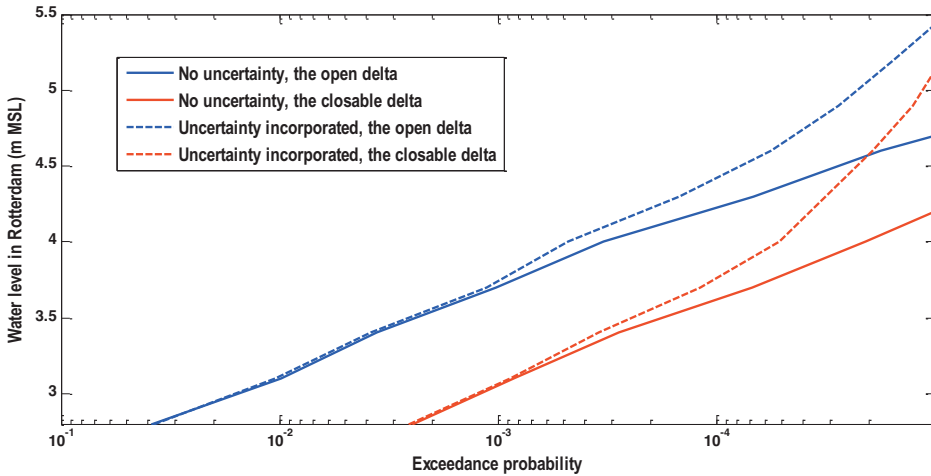


Figure 7-11: The high water level frequency considering the statistical uncertainty in all three marginal distributions

In Figure 7-8, the high water level frequency curves in Rotterdam are estimated from two different marginal distributions of h_{smax} respectively. Generally incorporating the statistical uncertainty in the marginal distribution of h_{smax} significantly increases the high water level frequency in Rotterdam for the exceedance probabilities lower than 10^{-3} .

In Figure 7-9, incorporating the statistical uncertainty in the marginal distribution of T_s does not affect the high water level frequency in Rotterdam.

In Figure 7-10, incorporating the statistical uncertainty in the marginal distribution of Q_r significantly increases the high water level frequency in Rotterdam for the exceedance probabilities lower than 10^{-4} .

In conclusion, the statistical uncertainty in each marginal distribution differs and its impact on the high water level frequency also varies.

In Figure 7-11, incorporating the statistical uncertainty in all three marginal distributions significantly increases the high water level frequency in Rotterdam. Generally for higher exceedance probabilities (lower return periods), the statistical uncertainty has a negligible effect on the high water level frequency, while for lower exceedance probabilities (higher return periods), the effect on the high water level frequency becomes more substantial.

The design water level in Rotterdam is regarded as the water level with an exceedance frequency of 1/10,000; and its present value is 3.60 m MSL (Ministerie van Verkeer and Waterstaat, 2007). As can be seen in Figure 7-11, the design water level of Rotterdam corresponds to 3.60 m MSL without considering the statistical uncertainty in three marginal distributions, while it corresponds to 3.75 m with considering the statistical uncertainty in three marginal distributions.

7.4 Conclusions and Recommendations

Quantifying high water level frequency is critical but complex in deltas or estuaries. The joint probability approach using a deterministic hydrodynamic model was widely applied to estimate the high water level frequency. This chapter aims at investigating statistical uncertainty of marginal distributions of the joint probability distribution and its impact on the high water level frequency. In the Lower Rhine Delta, the results show that incorporating the statistical uncertainty in the marginal distributions will increase the high water level frequency because the probability of extreme hydraulic boundary conditions increases. However, the statistical uncertainty in each marginal distribution differs and its impact on the high water level frequency also varies.

The statistical uncertainty in the marginal distributions can be reduced by improving the relevant knowledge or extending the available data. In addition, when considering the physical conditions, the statistical uncertainty needs to be constrained at extreme return periods in order to avoid unrealistic situations. The reduction of the statistical uncertainty needs discussion for future research.

Chapter 8. Conclusions and recommendations

The objectives of this thesis are to (1) quantify the high water level frequency in the Lower Rhine Delta; (2) quantify the impact of climate change and the operational water management system on the high water level frequency; (3) quantify the statistical uncertainty of the distributions in terms of the storm surge and Rhine discharge, and their impact on the high water level frequency; (4) investigate into adaptations of the operational water management system and the optimization of the control parameters, as well as their effect on the high water level frequency.

8.1 Summary of conclusions

8.1.1 High water level frequency assessment in the Lower Rhine Delta

A fully-probabilistic approach was applied, in which the relevant hydrodynamic loading parameters, namely the astronomical tide, the wind induced storm surges, the Rhine flow and the Meuse flow were jointly investigated. This method considered not only the peak values of the loading parameters but also the other characteristics of the loading parameters. For example the surge duration which used to be pre-determined was taken into account as a random parameter. This new approach was beneficial to the operational water management system, as the derived stochastic scenarios can estimate the consequence of the present operational water management system. For example, the closure duration of the Maeslant Barrier and the Haringvliet dam depends mostly on the storm surge duration which can be randomly generated by the above approach.

The stochastic scenarios derived from the joint probability approach were used to drive the conceptual model 'Equal Level Curves' to estimate the high water level frequency in the Lower Rhine Delta. The high water level frequency assessment with the conceptual model demonstrates how the closable delta strongly reduces the high water level frequency in the delta. For example, under the operation of the Maeslant barrier the return period of 3.0 m MSL in Rotterdam is increased from 11 years to about 2000 years. The return period of 3.6 m MSL (the design safety level) is increased from 10^2 years to more than 10^4 years.

However, due to the mean sea level rise, the frequency of the closure of the delta will increase. Under the present operational control rule, the delta will be closed if Rotterdam water level exceeds the critical water level 3.0 m MSL. In the future, the port of Rotterdam will be closed once every 3.2 years in 2050. The high frequency of the closure of the delta will harm navigation in the

harbor. Estimated losses of 5 million euro per closure at present and will even cost more in the future. On the one hand, the critical water level should be as high as possible to reduce the frequency of the closure; on the other hand it is better to lower the critical water level when the flood safety is at stake.

The stochastic scenarios derived from the joint probability approach were also used to drive the simplified 1-D model to estimate the high water level frequency in the Lower Rhine Delta. The 1-D model enabled assessment of the high water level frequency in a changing environment with associated effects from the operation of the infrastructures. The high water level frequency curves in Rotterdam and Dordrecht were compared to the exceedance probabilities of the present design water level. The results indicated that the high water level frequency complied with the required norm for safety at present. However, the threat of water levels exceeding the design water level still exists for the cities but with a lower probability.

The coinciding events of storm surges and high Rhine flows become the main flood threat to the Lower Rhine Delta and climate change will increase this threat. The future high water level frequency curves (the dashed lines in Figure 4-11) are about 0.2 to 0.4 m higher than the present curves (the solid lines in Figure 4-11) in Rotterdam and Dordrecht. The increase in the high water level frequency requires further adaptation measures in the operational water management system and/or in the flood defense system to maintain the required safety level.

A fast and new stochastic storm surge computing model was applied to the mouth of the Lower Rhine Delta. The results highlighted the importance of the storm surge duration on the high water level frequency assessment within the delta. Since the storm surge duration takes an important role in the high water level frequency assessment in the delta, the stochastic storm surge model with random storm surge duration is recommended for the flood risk assessment in the Lower Rhine Delta.

8.1.2 Statistical uncertainty of the hydraulic boundary conditions

In the fully-probabilistic approach, the critical marginal distributions (for example, the wind induced surge peak level h_{smax}) may contain large statistical uncertainty due to the distributions' parameters estimated from a limited length of observations. The statistical uncertainty of three important marginal distributions were investigated and incorporated into these marginal distributions. The results indicated that incorporating the statistical uncertainty in the marginal distributions will increase the high water level frequency because the probability of extreme hydraulic boundary conditions increases. However, the statistical uncertainty in each marginal distribution differs and its impact on the high water level frequency also varies.

8.1.3 The proposed adaptation of the operational water management system

To cope with climate change, adaptation measures of the operational water management system or the flood defense system are needed to maintain the required safety level. The operational management of the proposed four new floodgates was explored and their effects on the high water level frequency were assessed. The results indicated that (1) the operation of the Pannerdensch floodgate itself cannot reduce the high water level frequency in Rotterdam and Dordrecht; neither can the operation of the other three floodgates themselves; (2) the operation of the above four floodgates together can reduce the design water level significantly in Rotterdam and Dordrecht. However, this project will increase the high water level frequency significantly in Hollandsch Diep and Haringvliet where most flooding water is delivered. In conclusion, the new operational water management system avoids extreme water levels in the highly urbanized Rotterdam and Dordrecht by allowing high water levels occurring in Hollandsch Diep and Haringvliet where farmlands are located. The potential damage loss in Hollandsch Diep and Haringvliet is much lower than in Rotterdam and Dordrecht.

To look into the climate scenario of 2050, the increase in the mean sea level and the peak Rhine flow will increase the high water level frequency. The suggested adaptation measure makes Rotterdam and Dordrecht cope with climate change.

8.2 Recommendations

While deltas will follow adaptation paths that may differ, sometimes substantially, each delta can learn from the others (Aerts et al., 2009). Several recommendations based on this thesis are made:

1. Instead of the conceptual model and the simplified 1-D model, a more detailed numerical hydrodynamic model will be applied in order to investigate the areas of interest in a more detailed scale. In addition, the model uncertainties that arise from spatial variability combined with limited observations (sparse geotechnical data) need to be reduced through research and /or data collection.
2. The methods in terms of re-sampling of extreme hydrodynamic boundary conditions solely depend on the historical data. To incorporate the knowledge of the subjects such as meteorology, hydrology and coastal dynamics, and the information of the reconstruction of extreme floods in the past centuries, is expected to improve the re-sampling methods and results.

3. The statistical uncertainty in the hydraulic boundary conditions needs to be constrained at extreme return periods in order to avoid unreal situations due to the physical conditions. The statistical uncertainty can be reduced with improvement of knowledge and extended data. The reduction of the statistical uncertainty needs discussion. The investigation on the impact of the statistical uncertainty reduction on the high water level frequency will be interesting.
4. Climate change will increase the high water level frequency in the Lower Rhine Delta. At the same time, the future development of local economy and urbanization will increase the potential flood losses (Linde et al., 2011). New adjustable hydraulic structures have been proposed to cope with the expected climate change. However, the advantage of modern technologies in terms of the information of forecasting and better meteorological, hydrological and hydrodynamic models have not been taken into account. A centralized Model Predictive Control algorithm on the operational water management system has been available (van Overloop et al., 2010). It is expected that the application of the new algorithm will further lower the high water level frequency in the delta. It is an interesting topic to assess the high water level frequency of the delta under the new operational water management system which applies the centralized Model Predictive Control algorithm.
5. All the efforts in the operational water management system to reduce the high water level frequency may fail due to human or non-human errors. From this point, there is no absolute flood safety. The failure probability of the operational water management system should be further incorporated.
6. This thesis presents the high water level frequency in specific locations, with the impact of climate change and of adaptation measures of the operational water management system. However, the results are restricted to the high water level frequency in Rotterdam and Dordrecht. Further study should continue to incorporate flood damages and human losses induced by extreme hydraulic boundary conditions in order to assess flood risk at the locations of interest in the Lower Rhine Delta. The flood risk can be valuable for rational decision-making related to the flood risk management in the Lower Rhine Delta.

References:

Acreman, M. C.: Assessing the joint probability of fluvial and tidal floods in the river roding, *Water and Environment Journal*, 8, 490-496, 1994.

Adib, A., Vaghefi, M., Labibzadeh, M., Rezaeian, A., Tagavifar, A., and Foladfar, H.: Predicting extreme water surface elevation in tidal river reaches by different joint probability methods, *J. Food Agric. Environ.*, 8, 988-991, 2010.

Aerts, J., Major, D. C., Bowman, M. J., Dircke, P., and Aris Marfai, M.: Connecting delta cities: Coastal cities, flood risk management and adaptation to climate change, 2009.

Alexandersson, H., Schmith, T., Iden, K., and Tuomenvirta, H.: Long-term variations of the storm climate over nw europe, *The Global atmosphere and ocean system*, 6, 97-120, 1998.

Alexandersson, H., Tuomenvirta, H., Schmith, T., and Iden, K.: Trends of storms in nw europe derived from an updated pressure data set, *Climate Research*, 14, 71-73, 10.3354/cr014071, 2000.

Baart, F., Bakker, M. A. J., van Dongeren, A., den Heijer, C., van Heteren, S., Smit, M. W. J., van Koningsveld, M., and Pool, A.: Using 18th century storm-surge data from the dutch coast to improve the confidence in flood-risk estimates, *Nat. Hazards Earth Syst. Sci.*, 11, 2791-2801, 10.5194/nhess-11-2791-2011, 2011.

Barring, L., and von Storch, H.: Scandinavian storminess since about 1800, *Geophysical Research Letters*, 31, L2020210.1029/2004gl020441, 2004.

Bayliss, A., and Reed, D.: The use of historical data in high water level frequency estimation, Report to MAFF, Centre for Ecology and Hydrology, Wallingfor, available from: <http://www.nwl.ac.uk/feh/historical_floods_report.pdf>, 2001.

Bijl, W.: Impact of a wind climate change on the surge in the southern north sea, *Climate Research*, 8, 45-59, 10.3354/cr008045, 1997.

Bijlsma, A.: Investigation of surge-tide interaction in the storm surge model csm-16, *WL Rapporten*, 311, 1989.

Bol, R.: Operation of the 'Maeslant Barrier': storm surge barrier in the Rotterdam new waterway, *Flooding and Environmental Challenges for Venice and Its Lagoon: State of Knowledge*, 311-316, 2005.

Bowman, M. J., Bowman, M. H., Hill, D., and Khinda, J.: Hydrologic feasibility of storm surge barriers, Storm surge barriers to protect New York City: against the deluge, New York University, USA, 30-31 March 2009., 2013, 71-98,

Bulkeley, H.: Cities and climate change, Routledge, 2013.

Chan, F. K. S., Adekola, O., Mitchell, G., Ng, C. N., and McDonald, A.: Towards sustainable flood risk management in the chinese coastal megacities. A case study of practice in the pearl river delta, Irrig. Drain., 2013.

Chbab, E.: How extreme were the 1995 flood waves on the rivers rhine and meuse?, Physics and Chemistry of the Earth, 20, 455-458, 1995.

Chow, V. T.: Open-channel hydraulics, McGraw-Hill College Press, New York, 1959.

Chu, M., Knouft, J., Ghulam, A., Guzman, J., and Pan, Z.: Impacts of urbanization on river flow frequency: A controlled experimental modeling-based evaluation approach, Journal of Hydrology, 2013.

Cunge, J. A., Holly, F. M., and Verwey, A.: Practical aspects of computational river hydraulics, Pitman, London, 1980.

Dantzig, D., Hemelrijk, J., Kriens, J., and Lauwerier, H.: Rapport deltagcommissie, Staatsdrukkerij En Uitgeverijbedrijf,'s-Gravenhage, 3, 218, 1960.

Davison, A. C., and Hinkley, D. V.: Bootstrap methods and their application, Cambridge university press, 1997.

Dawson, R., Hall, J., Sayers, P., Bates, P., and Rosu, C.: Sampling-based flood risk analysis for fluvial dike systems, Stochastic Environmental Research and Risk Assessment, 19, 388-402, 2005.

De Bruijn, K. M., and Klijn, F.: Risky places in the netherlands: A first approximation for floods, J. Flood Risk Manag., 2, 58-67, 10.1111/j.1753-318X.2009.01022.x, 2009.

de Kraker, A. M.: Storm surges, high tides and storms as extreme weather events, their impact on the coastal zone of the north sea and the human response, 1350 to 2000, Reconstructions of climate and its modelling. Millennium images and reconstructions of weather and climate over the last millennium, Institute of Geography of the Jagiellonian University, Cracow, 85-101, 2000.

de Kraker, A. M.: Reconstruction of storm frequency in the north sea area of the preindustrial period, 1400–1625 and the connection with reconstructed time series of temperatures, *History of Meteorology*, 2, 51-69, 2005.

De Kraker, A. M.: Flood events in the southwestern netherlands and coastal belgium, 1400–1953, *Hydrological Sciences Journal*, 51, 913-929, 2006.

De Michele, C., Salvadori, G., Passoni, G., and Vezzoli, R.: A multivariate model of sea storms using copulas, *Coast. Eng.*, 54, 734-751, 2007.

de Moel, H., Lin, N., Emanuel, K., Botzen, W., and Aerts, J.: Hurricane flood risk to buildings in new york city–future projections and adaptation options, Working paper, http://www.turas-cities.eu/uploads/biblio/document/file/221/NYC_RiskModel_WorkingPaper.pdf, 2013.

de Ronde, J. G.: *Wisselwerking tussen opzet en verticaal getij*, Rijkswaterstaat Dienst Getijdewateren, 1985.

Delft Hydraulics: Sobek-re 1dflow technical reference 2.52. 005, Delft, the Netherlands: Institute for Inland Water Management and Waste Water Treatment (RWS-RIZA) and Delft Hydraulics, 2005.

Efron, B.: Bootstrap methods: Another look at the jackknife, *The annals of Statistics*, 1-26, 1979.

Engel, H.: The flood events of 1993/1994 and 1995 in the rhine river basin, *IAHS Publications-Series of Proceedings and Reports-Intern Assoc Hydrological Sciences*, 239, 21-32, 1997.

Gerritsen, H., de Vries, H., and Philippart, M.: The dutch continental shelf model, *Coastal and Estuarine Studies*, 47, 425-467, 1995.

Gerritsen, H.: What happened in 1953? The big flood in the netherlands in retrospect, *Philosophical Transactions of the Royal Society A: Mathematical, Physical and Engineering Sciences*, 363, 1271-1291, 2005.

Glaser, R., and Stangl, H.: Historical floods in the dutch rhine delta, *Natural Hazards and Earth System Science*, 3, 605-613, 1999.

Glynn, P. W., and Iglehart, D. L.: Importance sampling for stochastic simulations, *Management Science*, 35, 1367-1392, 10.1287/mnsc.35.11.1367, 1989.

Gönnert, G., Buß, T., and Thumm, S.: Coastal protection in hamburg due to climate change. An example to design an extreme storm surge event,

Proceedings of the First International Conference “Coastal Zone Management of River Deltas and Low Land Coastlines, 2010,

Genest, C., B. Remillard., and D. Beaudoin.: Goodness-of-fit tests for copulas: A review and a power study, *Insurance: Mathematics and Economics*, 44, 199-213, 2009.

Gorji-Bandpy, M.: The joint probability method of determining the flood return period of a tidally affected pond, *Iranian Journal of Science and Technology*, 25, 599-610, 2001.

Gouldby, B., Sayers, P., Mulet-Marti, J., Hassan, M., and Benwell, D.: A methodology for regional-scale flood risk assessment, *Proceedings of the ICE-Water Management*, 161, 169-182, 2008.

Hall, J., Dawson, R., Sayers, P., Rosu, C., Chatterton, J., and Deakin, R.: A methodology for national-scale flood risk assessment, *Water and Maritime Engineering*, 156, 2003.

Hanson, S., Nicholls, R., Ranger, N., Hallegatte, S., Corfee-Morlot, J., Herweijer, C., and Chateau, J.: A global ranking of port cities with high exposure to climate extremes, *Clim. Change*, 104, 89-111, 2011.

Hooijer, A., Klijn, F., Pedroli, G. B. M., and Van Os, A. G.: Towards sustainable flood risk management in the rhine and meuse river basins: Synopsis of the findings of irma-sponge, *River research and applications*, 20, 343-357, 10.1002/rra.781, 2004.

Hosking, J., and Wallis, J.: The value of historical data in high water level frequency analysis, *Water Resources Research*, 22, 1606-1612, 1986.

Hydrologic Engineering Centre.: HEC-RAS, version 3.1.0.0. U.S. Army Corps of Engineers, Davis, CA, 2002.

Jacobs, P., Blom, G., and Van Der Linden, M.: Climatological changes in storm surges and river discharges: The impact on flood protection and salt intrusion in the rhine-meuse delta, *Climate Scenarios for Water-Related and Coastal Impacts. ECLAT-2 KNMI Workshop Report*, 2000, 35,

Jonkman, S., and Kelman, I.: Deaths during the 1953 north sea storm surge, *Proceedings of the Solutions to Coastal Disasters Conference*, American Society for Civil Engineers (ASCE), Charleston, South Carolina, 2005, 8-11,

Jorigny, M., Diermanse, F., Hassan, R., and van Gelder, P.: Correlation analysis of water levels along dike-ring areas, *DEVELOPMENTS IN WATER SCIENCE*, 47, 1677-1684, 2002.

Kew, S., Selten, F., Lenderink, G., and Hazeleger, W.: The simultaneous occurrence of surge and discharge extremes for the rhine delta, *Natural Hazards and Earth System Sciences Discussions*, 1, 111-141, 2013.

Klemeš, V.: Tall tales about tails of hydrological distributions. II, *Journal of Hydrologic Engineering*, 5, 232-239, 2000a.

Klemeš, V.: Tall tales about tails of hydrological distributions. I, *Journal of Hydrologic Engineering*, 5, 227-231, 2000b.

Kuenzer, C., and Renaud, F. G.: Climate and environmental change in river deltas globally: Expected impacts, resilience, and adaptation, in: *The Mekong delta system*, Springer, 7-46, 2012.

Kundzewicz, Z. W., and Robson, A. J.: Change detection in hydrological records - a review of the methodology, *Hydrological Sciences Journal-Journal Des Sciences Hydrologiques*, 49, 7-19, 10.1623/hysj.49.1.7.53993, 2004.

Kwadijk, J., and Middelkoop, H.: Estimation of impact of climate-change on the peak discharge probability of the river rhine, *Clim. Change*, 27, 199-224, 10.1007/bf01093591, 1994.

Lehmann, E. L.: *Nonparametric statistical methods based on ranks.*, in, San Francisco, CA: Holden-Day, 1975.

Lian, J. J., Xu, K., and Ma, C.: Joint impact of rainfall and tidal level on flood risk in a coastal city with a complex river network: A case study of Fuzhou city, China, *Hydrology and Earth System Sciences*, 17, 679-689, 10.5194/hess-17-679-2013, 2013.

Linde, A. H. T., Aerts, J., Bakker, A. M. R., and Kwadijk, J. C. J.: Simulating low-probability peak discharges for the rhine basin using resampled climate modeling data, *Water Resources Research*, 46, W0351210.1029/2009wr007707, 2010.

Linde, A. H. T., Bubeck, P., Dekkers, J. E. C., de Moel, H., and Aerts, J. C. J. H.: Future flood risk estimates along the river rhine, *Natural Hazards and Earth System Sciences*, 11, 459-473, 10.5194/nhess-11-459-2011, 2011.

Mann, H. B.: Nonparametric tests against trend, *Econometrica*, 13, 245-259, 10.2307/1907187, 1945.

Mantz, P. A., and Wakeling, H. L.: Forecasting flood levels for joint events of rainfall and tidal surge flooding using extreme value statistics, *Proceedings of the Institution of Civil Engineers Part 2-Research and Theory*, 67, 31-50, 1979.

Middelkoop, H., and Kwadijk, J. C. J.: Towards integrated assessment of the implications of global change for water management - the rhine experience, *Physics and Chemistry of the Earth Part B-Hydrology Oceans and Atmosphere*, 26, 553-560, 10.1016/s1464-1909(01)00049-1, 2001.

MIKE.: MIKE 2012, Danish Hydraulic Institute (DHI) Software Package, 2012.

Ministerie van Verkeer and Waterstaat.: Hydraulische randvoorwaarden primaire waterkeringen voor de derde toetsronde 2006-2011 (hr 2006), Den Haag, 2007. (in Dutch)

Nguyen, H. N., Vu, K. T., and Nguyen, X. N.: Flooding in mekong river delta, viet nam, UNDP, Hanoi, 2007.

Nicholls, R. J., and Cazenave, A.: Sea-level rise and its impact on coastal zones, *science*, 328, 1517-1520, 2010.

Oumeraci, H.: Sustainable coastal flood defences: Scientific and modelling challenges towards an integrated risk-based design concept, Proc. First IMA International Conference on Flood Risk Assessment, IMA-Institute of Mathematics and its Applications, Session, 2004, 9-24,

Parmet, B., Van de Langemheen, W., Chbab, E. H., Kwadijk, J. C. J., Diermanse, F. L. M., and Klopstra, D.: Analyse van de maatgevende afvoer van de rijen te lobith, RIZA Report, 2002a.

Parmet, B., Van de Langemheen, W., Chbab, E. H., Kwadijk, J. C. J., Lorenz, N. N., and Klopstra, D.: Analyse van de maatgevende afvoer van de maas te borgharen, RIZA Report, 2002b.

Pilarczyk, K. W.: Flood protection and management in the netherlands, in: *Extreme hydrological events: New concepts for security*, Springer, 385-407, 2007.

Pinter, N., van der Ploeg, R. R., Schweigert, P., and Hoefler, G.: Flood magnification on the river rhine, *Hydrological Processes*, 20, 147-164, 10.1002/hyp.5908, 2006.

Praagman, N., and Roos, A.: Probabilistic determination of design waterlevels in the eastern scheldt, 1987.

Roscoe, K. L., and Diermanse, F.: Effect of surge uncertainty on probabilistically computed dune erosion, *Coast. Eng.*, 58,,1023-1033, 10.1016/j.coastaleng..2011. 05.014, 2011.

Rosenblatt, M.: Remarks on a multivariate transformation, *The Annals of Mathematical Statistics*, 23(3), 470-472, 1952.

Rosenzweig, C., Solecki, W. D., Blake, R., Bowman, M., Faris, C., Gornitz, V., Horton, R., Jacob, K., LeBlanc, A., and Leichenko, R.: Developing coastal adaptation to climate change in the new york city infrastructure-shed: Process, approach, tools, and strategies, *Clim. Change*, 106, 93-127, 2011.

Samuels, P. G., and Burt, N.: A new joint probability appraisal of flood risk, *Proceedings of the Institution of Civil Engineers-Water and Maritime Engineering*, 154, 109-115, 2002.

Schielen, R., Havinga, H., and Lemans, M.: Dynamic control of the discharge distributions of the Rhine River in the Netherlands, *Proc. Int. Conf. on Fluvial Hydraulics, River Flow*, 2008. Turkey, Sep. 3-5, 2008.

Second Delta Commission.: Working together with water: A living land builds for its future, findings of the deltacommissie 2008, Den Haag, the Netherlands: Hollandia Printing, 2008.

Smith, R. L.: Statistics of extremes, with applications in environment, insurance, and finance, *Extreme values in finance, telecommunications, and the environment*, edited by: Finkenstadt, B., and Rootzen, H., 1-78 pp., 2004.

Sneyers, R.: On the statistical analysis of series of observations, 143, 1991.

Stelling, G., and Duinmeijer, S.: A staggered conservative scheme for every froude number in rapidly varied shallow water flows, *International Journal for Numerical Methods in Fluids*, 43, 1329-1354, 2003.

Sterl, A., Van den Brink, H., De Vries, H., Haarsma, R., and Van Meijgaard, E.: An ensemble study of extreme storm surge related water levels in the north sea in a changing climate, *Ocean Science*, 5, 369-378, 2009.

Sveinsson, I. G. B., Salas, J. D., and Boes, D. C.: Prediction of extreme events in hydrologic processes that exhibit abrupt shifting patterns, *Journal of Hydrologic Engineering*, 10, 315-326, 10.1061/(asce)1084-0699(2005)10:4(315), 2005.

Syvitski, J. P., and Saito, Y.: Morphodynamics of deltas under the influence of humans, *Global and Planetary Change*, 57, 261-282, 2007.

Syvitski, J. P., Kettner, A. J., Overeem, I., Hutton, E. W., Hannon, M. T., Brakenridge, G. R., Day, J., Vörösmarty, C., Saito, Y., and Giosan, L.: Sinking deltas due to human activities, *Nature Geoscience*, 2, 681-686, 2009.

Tortosa, Alejandra.: Calibración de un modelo simplificado del sistema de canalizaciones hidráulicas de Holanda, Master thesis. Escuela Técnica Superior de Ingenieros de Sevilla, 2012. (in Spanish)

van den Hurk, B., Klein Tank, A., Lenderink, G., van Ulden, A., Van Oldenborgh, G., Katsman, C., Van den Brink, H., Keller, F., Bessembinder, J., and Burgers, G.: Knmi climate change scenarios 2006 for the netherlands, Citeseer, 2006.

van der Made, J. W.: Design levels in the transition zone between the tidal reach and the river regime reach, Hydrology of Deltas, Vol. 2 of Proceedings of the Bucharest Symposium, May, 1969, 246-257, 1969.

van Gelder, P.H.A.J.M: A new statistical model for extreme water levels along the dutch coast, Stochastic hydraulics 96, proceeding of the seventh IAHR International Symposium, edited by: Tickle, K. S., Goulter, I.C., Xu,C.C., Wasimi, S.A., and Bouchart, F., 243-249, 1996.

van Overloop, P. J.: Model Predictive Control on open water systems, PhD thesis, Delft University of Technology, Delft, the Netherlands, 2006.

van Overloop, P. J.: Operational water management of the main waters in the netherlands, Technical Report, Delft University of Technology, Delft, the Netherlands, 2009.

van Overloop, P. J., Negenborn, R., Schutter, B. D., and Giesen, N.: Predictive control for national water flow optimization in the netherlands, Intelligent Infrastructures, 439-461, 2010.

van Overloop, P. J.: Optimization of ‘Everything’, Prediction and Control of the entire Delta and River System of The Netherlands, Technical Report for Water INNOvation (WINN), Delft University of Technology, Delft, the Netherlands, 2011.

Verlaan, M., Zijderveld, A., de Vries, H., and Kroos, J.: Operational storm surge forecasting in the netherlands: Developments in the last decade, Philosophical Transactions of the Royal Society A: Mathematical, Physical and Engineering Sciences, 363, 1441-1453, 2005.

Vries, M.: Considerations about non-steady bed-load-transport in open channels, Delft Hydraulics Laboratory, 1965.

Vrijling, J. K, and Bruinsma, J.: Hydraulic boundary conditions, Symposium on hydraulic aspects of coastal structures, 1980, 109-132,

Vrijling, J. K., and van Gelder, P.H.A.J.M.: Probabilistic design in hydraulic engineering, Delft University of Technology, 1996.

Wahl, T., Jensen, J., and Mudersbach, C.: A multivariate statistical model for advanced storm surge analyses in the north sea, *Coast. Eng.*, 2, 2010.

Wahl, T., Mudersbach, C., and Jensen, J.: Assessing the hydrodynamic boundary conditions for risk analyses in coastal areas: A stochastic storm surge model, *Nat. Hazards Earth Syst. Sci.*, 11, 2925-2939, 10.5194/nhess-11-2925-2011, 2011.

Wahl, T., Mudersbach, C., and Jensen, J.: Assessing the hydrodynamic boundary conditions for risk analyses in coastal areas: A multivariate statistical approach based on copula functions, *Nat. Hazards Earth Syst. Sci.*, 12, 495-510, 2012.

Wall, F. J.: *Statistical data analysis handbook*, McGraw-Hill New York, 1986.

WASA-Group: Changing waves and storms in the northeast atlantic?, *Bulletin of the American Meteorological Society*, 79: 741-760, 1998.

Waterstaat, M. v. V.: *Hydraulische randvoorwaarden primaire waterkeringen voor de derde toetsronde 2006-2011 (hr 2006)*, Den Haag, 2007.

Weichselgartner, J.: From the field: Flood disaster mitigation in the mekong delta, *Seventh European Sociological Association Conference, Rethinking Inequalities*, Torun, Poland, 2005.

White, C. J.: *The use of joint probability analysis to predict high water level frequency in estuaries and tidal rivers*, PhD Dissertation, University of Southampton, 2013.

Winkelhorst, J.: *Hydraulic analysis of a flood channel from the Afgedamde Maas to the Biesbosch and Bergse Maas*, Master Thesis, Delft University of Technology, Delft, the Netherlands, 2013.

Yevjevich, V., Engineer, Y., Ingenieur, J., and Ingénieur, Y.: *Probability and statistics in hydrology*, Water Resources Publications Fort Collins, CO, 1972.

Zheng, F., Westra, S., and Sisson, S. A.: Quantifying the dependence between extreme rainfall and storm surge in the coastal zone, *Journal of Hydrology*, 505, 172-187, 2013.

Zhong, H., van Overloop, P. J., van Gelder, P., and Rijcken, T.: Influence of a storm surge barrier's operation on the high water level frequency in the rhine delta area, *Water*, 4, 474-493, 2012.

Zhong, H., Overloop, P.-J. v., and Gelder, P. v.: A joint probability approach using a 1-d hydrodynamic model for estimating high water level frequencies in the lower rhine delta, *Natural Hazards and Earth System Science*, 13, 1841-1852, doi:10.5194/nhess-13-1841-2013, 2013.

Index of notation and abbreviations

Symbol	Description
R	Flood risk
P	Probability of flooding
D	Flood induced damage
h_{smax}	Wind surge peak level
T_s	Wind surge duration
h_s	Wind surge level
h_{HW}	High astronomical tide level (excluding wind surge level)
h_{LW}	Low astronomical tide level (excluding wind surge level)
h_a	Astronomical tide level (excluding wind surge level)
u	Time shift between wind surge peak and high astronomical tide peaks
h_0	Mean sea level
h	Sea water level
h_R	Rotterdam water level
Q_r	Rhine discharge in Lobith
Q_m	Meuse discharge in Borgharen
h_{hvh}	Sea water level at Hook of Holland
A	Surface area of the cross section in Hook of Holland
g	Gravitational acceleration
μ	Discharge coefficient
ΔT	Delta closure duration
$h_{R,c}$	Rotterdam water level at the moment right after Rhine delta closure
B	Surface area of Lower Rhine Delta where water can be stored
h_G	Goidschalxoord water level
h_D	Dordrecht water level
h_M	Moerdijk water level
H_d	The closing decision level in Rotterdam
C	The Chézy friction coefficient
R_f	The hydraulic radius
A_f	The wetted area
q_{lat}	The lateral inflow per unit length ,
I	Indication function
P_i	Parameters in the alternative stochastic storm surge model
r	Root-Mean-Square Error (RMSE)
ε	Normal distribution random value
α	Occurrence probability of a combination event (Category III)

Acknowledgements

Four-year Ph.D looks like a precious journey to me. I would like to acknowledge people I met in this journey for their guidance, accompany and support.

First, I give my thanks to Prof. J.K Vrijling, for his sound suggestions on my dissertation. His profound knowledge, broad horizon, guided me. I also give the best gratitude to Prof. Pieter van Gelder, for his supervision and encouragement. My sincere appreciation is to Associate Prof. Peter-Jules van Overloop for his kind suggestions, stimulation and discussion.

Second, I give my gratitude to Xin Tian and Alejandra Tortosa for their work on the simplified 1-D hydrodynamic model of the Netherlands which I applied in the dissertation; to Ms. Marrette van Tilburg for improving English writing in my dissertation and other articles; to Ir. Ties Rijcken for sharing knowledge and opinions on the Rijnmond project ‘Rhine estuary closable but open’(in Dutch ‘Afsluitbaar Open Rijnmond’) at the beginning stage of my research; to Xuefei Mei and Lu Wang for the great academic air in the office room 3.93 of CiTG. I also thank all colleges and ex-colleges in our department for the great honour to work with such talented and diligent researchers.

Third, thanks committee members: Dr. Thomas Wahl, Dr. Joost Beckers, Prof. Matthijs Kok and Prof. Bas Jonkman for their valuable comments and suggestions on the dissertation. Specially, I appreciate Prof. Wang Wen from Hohai University for his kind recommendations, not only the Ph.D opportunity in TU Delft but also the future job in Nanjing Hydraulic Research Institute.

Fourth, I want to mention good friends in Delft: Junchao, Mingliang, Wenchao, Yutian, Jiao, Fan, Qian, Haiyang, Huayang, Congli, Dongju, Xuexue, Lixia, Gensheng, Wei, Hong, Zhan (HU), Xiuhan, Yajun, Kang, Kun, Miao, Yankai, Zhan (LUO), Xin, Hongkai and others.

Fifth, I give my heartfelt appreciation to my parents, Lijun Zhong and Guoying Zhao, and also my aunt, Yanchun Zhong. No matter what happened to me, good or bad, they always did their best to guide and support me. Every step I made contains their love. My beloved grandmother passed away when I was writing the dissertation. It broke my heart.

Sixth, special thanks to my girlfriend Junyu Li. Love sometimes comes unexpectedly. When I met her again in Nanjing, I could not take my eyes off her.

Last, I would like to mention and thank China Scholarship Council and TU Delft for offering me this precious Ph.D research opportunity.

Hua Zhong
February 2014 in Delft, the Netherlands

Curriculum Vitae

Hua ZHONG was born in Gongyi, Henan province, China, on 1st October 1984. In 2004 he went to Hohai University, Nanjing and began to study Hydrology and Water Resources Engineering. In 2008 he continued his master program at Hohai University. In 2009 he went to Delft University of Technology for his Ph.D research financially supported by China Scholarship Council. His Ph.D research in Department of Hydarulic Engineering focuses on the flood risk assessment in the Lower Rhine Delta. In 2014, He took a research position in Department of Hydrology and Water Resource, Nanjing Hydraulic Research Institute, Nanjing, China.

Publications

Peer-reviewed Journal articles

- 1.**Zhong, H.**, van Overloop, P. J., van Gelder, P., and Rijcken, T.: Influence of a storm surge barrier's operation on the high water level frequency in the Rhine delta area, *Water*, 4, 474-493, doi:10.3390/w4020474, 2012.
- 2.**Zhong, H.**, van Overloop, P.J., and van Gelder, P. H. A. J. M.: A joint probability approach using a 1-D hydrodynamic model for estimating high water level frequencies in the Lower Rhine Delta, *Nat. Hazards Earth Syst. Sci.*, 13, 1841-1852, doi:10.5194/nhess-13-1841-2013, 2013.
- 3.**Zhong, H.**, van Gelder, P. H. A. J. M., van Overloop, P. J., Wang, W.: Application of a fast stochastic storm surge model on the high water level frequency estimation in the Lower Rhine Delta, *Nature Hazards*, 2014 (accepted)
- 4.**Zhong, H.**, van Gelder, P. H. A. J. M., van Overloop, P. J., Wang, W.: The effect of statistical uncertainty in the hydraulic boundary conditions on the high water level frequency in the Lower Rhine Delta, Submitted to *Journal of Flood Risk Management*.

Conference articles

- 1.**Zhong, H.**, van Overloop, P. J., van Gelder, P., Tian, X.: The effect of four new floodgates on the high water level frequency reduction in the Lower Rhine Delta, the 8th European Water Resources Association conference, Porto, Portugal, 2013.